Aus der Klinik und Poliklinik für Psychiatrie und Psychotherapie

Klinik der Ludwig-Maximilians-Universität München

Direktor: Prof. Dr. med. Peter Falkai

Effects of prefrontal transcranial direct current stimulation on resting-state functional MRI: variability and target specificity in healthy subjects

---

Dissertation

zum Erwerb des Doktorgrades der Humanbiologie

an der Medizinischen Fakultät der

Ludwig-Maximilians-Universität zu München

vorgelegt von

Jana Vera Werle (geb. Wörsching)

aus Gräfelfing

2019

Mit Genehmigung der Medizinischen Fakultät

der Universität München

Berichterstatter:	Prof. Dr. med. Frank Padberg
Mitberichterstatter:	Prof. Dr. Kai Bötzel
	Prof. Dr. Olaf Dietrich
	Prof. Dr. Bertram Müller-Myhsok
	Prof. Dr. Rüdiger Ilg
Mitbetreuung durch den promovierten Mitarbeiter:	Dr. Daniel Keeser
Dekan:	Prof. Dr. med. dent. Reinhard Hickel
Tag der mündlichen Prüfung:	09.09.2019

Eidesstattliche Versicherung

Werle, Jana

Ich erkläre hiermit an Eides statt,

dass ich die vorliegende Dissertation mit dem Thema

Effects of prefrontal transcranial direct current stimulation on resting-state functional MRI: variability and target specificity in healthy subjects

selbständig verfasst, mich außer der angegebenen keiner weiteren Hilfsmittel bedient und alle Erkenntnisse, die aus dem Schrifttum ganz oder annähernd übernommen sind, als solche kenntlich gemacht und nach ihrer Herkunft unter Bezeichnung der Fundstelle einzeln nachgewiesen habe.

Ich erkläre des Weiteren, dass die hier vorgelegte Dissertation nicht in gleicher oder in ähnlicher Form bei einer anderen Stelle zur Erlangung eines akademischen Grades eingereicht wurde.

München, 17.09.2019	Jana Werle
Ort, Datum	Unterschrift Doktorandin

Table of contents

List of abbreviations

DLPFC, Dorsolateral prefrontal cortex

DMN, Default mode network

ECT, Electro-convulsive therapy

fMRI, Functional magnetic resonance imaging

ICC, Intra-class correlation-coefficients

mA, Milliampere

MD, Major depression

MEP, Motor-evoked potentials

min, Minutes

MRI, Magnetic resonance tomography

NIBS, Non-invasive brain-stimulation

PFC, Prefrontal cortex

RS, Resting state

RSN, Resting-state network

tDCS, Transcranial direct current stimulation

TMS, Transcranial magnetic stimulation

TRT, Test retest

WM, Working memory

List of publications

Original research articles

- **Wörsching, J.**, Padberg, F., Helbich, K., Hasan, A., Koch, L., Goerigk, S., Stoecklein, S., Ertl-Wagner, B., & Keeser, D. (2017). Test-retest reliability of prefrontal transcranial Direct Current Stimulation (tDCS) effects on functional MRI connectivity in healthy subjects. *Neuroimage, 155,* 187-201.
- **Wörsching, J.***, Padberg, F.*, Goerigk, S., Heinz, I., Bauer, C., Ertl-Wagner, B., & Keeser, D. (2018. Testing assumptions on prefrontal transcranial direct current stimulation: Comparison of electrode montages using multimodal fMRI. *Brain Stimulation, 11(5), 998-1007.*

Other publications related to the dissertation

- **Wörsching, J. ***, Padberg, F. ***, Ertl-Wagner, B., Kumpf, U., Kirsch, B., & Keeser, D. (2016). Imaging transcranial direct current stimulation (tDCS) of the prefrontal cortex-correlation or causality in stimulation-mediated effects? *Neurosci Biobehav Rev, 69*, 333-356.
- Palm, U., Kumpf, U., Behler, Nora, Wulf, L., Kirsch, B., **Wörsching, J.**, Keeser, D., Hassan, A., & Padberg, F. (2017). Home-use, remotely supervised and remotely controlled transcranial direct current stimulation (tDCS): a systematic review of the available evidence. *Neuromodulation, 21(4), 323-333.*

Oral presentations related to the dissertation

- Wörsching, J. (2017). Test-retest reliability of prefrontal tDCS effects on resting-state connectivity in healthy subjects. *2nd European Conference on Brain Stimulation in Psychiatry, Munich, Germany.*
- Wörsching, J. (2017). Test-retest reliability of prefrontal tDCS effects on resting-state connectivity in healthy subjects. *Organization for Human Brain Mapping (OHBM), Vancouver, Canada.*
- Wörsching, J. (2016). Test-retest reliability of prefrontal transcranial Direct Current Stimulation (tDCS) effects on functional MRI connectivity in healthy subjects. *Research Festival, Clinic for Psychiatry and Psychotherapy, LMU, Munich, Germany.*

Poster presentations related to the dissertation

- **Wörsching, J.***, Padberg, F.*, Heinz, I., Bauer, C., Ertl-Wagner, B.., & Keeser, D. (2017). Effects of different prefrontal-tDCS electrode-montages on resting-state connectivity and cognitive control. *2nd European Conference on Brain Stimulation in Psychiatry, Munich, Germany.*
- Eva Mezger, Boris Rauchmann, **Jana Wörsching**, Matin Mortazavi, Andre Brunoni, Birgit Ertl-Wagner, Frank Padberg, Daniel Keeser (2017). Modulation of brain metabolites and resting state functional MRI connectivity by transcranial direct current stimulation (tDCS) over the left dorsolateral prefrontal cortex in healthy subjects. *2nd European Conference on Brain Stimulation in Psychiatry, Munich, Germany.*
- **Wörsching, J.**, Helbich, K., Koch, L., Stoecklein, S., Ertl-Wagner, B., Padberg, F., & Keeser, D. (2017). Test-retest reliability of prefrontal tDCS effects on resting-state connectivity in healthy subjects. *Organization for Human Brain Mapping (OHBM), Vancouver, Canada.*
- **Wörsching, J.**, Helbich, K., Koch, L., Stoecklein, S., Ertl-Wagner, B., Padberg, F., & Keeser, D. (2016). Test-retest reliability of prefrontal transcranial Direct Current Stimulation (tDCS) effects on functional MRI connectivity in healthy subjects. *6th International Conference on Transcranial Brain Stimulation, Göttingen, Germany.*
- Kumpf, U., Nolden, J., Behler, N., Palm, U., Wulf, L., Kirsch, B., **Wörsching, J.**, Keeser, J., Görlitz, T., Mansmann, U., Bajboujc, M., Plewnia, C., Langguth, B., Zwanzger, P., & Padberg, F. (2016). Transcranial Direct Current Stimulation (tDCS) as treatment for major depression – A prospective multicenter double blind randomized placebo controlled trial (DepressionDC) - Analysis of the first technical data from a blind selection of active tDCS sessions. *6th International Conference on Transcranial Brain Stimulation, Göttingen, Germany.*
- **Wörsching, J.**, Padberg, F., Ertl-Wagner, B., Kumpf, U., Kirsch, B., & Keeser, D. (2016). Imaging transcranial direct current stimulation (tDCS) of the prefrontal cortex – Correlation or causality in stimulation-mediated effects? *Research Festival, Clinic for Psychiatry and Psychotherapy, LMU, Munich, Germany.*
- Kumpf, U., Nolden, J., Behler, N., Palm, U., Wulf, L., Kirsch, B., **Wörsching, J.**, Keeser, J., Görlitz, T., Mansmann, U., Bajboujc, M., Plewnia, C., Langguth, B., Zwanzger, P., & Padberg, F. (2016). Transcranial Direct Current Stimulation (tDCS) as treatment for major depression – A prospective multicenter double blind randomized placebo controlled trial (DepressionDC) - Analysis of the first technical data from a blind selection of active tDCS sessions. *Research Festival, Clinic for Psychiatry and Psychotherapy, LMU, Munich, Germany.*
- **Wörsching, J.**, Helbich, K., Kumpf, U., Kirsch, B., Ertl-Wagner, B., Padberg, F., & Keeser, D. (2016). Repeated measure stability of prefrontal transcranial Direct Current Stimulation (tDCS) on functional MRI connectivity in healthy subjects. *Organization for Human Brain Mapping (OHBM), Genf, Switzerland.*

- **Wörsching, J.**, Padberg, F., Ertl-Wagner, B., Kumpf, U., Kirsch, B., & Keeser, D. (2016). Imaging transcranial direct current stimulation (tDCS) of the prefrontal cortex – Correlation or causality in stimulation-mediated effects? *Brain Stimulation and Imaging Meeting, Genf, Switzerland.*
- **Wörsching, J.**, Helbich, K., Hellerhoff, I., Kumpf, U., Kirsch, B., Ertl-Wagner, B., Padberg, F., & Keeser, D. (2015). Repeated measure stability of prefrontal transcranial Direct Current Stimulation (tDCS) on functional MRI connectivity in healthy subjects. *First European meeting for noninvasive brain stimulation techniques (NIBS) for psychiatric disorders, Gent, Belgien.*
- Kumpf, U., Palm, U., Nolden, J., Pfeiffer, A., Egert, S., Görlitz, T., Bajbouj, M., Plewnia, C., Langguth, B., Zwanzger, P., Kirsch, B., **Wörsching, J.**, Mansmann, U., Falkai, P., Keeser, D., Hasan, K., & Padberg, F. (2015). Transcranial Direct Current Stimulation (tDCS) as treatment for major depression – A prospective multicenter double blind randomized placebo controlled trial (DepressionDC). *1st European Conference on Brain Stimulation in Psychiatry, Gent, Belgien.*
- **Wörsching, J.**, Helbich, K., Hellerhoff, I., Kumpf, U., Kirsch, B., Ertl-Wagner, B., Padberg, F., & Keeser, D. (2015). Repeated measure stability of prefrontal transcranial Direct Current Stimulation (tDCS) on functional MRI connectivity in healthy subjects. *Annual Conference on Clinical Neurophysiology and NeuroImaging, Munich, Germany.*
- Helbich, K., **Wörsching, J.**, Hellerhoff, I., Kirsch, B., Kumpf, U., Ertl-Wagner, B., Padberg, F., & Keeser, D. (2015). Repeated measure stability of prefrontal transcranial Direct Current Stimulation (tDCS) on functional MRI connectivity in healthy subjects. *Research Festival, Clinic for Psychiatry and Psychotherapy, LMU, Munich, Germany.*
- **Wörsching, J.**, Heinz, I., Padberg, F., & Keeser, D. (2015). Introducing a novel delayed working memory task with emotional distraction for fMRI studies of the German Center for Brain Stimulation (GCBS). *Research Festival, Clinic for Psychiatry and Psychotherapy, LMU, Munich, Germany.*

Der Arbeitsanteil aller Ko-Autoren wird separat bestätigt und eingereicht zusammen mit der Erklärung zu Punkt A4 der Richtlinien für die kumulative Dissertation an der medizinischen Fakultät der LMU.

Introduction

Transcranial direct current stimulation (tDCS)

Transcranial direct current stimulation (tDCS) is a non-invasive brain-stimulation (NIBS) technique for cortical modulation (Nitsche et al. 2008). The potential of electric currents to influence mental processes has been demonstrated as early as 1800 and was first systematically studied in the 1960s (Bindman et al. 1963; Bindman et al. 1962; Creutzfeldt et al. 1962; Purpura and McMurtry 1965). Despite positive findings in the 1960s and 1970s, including clinical studies, the technique has been largely abandoned due to its mixed findings, negative repercussion of electro-convulsive therapy (ECT) and advances of pharmacotherapy and, later on, repetitive transcranial magnetic stimulation (TMS). Almost two decades ago, non-invasive transcranial current stimulation was reintroduced as tDCS in clinical neurophysiology (Nitsche and Paulus 2000; Priori et al. 1998) and since then meets increasing interest among neuroscientists and clinical practitioners (Bestmann et al. 2015; Dubljevic et al. 2014).

Action mechanisms of tDCS – a mechanistic view

Direct electrical currents can be passed through the skull via two surface electrodes (Datta et al. 2009) – usually 5x5 or 5x7 cm^2 – one of which is of positive (anode) and the other one of negative (cathode) polarity (Edwards et al. 2013; Miranda et al. 2006). The intensity of the electrical current can be determined by the voltage between both electrodes divided by the total resistance through the head/body from one electrode to the other (Ohm's law). However, because most of the current is attenuated by the skin, skull, and cerebrospinal fluid (Miranda et al. 2006; Zaghi et al. 2010), the electrical current reaching the brain parenchyma comprises only a fraction of the originally applied intensity (Wagner et al. 2007). Overall, electrical currents ranging between 1

to 3 milliampere (mA) intensity for up to 60 minutes (min) per day are utilised (Bikson et al. 2016; Nitsche, Liebetanz, Antal, et al. 2003) and within this range can be categorised as weak, safe (Iyer et al. 2005; Antal et al. 2017; Palm et al. 2017; Nitsche, Liebetanz, Lang, et al. 2003) and subthreshold, i.e. non action-potential releasing (Nitsche et al. 2008). While the current is flowing from the anodal to the cathodal pole, electrical charge is moving the opposite direction. Thereby, apical dendrites in close vicinity to the anodal pole are assumed to be shifted towards hyperpolarisation, while the soma of the respective cells may be directed towards depolarisation. For cathodal stimulation, i.e. cells receiving influences from the cathodal pole, hyper- and depolarised cell compartments may be reversed (see Figure 1). This concept of bipolar polarisation in an electric field (Bikson et al. 2004) especially applies to columns of pyramidal neurons, for which the current is flowing in parallel to the neuron axis (Radman, Ramos, et al. 2009). In case of electric fields perpendicular to a column, synaptic efficacy between pyramidal neurons and inter-neurons may be modulated consistent with the concept of terminal depolarisation (Rahman et al. 2013). As already mentioned, excitability changes are subthreshold: intracellular recordings have shown that the shift in membrane potential within pyramidal neurons induced by direct current

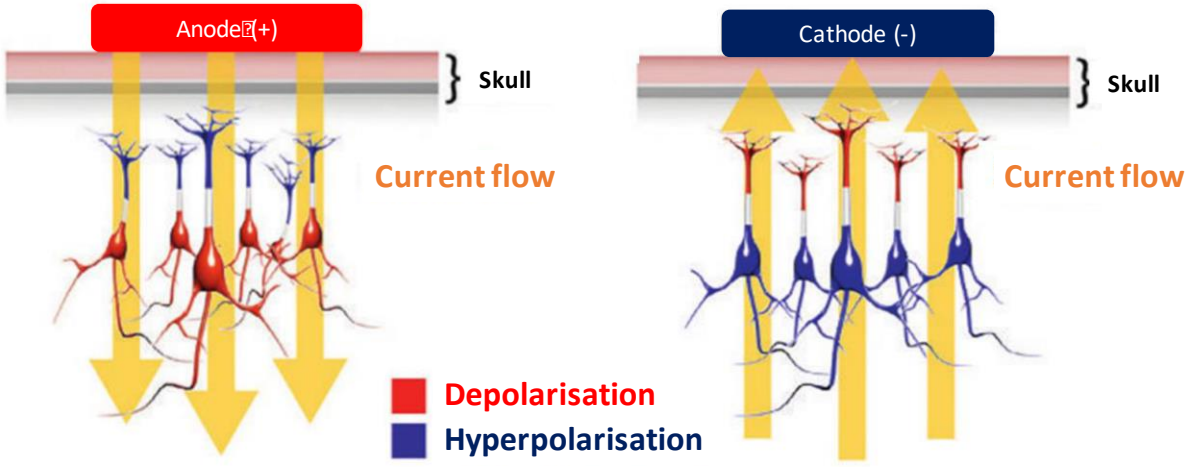

Figure 1. Action mechanisms of tDCS in the cortex beyond the anode and cathode.

Adapted from Moreno-Duarte et al. (2014)

stimulation does not exceed 0.3 mV (Bikson et al. 2004; Radman, Datta, et al. 2009). As a result, depending on the stimulation polarity, the cell's resting membrane-potential may be moved towards a more positive or negative charge, which, in turn, increases or decreases the probability of spontaneous neural firing (Wagner et al. 2007).

In line with this model, polarity-dependent excitatory or inhibitory effects of tDCS on neurophysiological parameters have been shown (see Figure 2). Following anodal tDCS over the motor cortex M1 with an intensity of up to 1 mA and a duration of 5-10 min, an increase in TMS-evoked motor-evoked potentials (MEP) could be observed (Nitsche and Paulus 2001, 2000), as compared to pre-tDCS MEPs. In contrast, MEP amplitudes decreased when the cathode was placed over the relevant cortical region (Nitsche, Nitsche, et al. 2003; Nitsche and Paulus 2000). Both mechanisms were found to be dependent on the stimulation duration in a linear way in these earlier studies (Nitsche, Nitsche, et al. 2003; Nitsche and Paulus 2001).

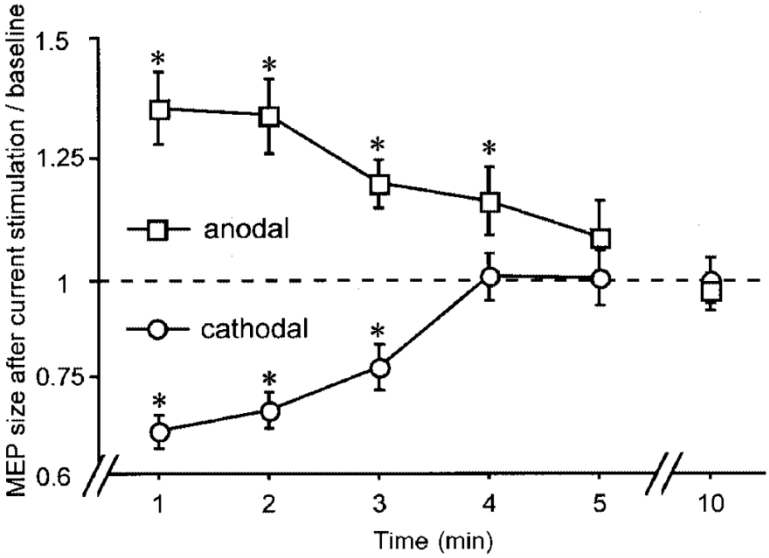

Figure 2. Polarity-specific excitability changes induced by tDCS. Excitability was measured as changes in TMS-evoked MEP amplitudes (y-axes). TDCS was applied for 5 min with 1 mA over M1 with either anodal or cathodal polarity. Asterisks indicate significant differences between MEP amplitudes after tDCS as compared to baseline. TDCS-effects on MEP amplitudes disappeared within 5 min.

Adapted from Nitsche and Paulus (2000)

Dose parameters of tDCS – non-linear relations and variability

While many motor-cortex tDCS-studies provide support for the hypothesis of electrode-specific subthreshold modulations of resting-membrane potentials (Been et al. 2007; Edwards et al. 1993; Nitsche et al. 2008; Nitsche and Paulus 2000, 2001; Paulus 2004), the direction of tDCS-induced neuromodulation and even the effectiveness of tDCS has been found to rely on selected stimulation parameters in a non-linear way (Batsikadze et al. 2013; Benwell et al. 2015; Brunoni, Ferrucci, et al. 2013; Hoy et al. 2013; Jacobson et al. 2012; Monte-Silva et al. 2013; Teo et al. 2011). For example, anodal tDCS over M1 with an intensity of 1 mA and a duration of 26 min led to a reduction of cortical excitability (Monte-Silva et al. 2013), arguing against dichotomous excitation versus inhibition assumptions. Beyond, using an intensity of 2 mA, cathodal M1-stimulation resulted in an MEP-amplitude increase (Batsikadze et al. 2013) and pharmacological studies show that drugs can change the direction of the effects (Nitsche, Fricke, et al. 2003).

In general, stimulation parameters such as current intensity (Nitsche and Paulus 2000), electrode size (Wagner et al. 2007), duration of stimulation (Nitsche et al. 2008; Nitsche and Paulus 2001), number of treatment sessions (Nitsche, Liebetanz, Antal, et al. 2003; Nitsche and Paulus 2000, 2001), the interval between sessions (Monte-Silva et al. 2013) and electrode montage may interact with each other and influence the final outcome as well as the duration of post-stimulation effects.

With regard to electrode placement, computational models suggest that even small displacements of 1 cm may affect both the distribution of the electric field across the brain as well as the peak electric-field intensity in the brain (Woods et al. 2015). This was also shown behaviourally: In a study by Ironside et al. (2016), anodal-F3 and

cathodal-F4, but not anodal-F3 and cathodal-Fp2 tDCS was associated with reduced vigilance to threatening stimuli in healthy subjects.

In this context, the relative distance of the cathode with respect to the anode is also important, because it determines the amount of current reaching brain tissue (Datta et al. 2011; Miranda et al. 2006; Weaver et al. 1976), electric field intensity within the region of interest (Bai et al. 2014; Datta et al. 2011; Galletta et al. 2015) and the pattern of current flow, i.e. brain areas stimulated (Bai et al. 2014; Galletta et al. 2015). Therefore, inconsistent and unprecise electrode positioning may have a significant impact on mode of action and stresses the need for comparable electrode montages across studies and standardised positioning systems (Seibt et al. 2015). However, even with a standardised electrode montage and constant other stimulation parameters, inter- and intra-individual variations in response patterns can be observed (Strube et al. 2016; Chew et al. 2015). Sources of inter-individual variability may arise from differences in head anatomy (skull structure and brain anatomy) (Datta et al. 2011) as well as in structural and functional connections (Rosso et al. 2014). For example, individual anatomical differences may affect current-density clustering (Bai et al. 2014), such that the electric current does not necessarily peak under the electrode of interest (Datta et al. 2009; Dmochowski et al. 2011; Dmochowski et al. 2013). This was also demonstrated for common parameters such as age (Kessler et al. 2013; Laakso et al. 2015), gender (Russell et al. 2014; Russell et al. 2017) and obesity (Truong et al. 2013).

To conclude, in the parameter space, dose-response relations are not linear, and direction of effects clearly varies between studies, between individuals, and even within individuals. Possible explanations for the inconsistency may be variability induced by divergent stimulation parameters but also genuine variability arising from anatomical differences and intra-individual distinct response patterns. Taken together, these

findings indicate high inter- and intra-individual variability of tDCS responses at varying current intensities and thereby challenge the test-retest (TRT) reliability of this method (Chew et al. 2015; Dyke et al. 2016; Horvath et al. 2016; Lopez-Alonso et al. 2014; Lopez-Alonso et al. 2015).

Levels of monitoring tDCS effects and multiparametric assessment

Discrepant findings, i.e. dissenting tDCS effects between studies, may also arise from the selection of outcome measures. Effects of tDCS can be monitored at different levels, comprising behavioural (performance in a task, scores of questionnaires), clinical (symptom reduction), neurophysiological (MEPs, electro-encephalography) or neuroimaging (structural and functional magnetic resonance imaging [MRI], magnetic resonance spectroscopy, positron emission tomography) assessments. Neurophysiological and neuroimaging methods can be further divided into task-dependent or resting-state (RS) recordings. Because excitability changes are subthreshold, tDCS provides an indirect or correlative approach that relies on statistical relations between experimental conditions and outcome criteria. Therefore, tDCS studies may benefit from multiparametric assessment: if different outcome criteria are accumulated, evidence from different sources can be compared and merged, thus increasing the explanatory power of a study (see Figure 3). Such an approach would further allow for investigations into state-dependencies of tDCS-mediated effects (Gozenman and Berryhill 2016; Heinen et al. 2016; Hsu et al. 2016; Learmonth et al. 2015; Looi et al. 2016; Monte-Silva et al. 2010; Tseng et al. 2016; Tseng et al. 2012), i.e. how tDCS-induced RS-modulations relate to tDCS effects on task-based data. While the RS represents a chaotic and less controllable condition, a task may ensure a relatively stable state across and within individuals. Possibly, tDCS only acts at a certain cognitive load, i.e. tDCS-induced subtle neuronal excitability changes require

some amount of pre-existing activity within neurons or neuronal networks to exert a measurable behavioural or neurophysiological effect. Consequently, the induced baseline activity may have a significant impact on reproducibility of tDCS effects.

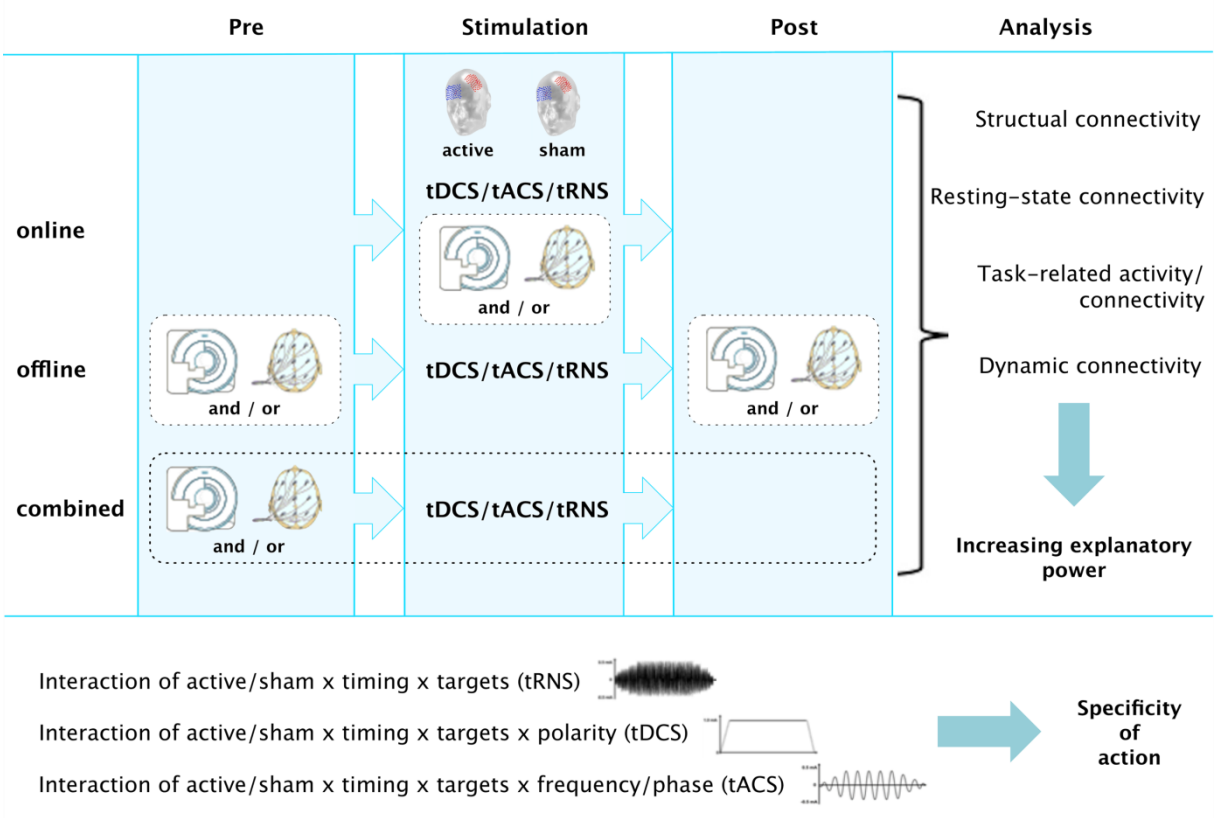

Figure 3. Different combinations of NIBS with functional MRI and/or EEG, considering different stimulation factors: stimulation condition (sham/active), timing of recording with respect to stimulation (online/offline/combined), targets (number of different electrode montages), polarity (anodal/cathodal, only for tDCS), and frequency/phase (only for tACS). Note: EEG = Electro-encephalography, tACS = transcranial alternating current stimulation, tRNS = transcranial random noise stimulation.

Adapted from Wörsching et al. (2016)

Specificity of tDCS effects

In addition to multiparametric assessment, tDCS studies further stand to benefit from systematic variations of the experimental-design parameters, i.e. the independent variables.

For example, the temporal coherence between stimulation and the recording of outcome measures is variable. Behavioural and physiological effects can be logged at different temporal scales, potentially influencing the strength and direction of

psychometric outcomes (Nitsche et al. 2005; Ohn et al. 2008): offline, i.e. after the stimulation period, or online, i.e. during the stimulation (see Figure 3). In order to trace the formation of tDCS-induced changes as well as tDCS after-effects, both online and offline recordings should be incorporated into a tDCS study.

Likewise, the general design of tDCS studies in terms of control and comparator conditions should be considered. Different conditions potentially allow demonstration of specificity of an effect by means of analysis of interactions between those conditions (e.g. active versus sham) and outcome criteria. If montage specificity is given, i.e. other montages produce no, considerably less or qualitatively different effects for the variable under study, a direct effect of tDCS on that variable can be accepted with a high level of certainty. Therefore, effects should be related to a specific interaction in the experimental design (see Figure 3).

In general, specificity of stimulation action can be demonstrated in space (e.g. electrode montages and polarity), time (e.g. online, offline, combined), and function (e.g. behavioural or neurophysiological measures). Theoretically, such specificity needs to be demonstrated for each single outcome variable (i.e. behavioural and neurophysiological). Unfortunately, the use of the above-mentioned design parameters varies considerably, leading to heterogeneous results, impaired reproducibility, less meaningful conclusions and reduced comparability between studies (for review see Worsching et al. 2016).

The prefrontal cortex as target for tDCS

One of the major advantages of motor-cortex assessment is the direct measurable output (MEPs), for which reason early research on tDCS mainly concentrated on stimulation of this region (Stagg and Nitsche 2011; Utz et al. 2010). More recently, regions other than M1, e.g. the prefrontal cortex (PFC), became of major interest in an effort to modulate more complex neuronal systems. So far, tDCS applied to non-motor cortex regions has been shown to have an effect on sensory (visual and somatosensory), affective, and cognitive functions (for review see Been et al. 2007), whereby visual stimulation resembles more motor than prefrontal stimulation as TMS-evoked phosphines are – like MEPs for M1 – a direct measurable outcome of this area.

Relevance of prefrontal tDCS: Field of application

The PFC subserves most cognitive functions and therefore can be considered a key target region in basic neuroscience and clinical research. On the one hand, prefrontal tDCS can be used to further elucidate the functional role of certain brain regions for a specific cognitive process (for review see Filmer et al. 2014). Accordingly, the effects of prefrontal tDCS on various cognitive domains have been studied in healthy volunteers (for review see Tremblay et al. 2014), including learning and automaticity (motor and categorisation learning), memory (working memory [WM], long-term memory, episodic, and declarative memory), decision making, mood, attention/vigilance, language, executive functions (problem solving, mental flexibility, inhibition, planning, impulsivity), emotion processing and regulation, semantic processing (language comprehension and naming, processing of action, congruence detection), verbal fluency, pain perception, social behaviours, food craving, and risk taking.

Because many of these cognitive domains are impaired in neurological and psychiatric diseases, which in turn are associated with prefrontal dysfunctions (for review see Flöel 2014; Kuo et al. 2014), on the other hand, prefrontal montages also provide an avenue for future development of tDCS towards a therapeutic application. So far, clinical benefits of prefrontal tDCS have been tested in patients with disorders of consciousness (Thibaut et al. 2014), chronic pain (Arul-Anandam et al. 2009; Valle et al. 2009), Parkinson's disease (Boggio et al. 2006; Fregni et al. 2006), major depression (MD) (Brunoni et al. 2017; Brunoni, Valiengo, et al. 2013), schizophrenia (Barr et al. 2012; Brunelin et al. 2012; Fitzgerald et al. 2014; Nawani et al. 2014; Vercammen et al. 2011), craving (Boggio et al. 2009; Boggio et al. 2008; Conti and Nakamura-Palacios 2014; da Silva et al. 2013; Nakamura-Palacios et al. 2012), attention deficit hyperactivity disorder (Prehn-Kristensen et al. 2014) and tinnitus (Frank et al. 2012; Vanneste and De Ridder 2011; Vanneste et al. 2011; Vanneste et al. 2010). Especially, in large samples of MD patients, prefrontal tDCS has been shown to be effective (Brunoni et al. 2017; Brunoni, Valiengo, et al. 2013).

In sum, a multitude of studies have described the application of prefrontal tDCS in various research fields dedicated to higher-order cognitive processes, such as memory and attention. At the same time, as demonstrated by clinical trials, prefrontal tDCS holds great potential as a therapeutic intervention. Anatomically targeted analyses of NIBS methods, including tDCS, in neuropsychiatric disorders have generated promising results (Fox et al. 2014; Fox et al. 2012) and meta-analyses show its potential to improves cognitive outcomes (Dedoncker et al. 2016). On the contrary, others question its efficacy (Horvath et al. 2015; Tremblay et al. 2014). The mixed outcomes may be caused by the heterogeneous effects of tDCS. To evaluate tDCS as a therapeutic tool its underlying mechanisms and effectiveness needs to be systematically investigated with respect to its specificity of action and explanatory

power. Studies of prefrontal tDCS in a clinical setting that used both clinical and neurophysiological information as outcome measures are rare and included heterogeneous patient groups (for overview see Table 1; Cavaliere et al. 2016; Meinzer et al. 2015; Palm et al. 2013; Palm et al. 2016; Sotnikova et al. 2017; Volpato et al. 2013; Yang et al. 2017).

Study	Target Measure(s)	Assessment	Condition(s) & Polarity*	Design	*n*	Targets**		Current [mA] / Duration [min]	Specific Interaction***
						1st electrode	2nd electrode		
Meinzer et al. (2015)	• RS fMRI • task fMRI • semantic-word retrieval	online	anodal tDCS sham tDCS	crossover double-blind	18 (MCI patients) 18 (matched HCs)	left ventral IFG (intersection of T3-F3, F7-C3, and F7-F3)	right supra-orbital region	1 / 20	active/sham x timing x target
		during sham: MCI patients > HCs: ↓ correct responses + widespread functional connectivity changes including medial frontal and lateral fronto-temporal cortices, bilateral sensorimotor regions, and right cerebellum; during tDCS > during sham: MCI patients ↑ performance to level of HCs + reversal of abnormal connectivity pattern; during tDCS for patients > sham for HCs: comparable connectivity patterns → "normalisation" in patients							
Palm et al. (2013)	• RS fMRI • clinical scales	offline	anodal tDCS		1 (patient with paranoid schizophrenia)	left DLPFC (F3)	right supra-deltoid area	2 / 20 (twice a day on 10 weekdays)	timing x target
	Results	post tDCS > pre tDCS: improvement in psychopathology + ↓ functional connectivity in anterior part of DMN							
Volpato et al. (2013)	• RS fMRI • psychopathological symptoms (clinical scales)	offline	cathodal tDCS sham tDCS	crossover	1 (patient with severe OCD and comorbid mood and anxiety disorders)	left DLFPC (F3)	posterior neck-base	2 / 10 (5 sessions for each condition)	active/sham x timing x target
	Results	baseline > controls: interhemispheric asymmetry with hyperactivation of the left and hypoactivation of the right anterior neural circuits; post tDCS > pre tDCS: no effect on OC symptoms, ↓ depression and anxiety + ↓ of interhemispheric imbalance							

Study	Target Measure(s)	Assessment	Condition(s) & Polarity*	Design	*n*	Targets**		Current [mA] / Duration [min]	Specific Interaction***
						1st electrode	2nd electrode		
Palm et al. (2016)	• RS fMRI • clinical outcomes	offline	anodal tDCS sham tDCS	parallel	16 (sub-sample) patients with paranoid schizophrenia or disorganised schizophrenia	left DLFPC (F3)	right orbitofrontal region (Fp2)	2 / 20 (on 10 days within 2 weeks)	active/sham x timing x target
	Results	(post 1st/10th tDCS > pre 1st/10th tDCS) > (post 1st/10th sham > 1st/10thpre sham): changes in seed-based functional connectivity (left and right DLPFC, left and right subgenual regions and the left insula); post tDCS > post sham: ↑ clinical improvements							
Sotnikova et al. (2016)	• RS fMRI • task fMRI • WM: 1-, 2-back	combined	anodal tDCS sham tDCS	crossover double-blind	16 adolescent ADHD patients	left DLPFC (F3)	Cz	1 / 20	active/sham x timing x target
	Results	during tDCS > during sham: ↑ activity in left DLPFC (under the electrode), left premotor cortex, left supplementary motor cortex and precuneus + more omission errors and less accuracy post tDCS > post sham: ↑ functional connectivity DLPFC seed – regions associated with WM functions							
Cavaliere et al. 2016	• task fMRI (4 sessions) • clinical assessment (evaluation of responses to tDCS)	offline (pre only)	anodal tDCS sham tDCS	crossover double blind	16 patients in subacute and chronic MCS → divided into responders and non-responders to tDCS	left DLPFC (F3)	right supra-orbital region	2 / 20	active/sham x timing x target
	Results	responders > non-responders: ↑ functional connectivity DLPFC – left IFG							

Study	Target Measure(s)	Assessment	Condition(s) & Polarity*	Design	*n*	Targets**		Current [mA] / Duration [min]	Specific Interaction***
						1st electrode	2nd electrode		
Yang et al. 2017	• RS fMRI • task fMRI • smoking cue reactivity & emotion task	offline (post only)	anodal tDCS sham tDCS	crossover double blind	32 male chronic smokers	left DLPFC (F3)	right DLPFC (F4)	1 / 30	active/sham x timing x target
	Results	post tDCS > post sham: ↓ craving during cue-reactivity task, ↓ activity in left superior frontal gyrus and left middle frontal gyrus during to smoking cues, ↑ functional connectivity left DLPFC – right parahippocampal gyrus → coupling correlated with craving change							

Table 1. Studies investigating prefrontal tDCS effects on RS connectivity in neuropsychiatric disorders using functional-imaging methods. Note: ADHD = attention deficit hyperactive disorder, Exp. = Experiment, HC = healthy control, IFG = inferior frontal gyrus, MCI = mild cognitive impairment, MCS = minimally conscious state, n = sample, OCD = obsessive compulsive disorder, ↑ = increase. ↓ = decrease.

* Polarity = tDCS condition according to the main hypothesis of the respective study (e.g. in a study investigating the main effect of anodal tDCS on verbal fluency the condition is described as “anodal tDCS/sham tDCS”).

** Targets = electrode montages, 1st and 2nd electrode = terms to indicate where the anodal and cathodal stimulation electrode is placed by referring to the given stimulation polarity (i.e. for anodal stimulation, the anode refers to the first electrode, for cathodal stimulation, the cathode refers to the first electrode).

*** Specific interaction = see Fig. 3.

Specificity of action: Electrode montages for prefrontal tDCS

For tDCS, diverse electrode-positioning methods are available and can be categorised into mono- or extra-cephalic versus (bi-)cephalic settings with the latter being further divisible into unilateral versus bilateral montages. In prefrontal settings, tDCS is typically applied bilaterally with either both electrodes placed on the right and left prefrontal hemispheres in a balanced manner, or the cathode or anode placed above the prefrontal region of interest and the other electrode located at a different region (e.g. supraorbital) on the contralateral hemisphere, i.e. in an un-balanced manner (see Figure 4). Extra-cephalic electrode-placements, in which the electrode of interest is put above the left or right PFC (e.g. F3 or F4) and the remaining electrode on another part of the body, e.g. the contralateral shoulder, are also used (Brunoni et al. 2012; Plewnia et al. 2015; Nasseri et al. 2015). Because there is no consensus in terms of suitable prefrontal stimulation-montages for a certain variable under study, most findings are likely to be a function of the stimulation parameters and monitoring levels at hand (for review see Worsching et al. 2016). Therefore, awareness should be raised for this drawback and systematic evaluations of prefrontal montages, i.e. reversing and changing the electrode arrangement with a proven value for the variable of interest, are warranted with the objective of identifying the most effective target location.

Monitoring levels: Imaging prefrontal tDCS

Application of stimulation currents to the PFC aims at enhancing higher-order cognitive processes. According to computational models, standard electrode montages for prefrontal tDCS, such as dorsolateral-PFC(DLPFC)-targeted montages (EEG 10–20 system: F3-F4 or F3-Fp2), were found to be suitable for effective stimulation of the

target area (Bai et al. 2014; DaSilva et al. 2015; Datta et al. 2011; Nelson et al. 2014; Neuling et al. 2012).

However, the neurophysiological response to tDCS and its methodological underpinnings are still not completely understood (Parkin et al. 2015). In combination with neuroimaging techniques such as functional MRI (fMRI), the mechanisms behind tDCS-modulated neural integration may be elucidated. MRI-compatible stimulation-systems are available, enabling the combination of tDCS with online neurophysiological measurements. This setup could inform in more detail about the temporal resolution of the method – i.e. the starting point at which and the length of time for which tDCS influences cortical processing. Moreover, besides investigations of tDCS-related plasticity, combined tDCS-fMRI can be used to demonstrate a link between a brain region and a cognitive process and to investigate the functional interactions between different brain areas. Finally, neurophysiological paradigms provide the advantage of specifically targeting and adjusting this method to physiological requirements, entailing state-dependencies (Benwell et al. 2015; Gozenman and Berryhill 2016; Hoy et al. 2013; Hsu et al. 2016; Learmonth et al. 2015; Looi et al. 2016; Tseng et al. 2016; Tseng et al. 2012). For a therapeutic application, state-related tDCS-outcomes may further inform about potential influences of different disorders and courses on the efficacy of this method. The optimal timing and setting of application – i.e. whether tDCS is most effective at prodromal or acute stages and whether tDCS should be applied during a relaxed or a cognitive demanding state such as learning processes activated during psychotherapeutic sessions – may be deduced from these data.

Effects of prefrontal tDCS on resting-state connectivity

Though RS-fMRI paradigms stand in contrast to cognitive demanding processes, RS networks (RSN) have been shown to be highly relevant for behaviour (Laird et al. 2011). For example, the magnitude of frontal-parietal RS-connectivity was positively associated with WM performance (Laird et al. 2011). Moreover, the most prominent RSNs conform to structurally defined networks and hubs (van den Heuvel and Hulshoff Pol 2010; van den Heuvel and Sporns 2013). Consequently, RS conditions allow for investigations of network effects of prefrontal stimulation (Fox et al. 2014) as a result of existing inter-regional connections, which may have behavioural implications in the absence of any task, providing an easily accomplishable study design. Moreover, RSNs have the advantage of being reliably reproducible across (Biswal et al. 2010; Iwabuchi et al. 2015; Kaiser et al. 2015) and within subjects (Finn et al. 2015; Mueller et al. 2013). For this reason, the impact of prefrontal tDCS on RSNs may entail important information about the specific mechanisms of action of this method. Several studies have investigated prefrontal-tDCS effects on RS-fMRI connectivity in healthy subjects by comparing RSN configurations and other functional couplings before and after stimulation (Keeser et al. 2011; Stagg et al. 2013; Meinzer et al. 2012; Meinzer et al. 2013; Park et al. 2013; Pena-Gomez et al. 2012; Weber et al. 2014). Overall, reported changes in RS connectivity following anodal tDCS may be evidence of a state reflecting enhanced alertness and improved information processing (for an overview see Table 2 and Worsching et al. 2016) and thereby add to the M1 literature. However, although changes in RS-fMRI connectivity observed after prefrontal tDCS support the assumption of polarity-specific excitability modulations, a causal link between the intervention and the outcome measure should not be established based on these studies being inconsistent in terms of stimulation and recording parameters. First, non-

standardized prefrontal electrode-positioning is used. Not only the prefrontal montage itself vary from balanced to unbalanced bi-cephalic settings (e.g. Keeser et al. 2011; Weber et al. 2014), but also the final target regions within the PFC differ, very often covering parts of the DLPFC (Keeser et al. 2011; Park et al. 2013; Pena-Gomez et al. 2012; Stagg et al. 2013; Weber et al. 2014) as well as the inferior frontal cortex in some cases (Meinzer et al. 2012; Meinzer et al. 2013). Secondly, studies differ in whether they apply tDCS offline (Keeser et al. 2011; Park et al. 2013; Pena-Gomez et al. 2012; Stagg et al. 2013) or online (Meinzer et al. 2012; Meinzer et al. 2013; Stagg et al. 2013). Finally, the studies do not vary the experimental conditions to the extent required to demonstrate specific relations between tDCS and its neurophysiological effects. Control conditions are not always conducted within the same individuals (Park et al. 2013; Stagg et al. 2013; Weber et al. 2014) and the advantage of comparator conditions is only rarely exploited (Pena-Gomez et al. 2012; Stagg et al. 2013). Given the lack of both comparability across and parameter variants within studies, specificity of action, such as polarity-dependence, cannot be taken for granted. Inconsistencies and incompleteness in the design of studies investigating tDCS-induced modulations in RS-fMRI sequences, are potentially reflected in discrepant findings, such as increased (Keeser et al. 2011) versus decreased default mode network (DMN) functional-connectivity (Pena-Gomez et al. 2012) after anodal tDCS of the left and concomitant cathodal tDCS of the contralateral supraorbital region as well as local, i.e. in close vicinity to the electrode (Keeser et al. 2011; Meinzer et al. 2012; Park et al. 2013) versus global effects, i.e. widespread RS changes (Keeser et al. 2011; Meinzer et al. 2013; Pena-Gomez et al. 2012; Stagg et al. 2013; Weber et al. 2014).

Study	Target Measure(s)	Assessment	Condition(s) & Polarity*	Design	*n*	Targets**		Current [mA] / Duration [min]	Specific Interaction***
						1st electrode	2nd electrode		
Keeser et al. (2011)	RS fMRI	offline	anodal tDCS sham tDCS	crossover double blind	13	left DLPFC (F3)	right supraorbital region	2 / 20	active/sham x timing x target
	Results	(post > pre tDCS) > (post > pre sham): ↑ coactivation in frontal parts of the DMN, parts of the left and right FPN, right PCC + ↑ coactivation outside RSNs within anodal ROI in frontal gyrus							
Pena-Gomez et al. (2012)	RS fMRI	offline (post only)	anodal tDCS sham tDCS	crossover	10	• left DLPFC (F3) • right DLPFC (F4)	contralateral supraorbital region	2 / 20	active/sham x timing x targets (1st and 2nd)
	Results	post tDCS (left and right) > post sham: ↑ functional connectivity prefrontal – parietal regions (, which are components of the AN) + ↓ spatial robustness of DMN							
Park et al. (2013)	RS fMRI	offline	anodal tDCS sham tDCS	parallel	25 + 14	left DLPFC (F3)	right supraorbital region	1 / 20	active/sham x timing x target
	Results	(post - pre tDCS) > (post - pre sham): ↑ functional connectivity DLPFC – right hemisphere + ↓ functional connectivity DLPFC – brain regions around the stimulation site in left hemisphere							
Stagg et al. (2013)	brain perfusion using ASL	combined	Exp. 1: anodal tDCS cathodal tDCS Exp. 2: sham tDCS	crossover (polarity) + parallel (condition)	12 for each Exp.	left DLPFC (F3)	right supraorbital region	1 / 20	active/sham x timing x target x polarity
	Results	during anodal tDCS > pre tDCS: ↑ functional connectivity left DLPF - right DLPFC and left sensorimotor cortex + ↓ functional connectivity left DLPFC - thalami bilaterally, brain stem, and cerebellum; post anodal tDCS > pre tDCS: ↑ functional connectivity left DLPFC – primary sensorimotor cortices bilaterally							

Study	Target Measure(s)	Assessment	Condition(s) & Polarity*	Design	*n*	Targets**		Current [mA] / Duration [min]	Specific Interaction***
						1st electrode	2nd electrode		
Meinzer et al. (2012)	• RS fMRI • task fMRI • semantic word-retrieval	online	anodal tDCS sham tDCS	crossover	20	left ventral IFG (intersection of T3-F3, F7-C3, and F7-F3)	right supraorbital region	1 / 17	active/sham x timing x target
	Results	during tDCS > during sham: ↑ functional connectivity of left IFG and hubs overlapping with language network							
Meinzer et al. (2013)	• RS fMRI • task fMRI • semantic word-retrieval	online	anodal tDCS sham tDCS	crossover	20 (healthy elderly adults) 20 (matched younger adults)	left ventral IFG (intersection of T3-F3, F7-C3, and F7-F3)	right supraorbital region	1 / 20	active/sham x timing x target
	Results	during tDCS > during sham: more “youth-like” connectivity-pattern during RS fMRI							
Weber et al. (2014)	• RS fMRI (ASL) • task fMRI • Balloon Analog Risk Task	offline	anodal tDCS sham tDCS	parallel	22 + 11	right DLPFC (F4)	left DLPFC (F3)	1.5 / 15	active/sham x timing x target
	Results	(post - pre tDCS) > (post - pre sham): ↓ functional connectivity right ACC – rest of brain							

Table 2. Studies investigating prefrontal tDCS effects on RS connectivity using functional-imaging methods. Note: ACC = anterior cingulate cortex, AN = attention network, ASL = arterial spin labelling, Exp. = Experiment, FPN = frontal parietal network, IFG = inferior frontal gyrus, n = sample, PCC = posterior cingulate cortex, ROI = region of interest, ↑ = increase. ↓ = decrease.

* Polarity = tDCS condition according to the main hypothesis of the respective study (e.g. in a study investigating the main effect of anodal tDCS on verbal fluency the condition is described as “anodal tDCS/sham tDCS”).

** Targets = electrode montages, 1st and 2nd electrode = terms to indicate where the anodal and cathodal stimulation electrode is placed by referring to the given stimulation polarity (i.e. for anodal stimulation, the anode refers to the first electrode, for cathodal stimulation, the cathode refers to the first electrode).

*** Specific interaction = see Fig. 1.

Research questions of the dissertation: Test-retest reliability and different electrode montages

Among NIBS techniques, tDCS is a particularly interesting method for modulating cortical excitability. The technology is easily applicable, appears to be rather safe and can be widely used in experimental and clinical settings (e.g. online combined with neuroimaging in neuroscience or clinically for treatment of psychiatric disorders in outpatient departments or even at home). The DLPFC is a promising target for tDCS in clinical applications and in combination with neuroimaging may advance research on plasticity in cognitive relevant neural systems and circuits. Because underlying mechanisms upon which tDCS exerts its effect are widely unknown, it is advantageous to investigate prefrontal tDCS-effects at a neurophysiological level. In this context, considering its behavioural relevance, stability, and relatively easy practicability, the RS is a neurophysiological outcome measure of particular interest for measuring prefrontal tDCS-effects. Recently, both TRT reliability of tDCS effects as well as the classical anodal-increase and cathodal-decrease assumption have been questioned. In addition, inter-individual variations in and state-dependencies of tDCS responses have been found. Yet, none of these issues have been systematically evaluated for tDCS-induced modulations in RS fMRI. Given the potential clinical relevance of prefrontal tDCS, and the need for better understanding the neurophysiological underpinnings of its effects, our aim was to

1. explore whether effects of prefrontal tDCS on RS-fMRI connectivity are reliable across different measurements within the same subjects.
2. test the effects of three common bifrontal tDCS-montages vs. sham on RS fMRI.

In consideration of moderate to good reliability of RSNs, for the first study, we hypothesised that the TRT reliability of prefrontal tDCS-effects as measured with RS-fMRI is moderate to good.

Based on classical assumptions derived from motor-cortex studies, for the second study, we hypothesised that observed effects follow polarity-specific directions, i.e. an anodal-tDCS associated increase and a cathodal-tDCS associated decrease in RS-fMRI connectivity.

Summary

TDCS is a NIBS technique widely applied in experimental and clinical research. While early research on tDCS mainly concentrated on the motor cortex M1, electrode montages are also increasingly motivated by upcoming clinical applications. Especially, the PFC may be a promising stimulation target for a therapeutic application in psychiatric disorders. However, studies using prefrontal stimulation face several shortcomings requiring basic methodological and systematic research based on neurophysiology measures to elucidate its neural underpinnings.

Because the TRT reliability of tDCS regarding its effects on motor-cortex excitability has recently been questioned, we first investigated the TRT reliability of prefrontal-tDCS-induced modulations in RS fMRI. In a between-subject design, 20 subjects were randomised to two groups (active versus sham) and underwent three testing sessions at one-week intervals, based on the same protocol: baseline RS-fMRI (10 min), active or sham stimulation (F3-F4, 2 mA, 20 min), post-tDCS RS-fMRI (10 min). To evaluate the TRT reliability, voxel-wise intra-class correlation-coefficients (ICC) of RS-connectivity maps were calculated across testing sessions, separately for each measure (baseline and post-tDCS) and group (active versus sham). Results revealed low to moderate ICCs at baseline levels independent of the group. However, for post-tDCS measures, ICCs were shifted to lower TRT reliability after active, but not after sham tDCS. When comparing our results to current literature, a discrepancy between previously reported moderate to good reliability for RS connectivity and low to moderate reliability of our baseline-RS measures becomes evident, which may arise from the small sample size of this study. Nevertheless, the drop of reliability from baseline to post-tDCS, which arose in the active but not sham group, argues for additional variability induced by tDCS. The assumption that tDCS effects are highly

variable at the individual level is consistent with available data showing high intra-individual variability of tDCS effects in motor regions.

To test assumptions on polarity-dependent directions and localisations of tDCS effects derived from motor-cortex studies, in a second empirical study, we investigated the influence of different prefrontal electrode-montages on RS fMRI. Within a cross-over design, 32 healthy male subjects underwent four testing sessions at one-week intervals, differing only with respect to the tDCS condition. The tDCS conditions comprised three active tDCS sessions (common bicephalic electrode-montages for DLPFC stimulation, 2 mA, 20 min) and sham tDCS, were presented in a pseudo-randomised order and always preceded as well as ensued by a RS-fMRI scan. Individual RS-connectivity maps were compared across stimulation conditions by means of a one-way repeated-measures ANOVA. Following cathodal tDCS of the left (F3) and concomitant anodal tDCS of the right DLPFC (F4), results indicated both a regional reduction in RS functional-connectivity within the left medial PFC and a regional increase in RS functional-connectivity within the DLPFC bilaterally. Whereas several previous studies have claimed an anodal-induced increase and a cathodal-related decrease of cortical excitability, the current study provides evidence for more complex electrode-montage-specific effects of tDCS.

Altogether, these results support the notion that tDCS modulates RS-fMRI connectivity and thereby justify prefrontal tDCS as a feasible tool in cognitive neuroscience and emphasise its potential in clinical practice, such as the treatment of depression. Moreover, our data point towards a high intra-individual variability and non-dichotomous montage-specific effects. Therefore, prior to a more extensive use of tDCS in clinical applications, it is important to better understand its modes of action. Reproducibility of prefrontal tDCS effects should be a major aim of future tDCS studies to investigate the individual determinants of such variability. Also, the impact of

stimulation parameters and brain target-regions are to be elucidated with the aim to identify effective protocols which are of use for therapeutic purposes.

Note: Task-related fMRI data of the 2nd publication („Testing assumptions on prefrontal transcranial direct current stimulation: Comparison of electrode montages using multimodal fMRI“) are part of M.D. projects, which will be submitted in a monographic format. Irmgard Heinz will focus on the task-fMRI analysis, while Christine Bauer will focus on the behavioural outcomes of the working-memory paradigm.

Zusammenfassung

Die transkranielle Gleichstromstimulation (tDCS) ist ein nicht-invasives Hirnstimulationsverfahren, das in der experimentellen und klinischen Forschung gut etabliert ist. Während frühe Untersuchungen zur tDCS hauptsächlich auf den Motorkortex fokussierten, sind mittlerweile nicht-motorische Regionen für viele klinisch-therapeutische Fragestellungen von besonderem Interesse. Vor allem der präfrontale Kortex (PFC) könnte eine vielversprechende Zielregion für die klinische Anwendung darstellen. Jedoch treten in Studien zur präfrontalen Stimulation verschiedene Probleme auf, welche grundlegende methodische und systematische Forschungsarbeit zur präfrontalen tDCS erfordern – unter Anwendung neurophysiologischer Messungen mit dem Ziel die neuronalen Grundlagen der Effekte zu verstehen.

Da die Test-Retest(TRT)-Reliabilität der tDCS-Effekte auf die Motorkortex-Erregbarkeit jüngst in Frage gestellt wurde, zielte die erste Studie darauf ab, die Reproduzierbarkeit von Effekten präfrontaler tDCS auf Resting-State(RS)-Konnektivität in der funktionellen Magnetresonanztomographie (fMRT) zu untersuchen. In einem Parallelgruppen-Design wurden 20 gesunde männliche Teilnehmer in zwei Gruppen (aktiv versus Plazebo) randomisiert und in drei Sitzungen, mit einem Abstand von einer Woche, anhand desselben Messprotokolls untersucht: Baseline-RS-fMRT (10 min), aktive oder Plazebo-Stimulation (F3-F4, 2 mA, 20 min), post-tDCS-RS-fMRT (10 min). Zur Bestimmung der TRT-Reliabilität wurden voxel-spezifische Intra-Klassen-Korrelationen (ICC) der RS-Bilder berechnet – unter Einbezug aller drei Messzeitpunkte, jedoch separat für jede Messsequenz (Baseline- und post-tDCS) und Gruppe (aktiv versus Plazebo). In den Ergebnissen zeigten sich niedrige bis moderate ICCs auf Baseline-Ebene unabhängig von der Gruppe. In den

post-tDCS-Messungen verschoben sich die ICCs in Richtung niedrigerer TRT-Reliabilität nach aktiver, nicht jedoch nach Plazebo-tDCS. Beim Vergleich dieser Ergebnisse mit der aktuellen Literatur zeigt sich eine Diskrepanz zwischen bisher berichteter moderater bis guter Reliabilität der RS-Konnektivität und niedriger bis moderater Reliabilität unserer Baseline-RS-Messungen. Letztere könnte der kleinen Stichprobengröße in unserer Studie zuzuschreiben sein. Dennoch spricht der Abfall in der Reliabilität von Baseline- zu post-tDCS, welcher sich in der aktiven, jedoch nicht in der Plazebo-Gruppe zeigte, für eine – durch die tDCS induzierte – Zunahme an Variabilität. Die Annahme, dass tDCS-Effekte auf individueller Ebene hoch variabel sind, steht in Übereinstimmung mit vorliegenden Daten, welche niedrige TRT-Reliabilität und hohe intra-individuelle Variabilität von tDCS-Effekten auf die Erregbarkeit des Motorkortex zeigen.

Um Annahmen bezüglich polaritätsabhängiger Effekte der präfrontalen tDCS zu überprüfen, welche aus Motorkortex-Untersuchungen abgeleitet wurden, untersuchten wir in einer zweiten empirischen Studie den Einfluss verschiedener präfrontaler Elektrodenmontagen auf RS-Konnektivität im fMRT. In einem Cross-Over-Design wurden 32 gesunde männliche Teilnehmer im Abstand von einer Woche an vier Testungen mit unterschiedlichen tDCS-Bedingungen in pseudo-randomisierter Reihenfolge untersucht. Die tDCS-Bedingungen umfassten drei aktive Stimulationen (übliche bifrontale Elektrodenmontagen zur Stimulation des DLPFC, 2 mA, 20 min) und eine Plazebo-Bedingung. Vor und nach jeder Stimulationsbedingung erfolgte eine 10-minütige RS-fMRT-Aufnahme. Anhand einer univariaten Messwiederholungs-ANOVA wurden individuelle RS-Bilder über die Stimulationsbedingungen hinweg miteinander verglichen. Nach kathodaler tDCS des linken (F3) und gleichzeitiger anodaler tDCS des rechten DLPFC (F4) zeigten die Ergebnisse sowohl eine regionale Reduktion funktioneller RS-Konnektivität innerhalb des medialen PFC als auch eine regionale

Zunahme funktioneller RS-Konnektivität innerhalb des DLPFC beidseitig. Während vorausgegangene Studien von einer anodal-bedingten Zunahme und einer kathodal-bedingten Abnahme kortikaler Erregbarkeit ausgingen, impliziert die vorliegende Studie komplexere montagespezifische Effekte der tDCS.

Insgesamt unterstützen diese Ergebnisse die Annahme einer durch aktive tDCS-induzierten Modulation der RS-fMRT-Konnektivität und bestätigen damit die Eignung präfrontaler tDCS als experimentelles Verfahren der kognitiven Neurowissenschaften. Zudem stellen sie das Potential der tDCS in der klinischen Anwendung als neue Therapiemethode (z.B. bei Depressionen) heraus. Weiterhin legen unsere Daten eine hohe intra-individuelle Variabilität und nicht-dichotome montagespezifische Effekte nahe. Deswegen sollte im Vorfeld eines intensiveren therapeutischen Einsatzes der tDCS ein umfassenderes Verständnis ihrer Wirkungsweise erlangt werden. Die Reproduzierbarkeit präfrontaler tDCS-Effekte sollte ein wichtiges Thema zukünftiger tDCS-Studien sein, um die individuellen Einflussfaktoren dieser Variabilität zu erforschen. Außerdem ist es empfehlenswert, den differentiellen Einfluss von Stimulationsparametern und Zielregionen zu untersuchen, um effektivere Protokolle für therapeutische Anwendungen zu identifizieren.

Die Daten des Task-fMRT (Arbeitsgedächtnis Paradigma) der 2. Publikation („Testing assumptions on prefrontal transcranial direct current stimulation: Comparison of electrode montages using multimodal fMRI“) sind Gegenstand medizinischer Doktorarbeiten, welche in monographischer Form eingereicht werden. Hierbei handelt es sich um die Doktorarbeit von Irmgard Heinz mit Fokus auf die Auswertung der fMRT-Daten sowie die Doktorarbeit von Christine Bauer mit Fokus auf die Verhaltensdaten im Arbeitsgedächtnis-Paradigma.

Publications

Test-retest reliability of prefrontal tDCS effects on functional MRI connectivity in healthy subjects

NeuroImage 155 (2017) 187–201

Contents lists available at ScienceDirect

NeuroImage

journal homepage: www.elsevier.com/locate/neuroimage

Test-retest reliability of prefrontal transcranial Direct Current Stimulation (tDCS) effects on functional MRI connectivity in healthy subjects

Jana Wörsching[a,*], Frank Padberg[a], Konstantin Helbich[a], Alkomiet Hasan[a], Lena Koch[a], Stephan Goerigk[b], Sophia Stoecklein[c], Birgit Ertl-Wagner[c], Daniel Keeser[a,c]

[a] Department of Psychiatry and Psychotherapy, Ludwig-Maximilians-University, Munich, Germany
[b] Department of Psychological Methodology and Assessment, Ludwig-Maximilians-University, Munich, Germany
[c] Institute for Clinical Radiology, Ludwig-Maximilians-University, Munich, Germany

ARTICLE INFO

Keywords:
Prefrontal transcranial direct current stimulation (tDCS)
Neuroimaging
Resting-state functional connectivity MRI (RS fcMRI)
Test-retest reliability
Intra-class correlation coefficient (ICC)
Variability

ABSTRACT

Transcranial Direct Current Stimulation (tDCS) of the prefrontal cortex (PFC) can be used for probing functional brain connectivity and meets general interest as novel therapeutic intervention in psychiatric and neurological disorders. Along with a more extensive use, it is important to understand the interplay between neural systems and stimulation protocols requiring basic methodological work. Here, we examined the test-retest (TRT) characteristics of tDCS-induced modulations in resting-state functional-connectivity MRI (RS fcMRI). Twenty healthy subjects received 20 minutes of either active or sham tDCS of the dorsolateral PFC (2 mA, anode over F3 and cathode over F4, international 10–20 system), preceded and ensued by a RS fcMRI (10 minutes each). All subject underwent three tDCS sessions with one-week intervals in between. Effects of tDCS on RS fcMRI were determined at an individual as well as at a group level using both ROI-based and independent-component analyses (ICA). To evaluate the TRT reliability of individual active-tDCS and sham effects on RS fcMRI, voxel-wise intra-class correlation coefficients (ICC) of post-tDCS maps between testing sessions were calculated. For both approaches, results revealed low reliability of RS fcMRI after active tDCS ($ICC_{(2,1)}$ = −0.09 – 0.16). Reliability of RS fcMRI (baselines only) was low to moderate for ROI-derived ($ICC_{(2,1)}$ = 0.13 – 0.50) and low for ICA-derived connectivity ($ICC_{(2,1)}$ = 0.19 – 0.34). Thus, for ROI-based analyses, the distribution of voxel-wise ICC was shifted to lower TRT reliability after active, but not after sham tDCS, for which the distribution was similar to baseline. The intra-individual variation observed here resembles variability of tDCS effects in motor regions and may be one reason why in this study robust tDCS effects at a group level were missing. The data can be used for appropriately designing large scale studies investigating methodological issues such as sources of variability and localisation of tDCS effects.

Introduction

Transcranial direct current stimulation (tDCS) is a non-invasive brain stimulation (NIBS) technique that modifies cortical excitability by passing weak electrical current through the brain via two surface electrodes (Datta et al., 2009; Jackson et al., 2016). The current is flowing constantly from the anodal to the cathodal pole with an applied intensity of up to 4 mA and usually with 1–2 mA (Bikson et al., 2016; Edwards et al., 2013; Miranda et al., 2006). Depending on dose parameters, such as stimulation polarity, electrode positioning and applied current intensity, distinct current flow patterns as well as current density distributions are observable (Bai et al., 2014; DaSilva et al., 2015; Galletta et al., 2015; Mendonca et al., 2011; Neuling et al., 2012; Seibt et al., 2015; Woods et al., 2015). At the primary motor cortex, anodal tDCS (i.e. the anode is placed over the brain region of interest) is associated with increased motor-cortical excitability whereas the opposite is true for cathodal stimulation (Nitsche and Paulus, 2000, 2001). Such tDCS-induced excitability changes may originate from shifted resting membrane potentials towards de- or hyperpolarization (Jackson et al., 2016; Liebetanz et al., 2002; Nitsche et al., 2003). However, dose-response relations do not appear to be linear and measured responses may often be a function of the selected dose parameters (for review see Worsching et al., 2016). For example, Monte-Silva et al. (2013) found anodal stimulation of the prefrontal cortex (PFC, 1 mA intensity for 26 min) to decrease cortical excitability. Moreover, the position and size of the return electrode may influence neuromodulation within the region of the active electrode (Bikson et al., 2010). For example, for bipolar bilateral montages (Nasseri et al.,

* Corresponding author.
E-mail address: Jana.Woersching@med.uni-muenchen.de (J. Wörsching).

http://dx.doi.org/10.1016/j.neuroimage.2017.04.052
Received 12 April 2017; Accepted 22 April 2017
Available online 24 April 2017

2015) as often used for PFC stimulation, cortex regions close to the electrodes may receive both anodal facilitation and cathodal inhibition.

Based on the role of the PFC in cognitive domains and neuropsychiatric disorders (Mega and Cummings, 1994; Tandon, 2013) and in consideration of the potential of prefrontal tDCS to specifically modulate cognitive functions (for review see Tremblay et al., 2014), tDCS of PFC regions seems to be especially promising for therapeutic applications. Accordingly, the behavioural effects of prefrontal tDCS have been investigated in neurological (for review see Flöel, 2014; Schulz et al., 2013) and psychiatric disorders (for review see Kekic et al., 2016; Kuo et al., 2014). To elucidate the neural substrate of NIBS effects, tDCS can be combined with functional magnetic resonance imaging (fMRI). For instance, effects of prefrontal tDCS on the blood oxygenation level dependent (BOLD) signal in task fMRI can be observed in areas under or close to the electrode position as well as in regions distant from the electrode site (Hauser et al., 2016; Holland et al., 2011; Meinzer et al., 2012; Meinzer et al., 2013; Meinzer et al., 2014; Sacco et al., 2016; Weber et al., 2014). Instead of investigating activity in isolated brain regions, functional-connectivity MRI (fcMRI) provides the possibility to identify coordinated or integrated activity across regions (Beckmann et al., 2005; van den Heuvel and Hulshoff Pol, 2010), which is a central characteristic of healthy brain functions (Catani et al., 2013; Park and Friston, 2013). Such functional relations involve spatially distinct networks that can be extracted by analysis of the temporal coherence between spontaneous BOLD-signal fluctuations measured in different brain areas (Friston et al., 1993). In the resting state (RS), functional networks are reproducible across (Biswal et al., 2010; Damoiseaux et al., 2006) and within subjects (Blautzik et al., 2013; Braun et al., 2012; Laumann et al., 2015). Moreover, functional networks acquired under resting conditions – so called resting-state networks (RSN) – resemble functional networks during activation (i.e. task performance) (Smith et al., 2009) and are highly relevant for cognitive functions and behaviour (Laird et al., 2011; Tavor et al., 2016). For this reason, the impact of tDCS on RS fcMRI entails important information about the effectiveness of this method regarding its influence on cognition without requiring an active task. Previous studies examining the influence of prefrontal brain stimulation have shown that tDCS modulates RS fcMRI (Keeser et al., 2011; Meinzer et al., 2012; Meinzer et al., 2013; Meinzer et al., 2014; Palm et al., 2013a; Palm et al., 2016; Park et al., 2013; Pena-Gomez et al., 2012; Pereira et al., 2013; Volpato et al., 2013). For example, increased connectivity within the Frontal Parietal Network (FPN) was found following anodal tDCS of the PFC (Keeser et al., 2011; Pena-Gomez et al., 2012), potentially reflecting a cognitive state of enhanced alertness. Consequently, tDCS may bear the potential to restore altered connectivity patterns (Meinzer et al., 2013; Meinzer et al., 2014) which are often found in neuropsychiatric disorders (Buckholtz and Meyer-Lindenberg, 2012; Filippi et al., 2013; Fornito et al., 2015; Insel, 2010; Menon, 2011; Zhou et al., 2012). Though imaging stimulation, i.e. imaging the on- and offline effects of NIBS on RS fcMRI, may theoretically provide an ideal paradigm to investigate how tDCS affects neural integration and to test state, disorder and course dependency of tDCS effects, combined fMRI-tDCS investigations have methodologically not yet been developed to this point and the neurophysiological response to tDCS is still not completely understood (Parkin et al., 2015). One major issue is the intra- and inter-individual stability of tDCS effects. For both the therapeutic application of tDCS and the investigation of tDCS-induced neuromodulation and tDCS-related plasticity, it is essential to know whether the same stimulation protocol produces predictable effects across different treatment sessions. However, only few studies have tested the test-retest (TRT) reliability of tDCS effects and that only in motor-evoked potential (MEP) paradigms (Chew et al., 2015; Dyke et al., 2016; Horvath et al., 2016; Jamil et al., 2016; Lopez-Alonso et al., 2015). To our knowledge, this is the first study investigating the TRT reliability of prefrontal tDCS-induced modulation in RS fcMRI. For this purpose, effects of active or sham tDCS on RS fcMRI were measured on three different days in the same healthy subjects. In a first step, RS fcMRI at baseline and post tDCS was determined at an individual level. In a second step, reproducibility of intra-individual baseline and post-tDCS RS-fcMRI was tested using voxel-wise intra-class correlations, enabling comparisons between baseline RS-fcMRI reliability and reliability following active-tDCS or sham-tDCS intervention.

Methods

Participants and sociodemographics

We tested 20 healthy male participants (mean age: 23.85 years, age range: 18–32 years) in a total of 60 tDCS-fMRI sessions. They were all right-handed (M = 99, SD = 3.08, $range$ = 90 – 100) according to the Edinburgh Handedness Questionnaire (Oldfield, 1971). Exclusion criteria were a history of neurological and psychiatric diseases and the intake of neuroactive medication. Participant selection was also restricted to non-smokers and to people without drug consumption during the past 6 months. The study was approved by the local ethics committee (Department of Psychiatry and Psychotherapy, Ludwig-Maximilians-University Munich, Germany) and all patients gave their written informed consent for participation in this study.

Experimental procedure

This study followed a sham-controlled and double-blind design with parallel groups, such that neither participants nor investigators were aware of the stimulation condition. The 20 participants were pseudo-randomised into two groups: one active-tDCS and one sham group. Each participant received 20 min of either active or sham tDCS in the MRI scanner, always preceded, accompanied and ensued by a RS-fcMRI examination (combined on- and offline measurements, though only offline results are presented here). This procedure was conducted three times with at least seven days between each testing session. Within one participant, the stimulation condition (active vs. sham tDCS) was the same across all testing sessions. Daytime of measurement was kept constant for each participant across all testing sessions (see Fig. 1).

Participants were asked to abstain from alcohol the day before and from caffeine the morning before each testing session. At the beginning of each session and prior to fMRI scanning, participants filled in several questionnaires based on an in-house digital Android tablet system. Afterwards, participants went into the MRI scanner and were asked to keep their eyes closed, to not fall asleep, to think about nothing in particular and to avoid movements. During each session, RS scans were repeated three times, directly following each other: baseline/pre tDCS (10 min), during tDCS (20 min), post tDCS (10 min) (see Fig. 1). Instructions were repeated before each RS scan started and participants were informed before stimulation started. At the end of each session, participants again filled in several questionnaires in order to assess possible stimulation effects on mood and other variables.

Questionnaires

Several questionnaires were administered once at the overall baseline including the Edinburgh Handedness Questionnaire (Oldfield, 1971), the trait scale of the Positive And Negative Affect Schedule (PANAS, missing the item “enthusiastic” on the positive affect scale) (Krohne et al., 1996; Watson et al., 1988), the trait scale of the State Trait Anxiety Inventory (STAI) (Laux, 1981; Laux and Spielberger, 1981; Spielberger et al., 1970) and a questionnaire for sociodemographic data. Additionally, the PANAS state scale and the STAI state scale were completed prior to each stimulation. After each stimulation, the PANAS state scale was filled in again in addition to the Comfort Rating Questionnaire (CRQ) (Palm et al., 2014).

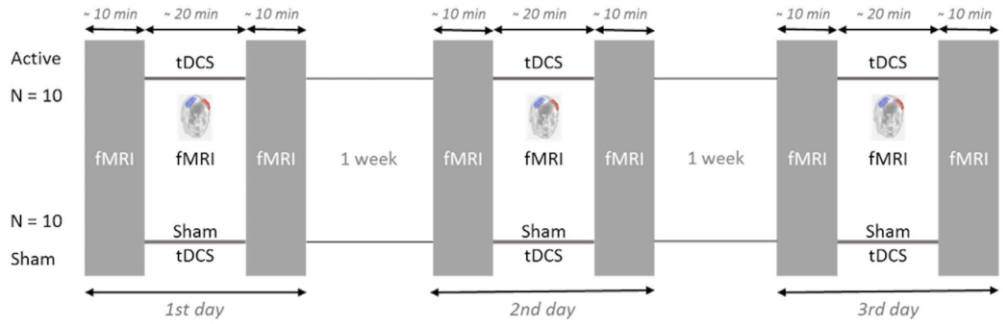

Fig. 1. Experimental protocol. Active- and sham-tDCS conditions were applied inside the MRI (online) after baseline fMRI scans according to a double-blind, between-subject design. The head model was created with Matlab/Comets (Jung et al., 2013).

Transcranial Direct Current Stimulation (tDCS)

TDCS was applied via two saline-soaked surface sponge electrodes (area = 7 × 5 cm^2) that were connected to an Eldith stimulator MR (neuroConn). In order to target the dorsolateral prefrontal cortex (DLPFC) bilaterally, the anode was placed over F3 and the cathode over F4 (according to the international 10–20 system). The impedance was kept below 10 kΩ. Distance between electrodes was at least 6 cm to avoid shunting effects (Miranda et al., 2006). TDCS was delivered for 20 min at an intensity of 2 mA (15 s ramp in and 15 s ramp out). For sham tDCS, the current was ramped up at the beginning and end of the stimulation period to mimic the somatosensory sensation of real tDCS, but turned off in between alternated with low-threshold direct-current impulses (Palm et al., 2013b). Operators and participants were kept blind to treatment conditions.

fMRI data processing

fMRI data acquisition

Subjects had to wear ear plugs and head phones for noise protection. FMRI was carried out at 3 T (SKYRA, Siemens) using a 20-channel head-coil. For functional imaging, an EPI sequence with the following parameters was used: repetition time (TR), 2000 ms; echo time (TE), 30 ms; flip angle (FA), 80°; spatial resolution, 3 × 3 × 3 mm^3; imaging matrix, 64 × 64; field-of-view (FoV), 192 × 192 mm^2; number of slices, 36; number of volumes, 250 (baseline), 620 (during tDCS), 250 (post tDCS). Functional images were acquired in axial orientation. For anatomical reference, a high-resolution MPRAGE was performed with the following specifications: FoV, 256 × 240 mm^2; spatial resolution, 0.8 × 0.8 × 0.8 mm^3; TR, 14 ms; TE, 7.61 ms; FA, 20°; number of slices, 160.

fMRI data pre-processing

Images were pre-processed using FSL 5.0.9 (http://www.fmrib.ox.ac.uk/fsl/index.html), AFNI (Analyses of Functional Images, http://afni.nimh.nih.gov/afni) and in-house scripts. Following brain extraction (BET; Smith, 2002), individual high-resolution T1-weightened images were reoriented to standard space, binarised, and segmented into grey matter (GM), white matter (WM), cerebrospinal fluid (CSF) using FAST (Smith, 2002). A linear and non-linear registration was applied using FLIRT and FNIRT (Jenkinson et al., 2002), a T1 atlas was generated and images were warped into MNI-standard space. Finally, calculations of the total amount of GM, WM and CSF, as well as of the volumetric proportion of all atlas regions were carried out. By means of a warping procedure, individual WM, GM and CSF deformation fields were created. The first ten volumes of functional MRI images were discarded to avoid non-steady-state effects. Functional image pre-processing comprised the following steps: (1) slice-time correction using 3dTshift to account for interleaved slice acquisition; (2) deobliquing using 3drefit and reorientation using 3dresample; (3) motion correction of time series using 3dTstat and 3dvolreg; (4) edge detection and removal of skull using 3dAutomask and 3dcalc; (5) linear and nonlinear spatial registration/normalisation to a standard EPI template in Montreal Neurological Institute (MNI) space using the T1 deformation field; (6) grand mean scaling; (7) de-trending; (8) calculation of motion outliers; (9) spatial smoothing using a 6 mm FWHM Gaussian kernel with high-pass temporal filtering (Gaussian-weighted, least-squares, straight-line fitting with σ = 50 s); (10) extraction of global signal, CSF and WM using 3dmaskave and creating a nuisance and motion parameter matrix; (11) obtaining residuals using 3dREMLfit; (12) demeaning of residuals using 3dTstat, 3dcalc and fslmaths; (13) band-pass filtering using 3dFourier (0.01 – 0.1 Hz, which are characteristic for RSNs according to: Boly et al., 2008; Damoiseaux et al., 2006; Fox et al., 2005; Greicius et al., 2003; Horovitz et al., 2009; Miller et al., 2009; Vincent et al., 2007); (14) smoothing; (15) warping of all fMRI images to the respective individual deformation template, resulting in normalised images in MNI space; (16) normalisation on segmented images (GM, WM and CSF); (16) censoring; (17) extraction of mean time courses in region-of-interest (ROI) masks using fslstats; (18) cross correlation using 3dfim, z-score normalisation using 3dcalc and normalisation to MNI space using applywarp.

ROI-based analysis

In a hypothesis-driven approach, ROIs were selected based on computational models that investigated current-flow patterns as generated with a F3-F4 electrode montage. Across studies, current distribution was widespread while current density clustered within the DLPFC (Bai et al., 2014; DaSilva et al., 2015; Nelson et al., 2014; Seibt et al., 2015; Woods et al., 2015). For this reason, ROIs were positioned within this region by means of the Sallet-atlas, which relies on a fMRI-based parcellation of the DLPFC (Sallet et al., 2013). Three different ROIs covering different parts of the DLPFC, in which an effect is to be expected, were chosen from the Sallet-atlas: area 46/9 dorsal, area 9 and area 10. These ROIs were drawn separately for the left and right hemisphere. The resulting masks are shown in inline supplementary figure 1. Additionally, by adding the beforementioned ROIs together, two hemisphere-specific total prefrontal ROIs were created for evaluation of group-tDCS effects. After converting them to a binary image, every mask was applied to each participant, each testing session and each measurement (baseline and post tDCS) using linear and non-linear registration (FLIRT, FNIRT). Connectivity values for each ROI and subject were generated by means of AFNI 3dfim command to cross correlate RS time-series within each ROI.

Independent component analysis (ICA)

In a complementary whole-brain approach, fcMRI data were analysed using the MELODIC (Multivariate Exploratory Linear

Optimized Decomposition into Independent Components) routine, version 3.14, implemented in FSL (Beckmann and Smith, 2004). Time courses of all participants, measurements (baseline and post tDCS) and testing sessions (t1, t2, t3), resulting in a total of 120 runs, were concatenated into a single 4D dataset. Decomposition into different functional networks was performed automatically by a dimensionality estimation of the MELODIC 3.14 tool. Four group-level components, which are known to involve brain regions within the DLPFC close to tDCS electrode sites, were selected for further analyses: the anterior Default Mode Network (DMN), the posterior DMN, the left FPN and the right FPN. An average z-score of $3 < z < 8$ was defined as the threshold for the resulting statistical group maps (see inline supplementary figure 2). Applying a threshold of $z = 3.0$, for each of these RSNs an independent-component (IC) mask was created. All ICA-derived group-level ICs containing the three RSNs of interest were reconstructed into individual ICs separately for each participant, measurement and testing session applying dual regression (Biswal et al., 2010; Filippini et al., 2009; Zuo et al., 2010).

Statistical analyses

Questionnaires

Group differences in scores for PANAS trait and STAI trait were analysed via independent t-tests using R (R Development Core Team (2008). R: A language and environment for statistical computing. R Foundation for Statistical Computing, Vienna, Austria. ISBN 3–900051-07-0, URL http://www.R-project.org). Scores of STAI state were evaluated with two-way ANOVAS with a mixed effect design. Testing session was treated as repeated-measures factor with three stages (t1, t2, t3) and group as independent factor with two stages (active, sham). Scores of PANAS state were analysed with a three-way ANOVA including an additional pre-post comparison factor. Sphericity was examined for all statistical analyses and in case of non-sphericity, results were corrected according to Greenhouse Geisser. All effects are reported as significant at $p < .05$.

FMRI contrasts

Voxel-wise nonparametric statistical contrasts (with 5000 permutations) were determined using PALM alpha86 (Permutation Analysis of Linear Models; Winkler et al., 2014; Winkler et al., 2015; Linear Models, http://fsl.fmrib.ox.ac.uk/fsl/fslwiki/PALM/). Due to the exploratory character of our study changes in RS fcMRI from pre to post tDCS were considered significant at an uncorrected $p < .001$ (cluster size > 20 voxels). Effects of active tDCS on RS fcMRI at each testing session were summarised with two directional contrasts: brain regions that showed an increase (post active-tDCS > pre active-tDCS) or decrease (post active-tDCS < pre active-tDCS) in RS fcMRI with or within the ROI or ICA network (RSN). Changes in the sham group following the placebo intervention were analysed for each testing session using the same directional contrasts: positive effects (post sham-tDCS > pre sham-tDCS) and negative effects (post sham-tDCS < pre sham-tDCS). Hereby, each active-tDCS effect, i.e. post active-tDCS > pre active-tDCS or post active-tDCS < pre active-tDCS, could be compared to its corresponding sham effect (post sham-tDCS > pre sham-tDCS or post sham-tDCS < pre sham-tDCS), to test whether significant changes in each contrast arose from a tDCS-unrelated increase/reduction in RS fcMRI from baseline to post tDCS. All active-tDCS effects were checked for overlaps with direction-specific sham effects at each testing sessions. Overlaps were defined as visually observable intersections between direction-specific active-tDCS and sham effects. All active-tDCS effects were also checked for consistency across testing sessions. Consistent tDCS effects were defined as spatially proximal clusters covering a common anatomical structure.

Test-retest approach

To evaluate intra-individual TRT reliability, voxel-wise intra-class correlation coefficients (ICC) were calculated based on a script by Zou and colleagues (Zuo et al., 2010): https://de.mathworks.com/matlabcentral/fileexchange/22122-ipn-tools-for-test-retest-reliability-analysis. Activity within voxels of individual baseline or post-tDCS maps – resulting from individual normalized z-score maps (derived from the ROI-connectivity analyses) and reconstructed individual probabilistic ICs (derived by means of dual regression) – of each participant at each testing session was extracted and then consistency of the two-way random single measures was determined using $ICC_{(2,1)}$ across all testing sessions (t1 and t2 and t3) as well as across pairs of sessions: t1 to t2, t1 to t3 and t2 to t3. In this way, reliability maps were generated for both baseline and post-tDCS measurements separately for the seed- and the ICA-based approach and separately for each group (active and sham). TRT reliability maps were summarised by calculating the median ICC-value within each IC mask or ROI. According to Cicchetti (1994), ICC values were rated as follows: low (ICC values < 0.4), moderate (ICC values between 0.4 and 0.59), good (ICC values between 0.6 and 0.74) and excellent (ICC values ≥ 0.75). Negative ICC values indicate that the measure is not reliable (Lahey et al., 1983).

Results

TDCS effects: ROI-based and dual-regression analyses

Peak voxels of contrast-specific effects are given in Inline Supplementary tables, separately for the active (see Inline Supplementary table 1) and sham group (see Inline Supplementary table 2). To identify regions which change in active tDCS and do not change in sham, visual maps of direction-specific effects in the active and sham group are provided. Visualisations also provide the opportunity to compare one contrast across testing sessions and thus to identify repeatedly appearing tDCS effects (see Figs. 2 and 3).

ROI-based analysis

Functional connectivity within ROIs did not change appreciably and only once exhibited a significant active-tDCS effect, namely an increase in right-hemispheric functional connectivity during the first testing session (see Inline Supplementary table 1). There was no effect of sham tDCS on within-ROI connectivity.

ICA approach

Based on whole-brain dual-regression analyses, results indicate that active tDCS affected the magnitude of correlation in time series between voxels within a given RSN (see Inline Supplementary table 1). For active tDCS, neither positive nor negative effects on connectivity clustered within a specific brain region but were rather widespread. Consistent active-tDCS effects across testing sessions could be identified for each RSN (see Figs. 2 and 3). The anterior DMN exhibited an increase in correlated time series with the right superior temporal gyrus/insula as well as the left thalamus across two active-tDCS testing-sessions. For the posterior DMN, a positive active-tDCS effect appeared throughout all testing sessions within the right and left medial frontal gyrus. Increased correlations with the left FPN were found within the right postcentral gyrus, right parietal lobule, left middle and inferior frontal gyrus, left and right precentral gyrus and left middle temporal gyrus across two active-tDCS testing-sessions. The left inferior parietal lobule, right (pre-)cuneus and right thalamus showed increased correlations with the right FPN across two testing sessions. Repeatedly, decreased correlations across two active-tDCS testing-sessions appeared between the anterior DMN and right precentral gyrus, posterior DMN and both the right inferior frontal gyrus and right cingulate gyrus, left FPN and right middle frontal gyrus, right FPN and both the right middle/superior frontal gyrus and left cingulate gyrus.

For sham tDCS, significant effects on RSNs were present as well

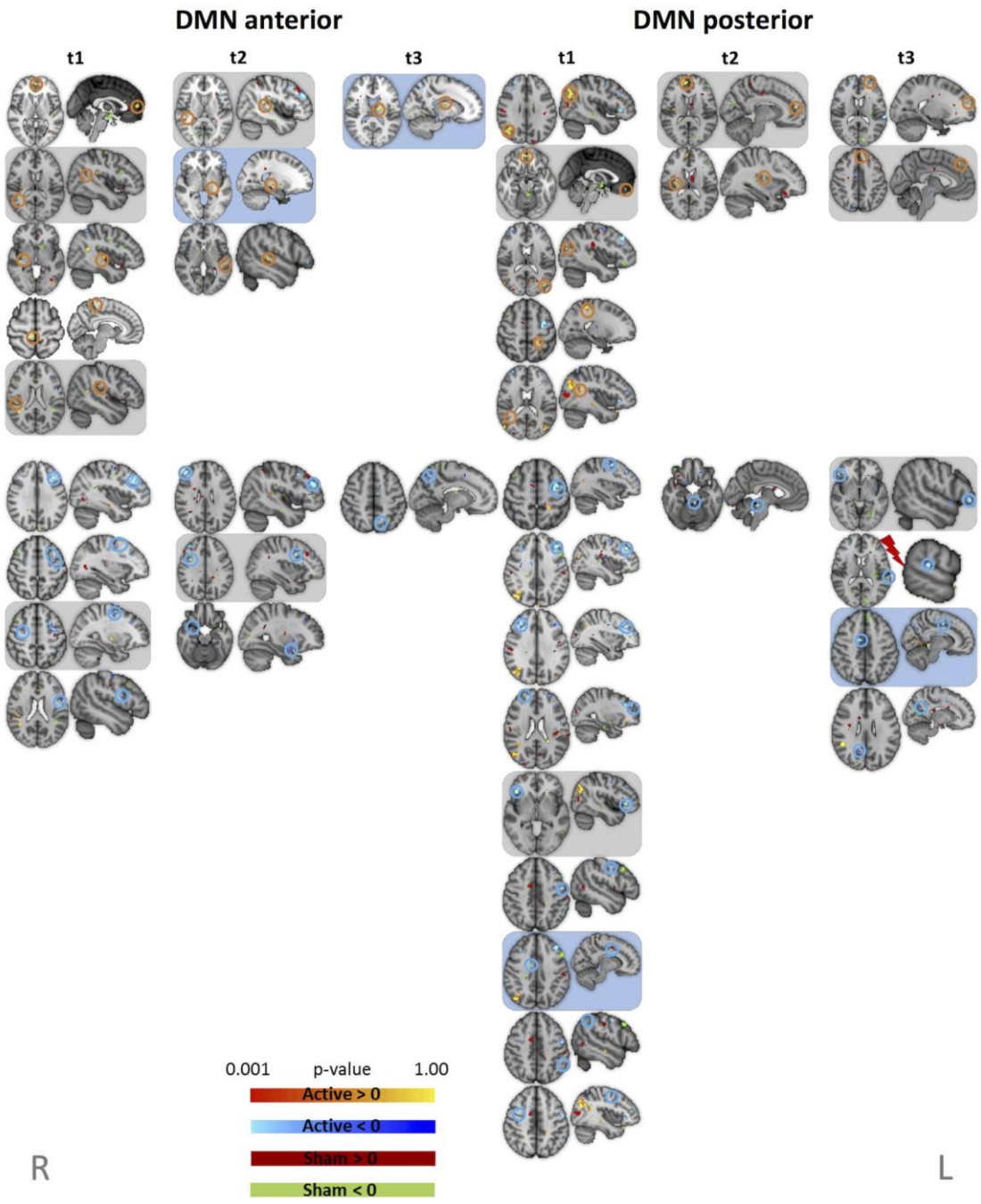

Fig. 2. Active-tDCS effects and sham effects on resting-state networks (RSN) at each testing session. Colours represent the following contrasts: orange = post active-tDCS > pre active-tDCS, blue = post active-tDCS < pre active-tDCS, dark red = post sham-tDCS > pre sham-tDCS, green = post sham-tDCS < pre sham-tDCS. Orange circles mark positive tDCS effects, i.e clusters that showed increased correlated time-series with the respective network after active tDCS as compared to baseline. Blue circles mark negative tDCS effects, i.e clusters that showed decreased correlated time-series with the respective network after active tDCS as compared to baseline. Framed effect clusters mark positive or negative tDCS effects in the active group that repeatedly appeared across different testing sessions ;colours mark effects that belong together. The flash indicates an overlapping negative effect between the active and sham group (orange and dark red). MNI coordinates (x, z) of each effect cluster is given in Inline supplementary table 1 and 2. Effects are sorted by cluster size. Correlated time series are shown at a threshold of $p < .001$, uncorrected, radiological convention. DMN = Default Mode Network, L/R = left/right, t1/2/3 = testing session 1/2/3.

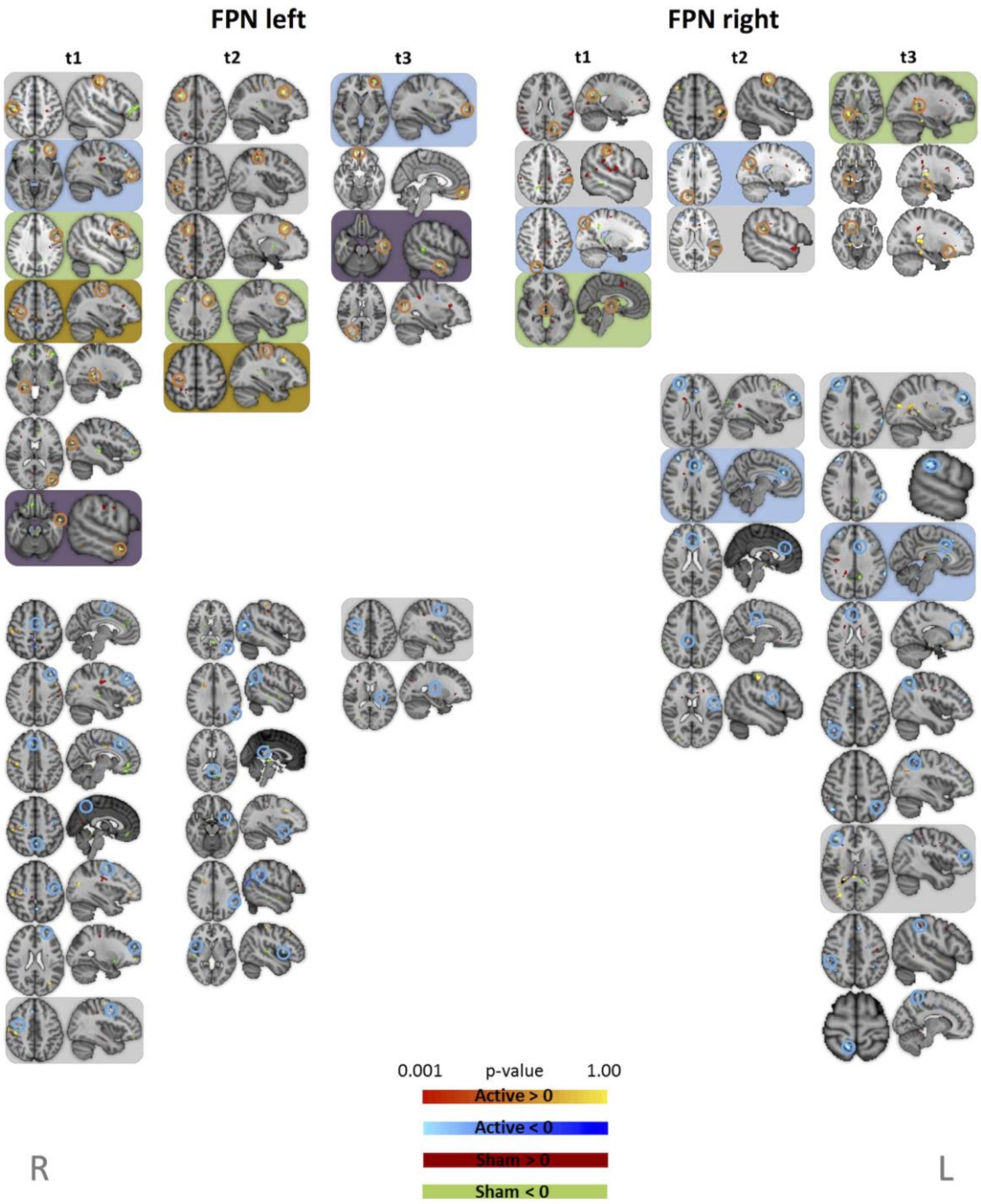

Fig. 3. Active-tDCS effects and sham effects on resting-state networks at each testing session. Colours represent the following contrasts: orange = post active-tDCS > pre active-tDCS, blue = post active-tDCS < pre active-tDCS, dark red = post sham-tDCS > pre sham-tDCS, green = post sham-tDCS < pre sham-tDCS. Orange circles mark positive tDCS effects. i.e. clusters that showed increased correlated time-series with the respective network after active tDCS as compared to baseline. Blue circles mark negative tDCS effects, i.e clusters that showed decreased correlated time-series with the respective network after active tDCS as compared to baseline. Framed effect clusters mark positive or negative tDCS effects in the active group that repeatedly appeared across different testing sessions; colours mark effects that belong together. MNI coordinates (x, z) of each effect cluster is given in Inline Supplementary table 1 and 2. Effects are sorted by cluster size. Correlated time series are shown at a threshold of $p < .001$, uncorrected, radiological convention. FPN = Frontal Parietal Network, L/R = left/right, t1//2/3 = testing session 1/2/3.

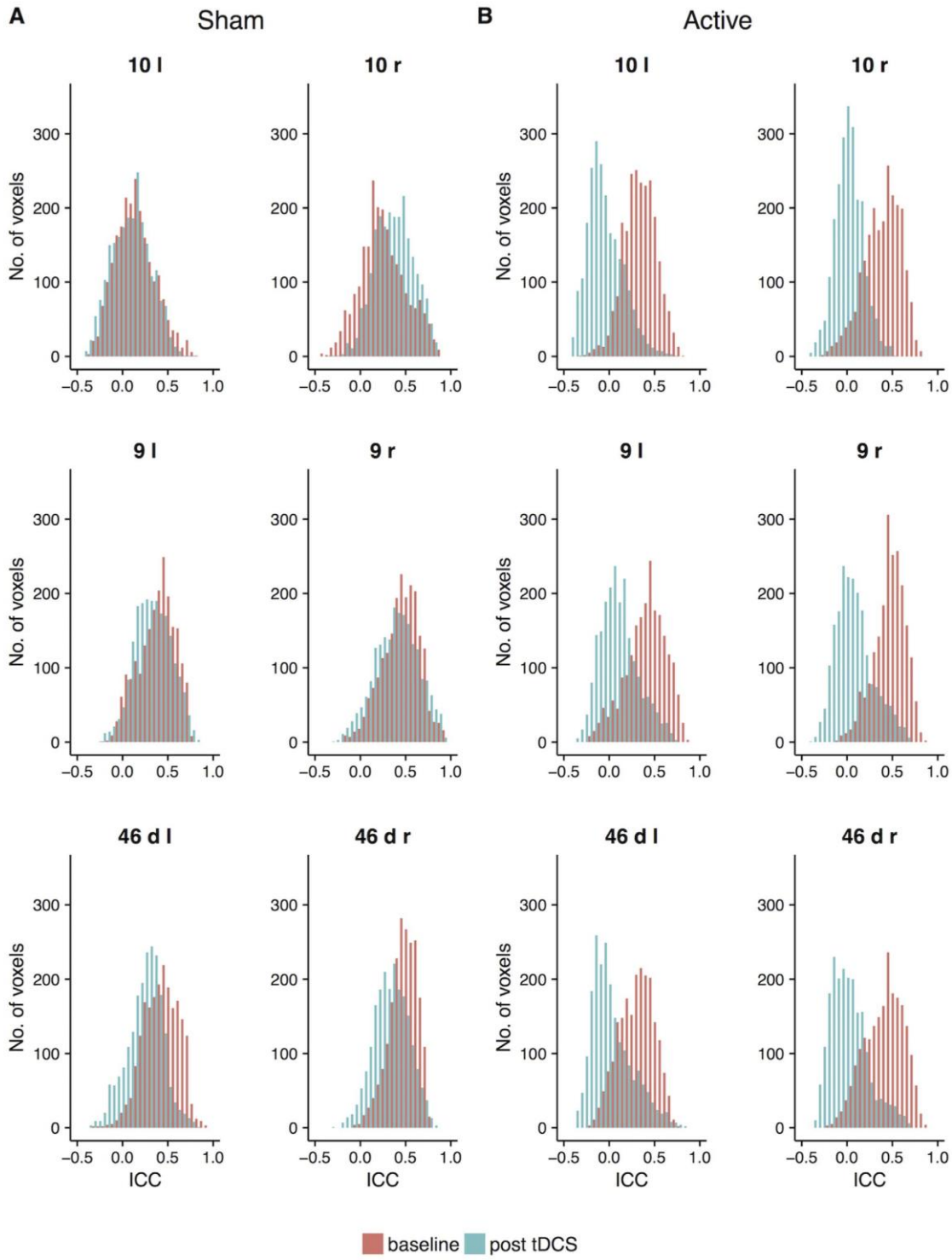

Fig. 4. Frequency distributions of voxel-wise ICC calculations within a region of interest (ROI). Colours represent frequency of ICC levels of baseline and post-tDCS measurements in a) the sham group. b) the active group. ICC = intra-class correlation coefficient, l/r = left/right, 10 = area 10 of the Sallet-atlas, 46d = area 46/9 dorsal of the Sallet-atlas, 9 = area 9 of the Sallet-atlas (Sallet et al., 2013).

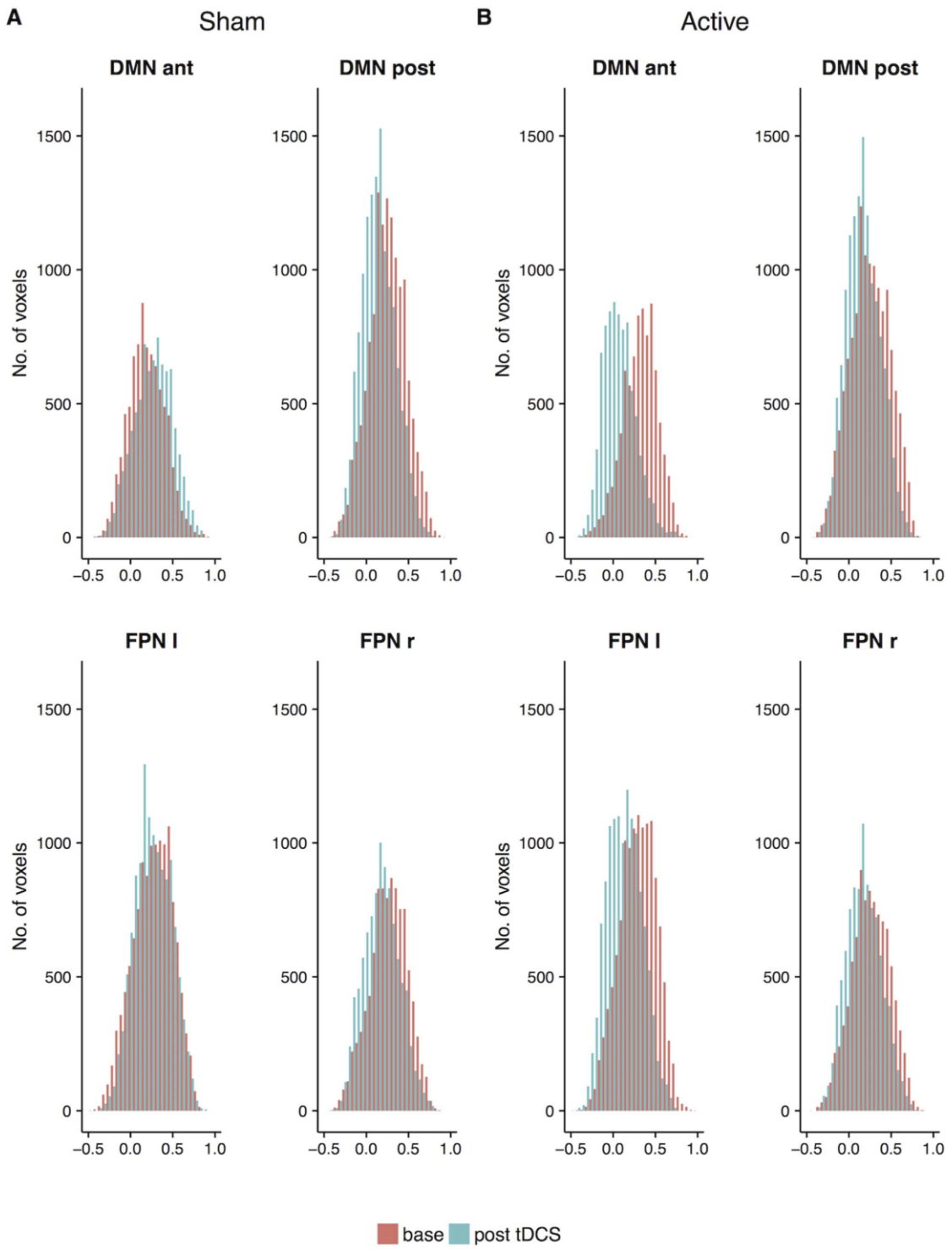

Fig. 5. Frequency distributions of voxel-wise ICC calculations within a resting-state network (RSN). Colours represent frequency of ICC levels of baseline and post-tDCS measurements in a) the sham group. b) the active group. ant = anterior, DMN = Default Mode Network, FPN = Frontal Parietal Network, ICC = intra-class correlation coefficient, l/r = left/right, post = posterior.

(see Inline Supplementary table 2). To visually identify regions for which changes from baseline to post-tDCS measurements were specific to active tDCS, flashes within contrast maps indicate overlapping direction-specific effects between the active and sham group (see Figs. 2 and 3). Only one overlap between direction-specific effects of active tDCS and sham tDCS occured: for the posterior DMN, both a negative active-tDCS effect and a negative sham effect were found within the left superior temporal gyrus at testing session 3.

Reliability analyses

Inter-session TRT reliability was represented by the degree of consistency of single measurements (activity within voxels). To descriptively compare ICC levels between and within groups, the frequency-distributions of single-voxel ICC-values within a ROI or RSN are shown in histograms (see Figs. 4 and 5). Histograms also conduced to trace differences between ICC pairs (t1-t2, t1-t3, t2-t3). Here, values of the ICC-pair 23 were contrasted with values of both ICC-pair 12 and ICC-pair 13 (see Inline Supplementary figure 4 and 5).

TRT reliability of baseline RS-fMRI connectivity

For baselines as investigated with the ROI-based approach, ICCs were poor to moderate for both groups with median values ranging from $ICC_{(2,1)}$ = 0.13 to $ICC_{(2,1)}$ = 0.50 (see Table 1). Thereby, half of the median ICC-values were showing poor and the other half moderate TRT reliability. For the ICA-based approach, baseline connectivity patterns rather showed poor reliability across groups as indicated by median ICC-values ranging from $ICC_{(2,1)}$ = 0.19 to $ICC_{(2,1)}$ = 0.34 (see Table 2).

Table 1
Inter-session test-retest reliability of ROIs.

Surface ROI localisation	ROI and hemisphere	sham		active	
		baseline	post	baseline	post
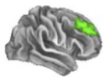	46 d l	0.44	0.26	0.33	−0.03
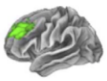	46 d r	0.50	0.33	0.44	−0.02
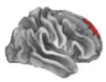	9 l	0.30	0.32	0.37	0.12
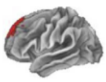	9 r	0.46	0.49	0.50	0.06
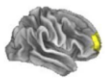	10 l	0.13	0.09	0.35	−0.09
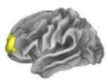	10 r	0.24	0.36	0.42	0.01

Note. Test-retest reliability of connectivity within ROIs, separately for both groups (active vs. sham) and both conditions (baselines and post tDCS). Test-retest reliability is expressed as median of voxel-wise intra-class correlation coefficients (ICC) between all testing sessions (t1, t2, t3). ROIs are illustrated in radiological convention. *d = dorsal, l/r = left/right, ROI = region of interest, 10 = area 10 of the Sallet-atlas, 46d = area 46/9 dorsal of the Sallet-atlas, 9 = area 9 of the Sallet-atlas (*Sallet et al., 2013*)* .

Table 2
Inter-session test-retest reliability of RSNs.

RSN localisation	RSN	sham		active	
		baseline	post	baseline	post
	DMN anterior	0.19	0.27	0.34	0.04
	DMN posterior	0.26	0.12	0.26	0.14
	FPN l	0.29	0.25	0.31	0.12
	FPN r	0.28	0.17	0.27	0.16

Note. Test-retest reliability of ICA-analyses-based RSN-connectivity, separately for both groups (active vs. sham) and both conditions (baselines and post tDCS). Test-retest reliability is expressed as median of voxel-wise intra-class correlation coefficients (ICC) between all testing sessions (t1, t2, t3). RSNs are illustrated in radiological convention. *DMN = Default Mode Network, FPN = Frontal Parietal Network, ICA = independent component analysis, l/r = left/right, RSN = resting-state network.*

TRT reliability of tDCS-related effects on RS-fMRI connectivity

For the ROI-based approach, reliability of individual post-tDCS maps differed depending on whether an active or sham tDCS intervention preceded the measurement. In the active group, median ICC-values ranged from $ICC_{(2,1)}$ = −0.09 to $ICC_{(2,1)}$ = 0.12 and in the sham group, median ICC-values ranged from $ICC_{(2,1)}$ = 0.09 to $ICC_{(2,1)}$ = 0.49 (see Table 1). Thereby, post-tDCS median ICC-levels of the active group can be rated as not reliable to poor, while median ICC-levels of the sham group are classifiable as poor to moderate. For the ICA-based approach, post-tDCS reliability could be classified as poor across groups as indicated by median ICC-values ranging from $ICC_{(2,1)}$ = 0.04 to $ICC_{(2,1)}$ = 0.16 in the active group and from $ICC_{(2,1)}$ = 0.12 to $ICC_{(2,1)}$ = 0.27 in the sham group (see Table 2). The described pattern is illustrated in Inline Supplementary figure 3.

Comparisons of TRT reliability

Based upon histograms, in the sham group, ICC frequency-distributions of baseline and post-tDCS measurements largely overlapped (see Figs. 4 and 5), pointing towards a close match in ICC levels between both RS-fcMRI examinations. By contrast, histograms of the active group indicate a distinction in ICC levels between baseline and post-tDCS measurements. Especially in the ROI approach, ICC frequency-distributions of baseline and post-tDCS measurements were so very far apart that the two peaks of each distribution were clearly discernible (see Fig. 4). This observation did not apply to ICA-based ICCs. Here, ICC frequency-distributions of the active group largely resembled those of the sham group, such that distributions were hardly

distinguishable. Only the anterior DMN exhibited a bimodal histogram (see Fig. 5).

Median ICC-values of ICC pairs ranged within the same values as median ICC-values resulting from overall ICC calculations across all three testing sessions (see Inline Supplementary table 3 and 4). Histograms of single-voxel ICCs show that the frequency distributions of different ICC pairs were quite similar, i.e. largely overlapping, across groups and measurements (see Inline Supplementary figure 4 and 5), again suggesting comparable ICC levels independent of the factor testing session.

Behavioural data

A significant difference was found between overall levels of positive affect (PANAS state), $F(1, 18) = 10.01$, $p < .01$, and overall levels of negative affect (PANAS state), $F(1, 18) = 9.80$, $p < .01$, before and after both active and sham tDCS, indicating that participants on average reported both higher positive and higher negative affects before measurement ($M_{POS} = 26.88$, $SD_{POS} = 6.54$; $M_{NEG} = 11.52$, $SD_{NEG} = 2.08$) than after ($M_{POS} = 24.27$, $SD_{POS} = 7.46$; $M_{NEG} = 10.67$, $SD_{NEG} = 0.90$). All other behavioural variables did not change significantly, neither between groups nor across testing sessions. There was also no difference in age between groups. Separate item analysis of CRQ showed that tDCS-related discomfort was low.

Discussion

In this study, we investigated the TRT reliability of effects that single prefrontal tDCS sessions exert on RS fcMRI and observed none or low reliability of responses (post-tDCS RS-fcMRI) in contrast to a more robust TRT reliability of baseline RS fcMRI. The underlying question is highly relevant as establishing imaging stimulation (tDCS) probes for exploring state, disorder or course dependency of tDCS effects would require a deeper understanding of the variability of tDCS-mediated RS-fcMRI changes. Moreover, the reliability of tDCS effects in general has recently been questioned by findings from three studies reporting variable inter- and intra-individual MEP responses to motor-cortex tDCS (Chew et al., 2015; Dyke et al., 2016; Horvath et al., 2016). Finally, varying RS-fcMRI response-patterns to NIBS may be related to the variation of responses observed in clinical applications of NIBS in psychiatry (for review see Lefaucheur et al., 2016). If neurophysiological effects of tDCS vary, variations in behavioural and clinical responses can be expected as well. And if significant variability of response-patterns to NIBS exist even at an intra-individual level, average measures of clinical responses should be replaced by intra-individual analyses.

In order to address the question of TRT reliability for prefrontal-tDCS RS-fcMRI effects, we chose a methodologically broad approach comprising both ROI-based as well as ICA-based analyses. Masks were seeded in prefrontal areas where a tDCS effect can be expected according to computational models. Next, voxel-wise ICCs were calculated for both individual baseline and individual post-tDCS RS-fcMRI separately for each group (active and sham). Mostly moderate TRT reliability was observed for RS-fcMRI measurements at baseline prior to tDCS using the ROI-based approach. For the ICA-based approach, low reliability of baseline RS fcMRI appeared. More reliable connectivity patterns in the ROI-based approach is in line with Craddock et al. (2012). According to this study, reliability increases as a function of the number of entities the brain is portioned out, which might be one reason why reliability within selected ROIs is slightly higher than in ICA-derived RS components. While the latter represents correlated time courses across the whole brain, our seeds comprised clearly defined small clusters within the DLPFC. The discrepancy between moderate to good RS-fcMRI ICC-values previously reported (Blautzik et al., 2013; Braun et al., 2012; Laumann et al., 2015; Zuo et al., 2010) and low to moderate baseline ICC levels may arise from our small sample size. Furthermore, low to moderate ICC values may be also due to network selection, which was based on anatomical proximity to stimulation sites. As a result, mainly prefrontal networks, which are associated with higher order cognitive functions, were considered stimulated networks. Because inter-subject variability of functional networks increases with their relevance for cognitive functions (Mueller et al., 2013), it is plausible that the networks selected here show lower reliability than networks associated with sensory or motor functions.

Regarding reliability of RS-fcMRI after tDCS, for the ROI-based approach, the ICC frequency distribution was shifted to lower TRT reliability in the active group. On the contrary, reliability of the post measurements following sham tDCS was low to moderate and, as suggested by ample overlap between frequency scales, did not seem to differ from baseline ICCs. On this descriptive level, active tDCS appears to induce additional variability and reduces TRT reliability in contrast to sham tDCS leaving TRT reliability largely on the baseline level. This supports the notion of active tDCS modulating RS-fcMRI, however, with variable and divergent effects. For the ICA-based approach, no clear difference between baseline and post-tDCS ICCs was observed, possibly due to the large spatial extend of IC-networks.

Test-retest reliability and sources of variability

The assumption that tDCS effects are highly variable at the individual level would be consistent with available data showing low TRT reliability of tDCS effects on MEPs. Similar to our results, in most studies investigating reproducibility of tDCS effects on MEPs, reliability values ranged from −0.50 to 0.28. Dyke et al. (2016) showed that effects of 2 mA anodal tDCS on MEPs, defined as ratio of post-tDCS and pre-tDCS slopes, were poorly reliable (ICC = 0.28). Poor intra-individual reliability was also found for MEPs over a 30-min interval following both anodal stimulation with 0.5 mA (ICC = −0.50) (Chew et al., 2015) and 1 mA (ICC = 0.06) (Horvath et al., 2016). For the same interval and stimulation intensity, Lopez-Alonso et al. (2015) detected fair reliability (ICC = 0.57) of anodal tDCS, but again poor reliability (ICC = −0.03) for MEPs obtained during the second half of the overall 60-min interval. Only in one recent motor-cortex study, intra-individual reliability over both early and late measurement periods following stimulation with 1 mA was reported to be satisfying (ICC = 0.74 and 0.64) (Jamil et al., 2016).

One may argue that ICCs must not be directly compared across MEP-tDCS and fMRI-tDCS studies, because different factors contribute to the overall variability in such paradigms, especially MEP/fMRI-related factors. Numerous studies have addressed TRT reliability of MEPs only and reported moderate to good reliability of different MEP measures (Carroll et al., 2001; Kamen, 2004; Livingston and Ingersoll, 2008; Malcolm et al., 2006). Though, to our knowledge, there is no single study directly comparing TRT reliability measures for MEPs alone and tDCS effects on MEPs. The above-mentioned studies have only investigated TRT reliability of MEPs following active and sham tDCS. Therefore, we can only speculate that ICCs of these measures may be different. In comparison with RS fcMRI, MEPs constitute an active intervention, i.e. measures cortical reactions to a single TMS (transcranial magnetic stimulation) pulse, that possibly influences baseline states and the mode of action of a subsequent intervention, namely tDCS. By contrast, RS fcMRI is task-free and represents a less controlled behavioural state. Besides, MEPs are specifically related to motor-cortex physiology, whereas tDCS-induced RS-fcMRI modulation can be also measured for other target regions (Callan et al., 2016; Krishnamurthy et al., 2015; Polania et al., 2012). Lastly, motor-cortex excitability can be neuropharmacologically modified (Ziemann, 2008), but very little is known about pharmacological effects on RS-fcMRI measures (Bartelle et al., 2016). If there were different contributions of MEPs and RS fcMRI to tDCS-related variability, it might be difficult to translate reliability estimations of tDCS effects on MEPs to tDCS effects

on RS fcMRI. However, the current debate in the literature is concerned with the reliability of tDCS and not with the reliability of MEP or fcMRI.

The variability of BOLD-responses has been investigated for task-fMRI studies. Here functional paradigms are used to evoke a BOLD signal in a certain brain region. In a study by Plichta et al. (2012), reliability of a task-fMRI battery targeting different systems (emotion, motivation and cognition) was assessed at both group and individual levels. While group-level activation maps were highly reliable independent of the task (whole brain level: ICC = 0.89 – 0.98, target ROIs: ICC = 0.66 – 0.97), within-subject reliability ranged from fair to good for the motivational and the cognitive task (ICC = 0.56 – 0.62 and ICC = 0.44 – 0.57, respectively) but remained low for the emotional task (ICC = −0.02 – 0.16) (Plichta et al., 2012). Furthermore, it has been shown that observed between-session variations in the spatial pattern of BOLD activation are mainly due to global effects that can be corrected by pre-processing steps such as spatial smoothing, for which reason the authors consider the localisation of fMRI signals as highly reliable. In contrast, variations in the amplitude of the activation were pronounced to a greater degree – especially for cognitive tasks – and may limit interpretations of the magnitude of brain activation (Raemaekers et al., 2012). Another study investigating variations in fMRI-task responses within subjects by means of within-subject variance-decompositions found that error in measurement contributes the most to the total variance (Gonzalez-Castillo et al., 2016). At the same time, within-subject variance across sessions and across runs or blocks within one session also constituted an important source of overall variance (Gonzalez-Castillo et al., 2016). Such natural within-subject variability in task-fMRI may reflect the potential of this method to capture intra-individual differences and point to the need for individual-subject analyses (Laumann et al., 2015; McGonigle, 2012; Shine et al., 2016). Consequently, sources of variability, which reside in intra- and inter-related factors other than natural differences in response to tDCS itself may limit reliability of individual measurements and hinder identification of the 'true' TRT level for tDCS. Therefore, it is essential to control for these factors.

Heterogenous groups and especially outliers add to the total variance and may affect the magnitude of ICCs. Consequently, it is important to ensure similar characteristics of the tested sample (Lopez-Alonso et al., 2015; Vaz et al., 2013). For this reason, behavioural control variables were carefully and elaborately reviewed and relevant individual covariates subsumed under 'sociodemographics' (see Results) were matched within and between groups. Importantly, there was no difference in trait and state aspects of both anxiety and affect between the active and the sham group, allowing for direct comparison between groups. Solely, changes in positive and negative affect were observed across groups, i.e. both positive and negative PANAS values were higher before each measurement compared to after. Importantly, PANAS scores that on average roughly changed to the same extend at each session (there was no interaction with the factor testing session), are unlikely to impact TRT reliability. Reduction in both positive and negative affect after as compared to before the beginning of each measurement (independent of stimulation condition) may reflect an overall tiring due to a one-and-a-half-hour testing session.

Apart from between-subject changes, we also took potential influences on intra-individual variability into account, such as attentional level, time of day and hormonal fluctuations (for review see Ridding and Ziemann, 2010). To exclude possible effects of hormonal cycles between sessions, we only included men in our study (De Bondt et al., 2015). In addition, we tried to keep day time of measurement constant between sessions within participants to avoid daily variations in vigilance and attention. Another possible source of within-subject variability is novelty. At first testing, most participants are naïve to MRI measurements and stimulation, implicating higher levels of anxiety, which in turn can affect cortical excitability (Wassermann et al., 2001). For example, heart rates have been shown to be especially high at the beginning of MRI investigations (van Minde et al., 2014) and equally sensing a stimulation for the first time may cause intensified physical and mental reactions. Our study design allows for verifying novelty as confounding factor and to ensure stable experiences with MRI and tDCS across participants. All participants attended three testing sessions, such that inter-session TRT reliability could be evaluated three times (testing session 1–2, 1–3 and 2–3), including one evaluation to which novelty aspects do not apply (testing session 2–3). Across groups and measurements, frequency distributions of novelty-unaffected ICC evaluations (ICC-pair 23) showed large overlap with ICC evaluations containing the first testing-session (ICC-pair 12 and ICC-pair13). Hence, ICC levels may be treated as comparable, suggesting no effect of the first measurement on neither baseline nor post-tDCS ICC values. Group-level analyses of active-tDCS effects at each time point also argue against an influence of the first testing session on ICC levels, because consistently appearing effects were not limited to the comparison between testing session 2 and 3, but already were present at first testing session. Taken together, novelty did not seem to influence ICC evaluations.

TDCS effect at each testing session

When discussing our results, we also must take into account the possibility that the main effect of tDCS on RS fcMRI has been missed. This consideration is presumably a methodical short-coming that is hardly avoidable because consistent ROIs across subjects are required for ICC calculations but are unsuitable for capturing individual responses to tDCS. However, analyses steps of our approach were considered thoroughly and relied on reviewed up-to-date literature. For example, ROIs were placed in regions where F3-F4 stimulation is most likely to exert an effect according to computational models (Bai et al., 2014; DaSilva et al., 2015; Nelson et al., 2014; Seibt et al., 2015; Woods et al., 2015). Additionally, our ROIs covered prefrontal regions where a tDCS effect was reported before (Keeser et al., 2011; Pena-Gomez et al., 2012). In order to account for local differences in the brain's responses to tDCS and thus to increase reliability, regions of expected effects were subdivided into clusters by means of the Sallet atlas, which provides a functional-connectivity-based parcellation of the DLPFC (Sallet et al., 2013). By evaluating a group-tDCS effect across ROIs in each hemisphere (i.e. the three different ROIs in each hemisphere were merged) at each testing session, we were provided with the possibility to roughly test our assumptions. Although comparisons between ICC levels and group-tDCS effects at each testing session is not optimal with this approach, approximations are possible.

With regard to the ROI-based approach, only the right-hemisphere ROI exhibited an effect after tDCS in terms of increased connectivity at testing session 1. Concurrently, within-ROI functional connectivity descriptively showed a clear difference in ICC frequency-distributions between baseline and post-tDCS measurements of the active group. This observation may reflect intra-individual variability of tDCS responses and fits to our group-level findings, showing only one tDCS effect at one testing session on within-ROI functional connectivity and thus missing any consistent pattern: When tDCS effects are highly variable already at an intra-individual level, it is likely that the effect is even less consistent at an inter-individual level averaged across groups. Altogether, in the ROI-based approach, reliability values may mirror the stability of tDCS effects observed at a group level. However, no definite comparison can be made between ICC levels and tDCS effects both based on coherent, yet different ROIs.

Therefore, we also followed a whole-brain approach by means of ICA. Here, more direct comparisons between tDCS effects and ICCs are possible, because group analyses of tDCS effects at all time points are available for each RSN separately. Following previous literature, RSNs showing a tDCS effect were selected (Keeser et al., 2011; Pena-Gomez et al., 2012). Again, this procedure keeps open the option of missed effects within another RSN. Still, within each RSN we were able to

investigate the whole brain in a hypotheses-free way. Here, group-level analyses revealed several active-tDCS effects. Most of these effects were unique to the active group (i.e. no overlapping directional contrasts between the active and sham group) with some of them even being repeatedly observable across two or three testing sessions. At an intra-individual level, no clear differences between ICC frequency-distributions appeared: in both groups distributions of baseline and post measurements were largely overlapping. Theoretically, tDCS may have exerted different effects on ICA- versus ROI-derived functional connections. In this case, it may be that comparable baseline and post-tDCS measurements in the active group, which range within the ICC levels of the sham group, may reflect a consistent tDCS effect. This speculation would be in accordance with repeatedly occurring tDCS effects observed at a group level. However, the uncorrected level, at which group-tDCS effects were reported, should not be overinterpreted. Therefore, it may also be that tDCS did not affect ICA networks at all, resulting in overlapping ICC-distributions for baseline and post-tDCS measurements similar to the sham group. Finally, it may also be possible, that low baseline TRT reliability undermined clear differences between baseline and post-tDCS measurements in the ICA approach.

Unspecific and placebo effects

Multiple factors may contribute to the considerable intra- and inter-subject variability observed here. For sham tDCS, baseline and post-tDCS TRT reliability were similar at an individual level. In contrast, group-level analyses showed differences between connectivity patterns before and after sham tDCS. Theoretically, it would be interesting to further analyse this placebo effect and its specific and non-specific compounds. Usually, an intervention, especially one that is physical sensible, triggers expectations (positive or negative ones), which contribute to the measured overall outcome (Gomm, 2009; Supino, 2012). Consequently, to receive the real or true effect induced by the intervention alone, it is necessary to subtract the specific placebo effect (including expectation and anxiety) from the effect as measured following an active intervention. However, we cannot further interpret our placebo effect because our design with two parallel groups does not allow discrimination between such placebo-specific effects, and non-specific overall effects of the intervention or setting. In order to analyse the effect of sham tDCS itself and its TRT reliability, a third arm including a second control group, i.e. a no-stimulation control, would be needed in future studies.

Limitations of the study

There are several methodological limitations of our study. Both inter- and intra-subject variability may be related to the stimulation itself. We did not employ a highly standardised or even MRI-guided electrode positioning system which would serve to minimalize variability of montages (Seibt et al., 2015). At the same time, tDCS with electrodes covering an area of 35 cm^2 is not focal and displacement of the electrodes by 1 cm may not have any significant impact on current flow (Bai et al., 2014). As we adhered to the EEG 10–20 system during positioning of the electrodes and always kept a distance of 6 cm between the sponges, we consider variability between montages within this range. Still, we cannot exclude influences of electrode positioning on TRT reliability, particularly because findings on small drifts in electrode positions are ambiguous and controversially discussed (Woods et al., 2015). Also, amount of NaCl was not standardised across participants and sessions, possibly, in the case of oversaturation of the sponges, leading to diverse stimulation targets due to irrepressible diffusion of the liquid and hence of the current.

Another limitation of our study is the small sample size that hampers inferences on the general population (Button et al., 2013). As this study was designed a pilot for further TRT experiments with larger sample sizes, only 10 subjects were investigated in each group. Consequently, our analyses should be considered as exploratory. Still, each subject was measured three times with two scans each time, resulting in a total of 120 RS scans.

Further, our study design, which followed practical needs on the one hand, faces statistical shortcomings on the other hand. We have chosen a parallel design to control potentially confounding factors. First, a parallel design allows to keep a sham-tDCS group free of any active tDCS across different time points and thus avoids carry-over effects from active to sham conditions. Secondly, subjects participating in a cross-over study can directly compare active and sham tDCS and may distinguish both based on subtly different skin reactions or sensations (Palm et al., 2014). Nevertheless, a crossover designs would have had statistical advantages, particularly at small sample sizes.

It is also important to emphasize that we investigated the main, i.e. group effect of tDCS by analysing changes from baseline to post tDCS, whereas we used only post-tDCS measurements for evaluating the TRT reliability of tDCS effects. This approach was chosen in order to assure a similar range of variability and allow comparisons between baseline reliability and reliability of tDCS responses. When individual contrast maps, i.e. differences between pre and post scans, are created, active-tDCS-related but also other variations, i.e. specific placebo as well as non-specific overall effects, may take effect and may artificially increase variability for both tDCS conditions. Similarities between post and baseline are subtracted out, leaving only non-specific and placebo-related variations in the sham group and a mixture of tDCS-related (if available) and non-specific changes in the active group. Consequently, as shown in Inline Supplementary table 5, no differences between groups in reliability of contrast maps could be found. To minimize the influence of these factors, we chose post-tDCS measurements as main output measure reflecting the tDCS response. Post active- and post-sham tDCS-effects – contrary to pre-post differences– showed rather distinct ICC values and can be regarded as independent, arguing in favour of our approach. Still, when comparing group tDCS effects with intra-individual TRT reliability of post-tDCS measurements, with this approach, we are examining different dimensions of tDCS responses.

The full extent of tDCS-related variability needs to be systematically addressed in future studies by including further control conditions (Atri et al., 2011; Plichta et al., 2012) into the experimental designs. Moreover, all efforts should be made to standardise the intervention (e.g. electrode positioning), individual predispositions (e.g. sleep, stress associated factors) and setting conditions (e.g. time of the day) as far as possible.

Conclusion

Reproducibility of data is an important issue in MRI research (Nichols et al., 2016), but also in combined neuroimaging-stimulation approaches in order to differentiate variable versus constant components of tDCS-induced modulation. Intra- as well as inter-individual variability in tDCS responses should be considered when evaluating tDCS as a therapeutic tool. Through identifying sources of this variability, possible responders could be distinguished from non-responders and effective treatment protocols with respect to time lag between stimulations and amount of treatment sessions could be designed.

This study investigated the TRT reliability of prefrontal tDCS-induced RS-fcMRI modulation for the first time. The analysis of individual responses to active tDCS across three testing sessions revealed none to low reliability, in comparison with baseline RS-fcMRI measurements and sham tDCS which did not reduce TRT reliability to such extend. Reduction in reliability from baseline to post tDCS was most notably for functional networks that also exhibited no consistent active-tDCS effect across testing sessions at a group level, suggesting that active tDCS induced additional variability and reduced TRT reliability. Further studies using a standardised positioning system and a higher sample size are warranted. Moreover, possible

sources of intra- and inter-subject variability need to be investigated in more detail.

Conflict of interest

F.P. has received speaker's honorarium from Mag & More GmbH and the neuroCare Group as well as support with equipment from neuroConn GmbH, Ilmenau, Germany, Mag & More GmbH and Brainsway Inc., Jerusalem, Israel. A. H. reports no conflicts of interest related to this work.

Acknowledgements

This work was supported by the German Center for Brain Stimulation (GCBS) research consortium (Work Package 5, grant number: 01EE1403E), funded by the Federal Ministry of Education and Research (BMBF). This work is part of the PhD thesis of J.W. We very much thank Julia Dillard for her support.

We plan to make all future data (http://www.gcbs.network/gcbs/projects/human-models/Work-Package-5.html) publicly available and try to provide this possibility for previous data as well. A general ethical approval has been submitted for the Psychiatric Imaging Network Germany (PING): http://www.ping.rwth-aachen.de/ to publish all neuroimaging data of several BMBF funded projects.

Appendix A. Supporting information

Supplementary data associated with this article can be found in the online version at doi:10.1016/j.neuroimage.2017.04.052.

References

Atri, A., O'Brien, J.L., Sreenivasan, A., Rastegar, S., Salisbury, S., DeLuca, A.N., O'Keefe, K.M., LaViolette, P.S., Rentz, D.M., Locascio, J.J., Sperling, R.A., 2011. Test-retest reliability of memory task functional magnetic resonance imaging in Alzheimer disease clinical trials. Arch. Neurol. 68, 599–606.

Bai, S., Dokos, S., Ho, K.A., Loo, C., 2014. A computational modelling study of transcranial direct current stimulation montages used in depression. Neuroimage 87, 332–344.

Bartelle, B.B., Barandov, A., Jasanoff, A., 2016. Molecular fMRI. J Neurosci. 36, 4139–4148.

Beckmann, C.F., Smith, S.M., 2004. Probabilistic independent component analysis for functional magnetic resonance imaging. IEEE Trans. Med Imaging 23, 137–152.

Beckmann, C.F., DeLuca, M., Devlin, J.T., Smith, S.M., 2005. Investigations into resting-state connectivity using independent component analysis. Philos. Trans. R Soc. Lond. B Biol. Sci. 360, 1001–1013.

Bikson, M., Datta, A., Rahman, A., Scaturro, J., 2010. Electrode montages for tDCS and weak transcranial electrical stimulation: role of "return" electrode's position and size. Clin. Neurophysiol. 121, 1976–1978.

Bikson, M., Grossman, P., Thomas, C., Zannou, A.L., Jiang, J., Adnan, T., Mourdoukoutas, A.P., Kronberg, G., Truong, D., Boggio, P., Brunoni, A.R., Charvet, L., Fregni, F., Fritsch, B., Gillick, B., Hamilton, R.H., Hampstead, B.M., Jankord, R., Kirton, A., Knotkova, H., Liebetanz, D., Liu, A., Loo, C., Nitsche, M.A., Reis, J., Richardson, J.D., Rotenberg, A., Turkeltaub, P.E., Woods, A.J., 2016. Safety of transcranial direct current stimulation: evidence based update 2016. Brain Stimul. 9, 641–661.

Biswal, B.B., Mennes, M., Zuo, X.N., Gohel, S., Kelly, C., Smith, S.M., Beckmann, C.F., Adelstein, J.S., Buckner, R.L., Colcombe, S., Dogonowski, A.M., Ernst, M., Fair, D., Hampson, M., Hoptman, M.J., Hyde, J.S., Kiviniemi, V.J., Kotter, R., Li, S.J., Lin, C.P., Lowe, M.J., Mackay, C., Madden, D.J., Madsen, K.H., Margulies, D.S., Mayberg, H.S., McMahon, K., Monk, C.S., Mostofsky, S.H., Nagel, B.J., Pekar, J.J., Peltier, S.J., Petersen, S.E., Riedl, V., Rombouts, S.A., Rypma, B., Schlaggar, B.L., Schmidt, S., Seidler, R.D., Siegle, G.J., Sorg, C., Teng, G.J., Veijola, J., Villringer, A., Walter, M., Wang, L., Weng, X.C., Whitfield-Gabrieli, S., Williamson, P., Windischberger, C., Zang, Y.F., Zhang, H.Y., Castellanos, F.X., Milham, M.P., 2010. Toward discovery science of human brain function. Proc. Natl. Acad. Sci. USA 107, 4734–4739.

Blautzik, J., Keeser, D., Berman, A., Paolini, M., Kirsch, V., Mueller, S., Coates, U., Reiser, M., Teipel, S.J., Meindl, T., 2013. Long-term test-retest reliability of resting-state networks in healthy elderly subjects and with amnestic mild cognitive impairment patients. J Alzheimers Dis. 34, 741–754.

Boly, M., Phillips, C., Balteau, E., Schnakers, C., Degueldre, C., Moonen, G., Luxen, A., Peigneux, P., Faymonville, M.E., Maquet, P., Laureys, S., 2008. Consciousness and cerebral baseline activity fluctuations. Hum. Brain Mapp. 29, 868–874.

Braun, U., Plichta, M.M., Esslinger, C., Sauer, C., Haddad, L., Grimm, O., Mier, D., Mohnke, S., Heinz, A., Erk, S., Walter, H., Seiferth, N., Kirsch, P., Meyer-Lindenberg, A., 2012. Test-retest reliability of resting-state connectivity network characteristics using fMRI and graph theoretical measures. Neuroimage 59, 1404–1412.

Buckholtz, J.W., Meyer-Lindenberg, A., 2012. Psychopathology and the human connectome: toward a transdiagnostic model of risk for mental illness. Neuron 74, 990–1004.

Button, K.S., Ioannidis, J.P., Mokrysz, C., Nosek, B.A., Flint, J., Robinson, E.S., Munafo, M.R., 2013. Power failure: why small sample size undermines the reliability of neuroscience. Nat. Rev. Neurosci. 14, 365–376.

Callan, D.E., Falcone, B., Wada, A., Parasuraman, R., 2016. Simultaneous tDCS-fMRI Identifies Resting State Networks Correlated with Visual Search Enhancement. Front Hum. Neurosci. 10, 72.

Carroll, T.J., Riek, S., Carson, R.G., 2001. Reliability of the input-output properties of the cortico-spinal pathway obtained from transcranial magnetic and electrical stimulation. J Neurosci. Methods 112, 193–202.

Catani, M., Dell'acqua, F., Thiebaut de Schotten, M., 2013. A revised limbic system model for memory, emotion and behaviour. Neurosci. Biobehav Rev. 37, 1724–1737.

Chew, T., Ho, K.A., Loo, C.K., 2015. Inter- and intra-individual variability in response to transcranial direct current stimulation (tDCS) at varying current intensities. Brain Stimul. 8, 1130–1137.

Cicchetti, D.V., 1994. Guidelines, criteria, and rules of thumb for evaluating normed and standardized assessment instruments in psychology. Psychol. Assess. 6, 284–290.

Craddock, R.C., James, G.A., Holtzheimer, P.E., 3rd, Hu, X.P., Mayberg, H.S., 2012. A whole brain fMRI atlas generated via spatially constrained spectral clustering. Hum. Brain Mapp. 33, 1914–1928.

Damoiseaux, J.S., Rombouts, S.A., Barkhof, F., Scheltens, P., Stam, C.J., Smith, S.M., Beckmann, C.F., 2006. Consistent resting-state networks across healthy subjects. Proc. Natl. Acad. Sci. USA 103, 13848–13853.

DaSilva, A.F., Truong, D.Q., DosSantos, M.F., Toback, R.L., Datta, A., Bikson, M., 2015. State-of-art neuroanatomical target analysis of high-definition and conventional tDCS montages used for migraine and pain control. Front Neuroanat. 9, 89.

Datta, A., Bansal, V., Diaz, J., Patel, J., Reato, D., Bikson, M., 2009. Gyri-precise head model of transcranial direct current stimulation: improved spatial focality using a ring electrode versus conventional rectangular pad. Brain Stimul. 2, 201–207.

De Bondt, T., Smeets, D., Pullens, P., Van Hecke, W., Jacquemyn, Y., Parizel, P.M., 2015. Stability of resting state networks in the female brain during hormonal changes and their relation to premenstrual symptoms. Brain Res. 1624, 275–285.

Dyke, K., Kim, S., Jackson, G.M., Jackson, S.R., 2016. Intra-subject consistency and reliability of response following 2 mA transcranial direct current stimulation. Brain Stimul. 9, 819–825.

Edwards, D., Cortes, M., Datta, A., Minhas, P., Wassermann, E.M., Bikson, M., 2013. Physiological and modeling evidence for focal transcranial electrical brain stimulation in humans: a basis for high-definition tDCS. Neuroimage 74, 266–275.

Filippi, M., van den Heuvel, M.P., Fornito, A., He, Y., Hulshoff Pol, H.E., Agosta, F., Comi, G., Rocca, M.A., 2013. Assessment of system dysfunction in the brain through MRI-based connectomics. Lancet Neurol. 12, 1189–1199.

Filippini, N., MacIntosh, B.J., Hough, M.G., Goodwin, G.M., Frisoni, G.B., Smith, S.M., Matthews, P.M., Beckmann, C.F., Mackay, C.E., 2009. Distinct patterns of brain activity in young carriers of the APOE-epsilon4 allele. Proc. Natl. Acad. Sci. U S A 106, 7209–7214.

Flöel, A., 2014. tDCS-enhanced motor and cognitive function in neurological diseases. Neuroimage 85 (Part 3), 934–947.

Fornito, A., Zalesky, A., Breakspear, M., 2015. The connectomics of brain disorders. Nat. Rev. Neurosci. 16, 159–172.

Fox, M.D., Snyder, A.Z., Vincent, J.L., Corbetta, M., Van Essen, D.C., Raichle, M.E., 2005. The human brain is intrinsically organized into dynamic, anticorrelated functional networks. Proc. Natl. Acad. Sci. USA 102, 9673–9678.

Friston, K.J., Frith, C.D., Liddle, P.F., Frackowiak, R.S., 1993. Functional connectivity: the principal-component analysis of large (PET) data sets. J Cereb. Blood Flow Metab. 13, 5–14.

Galletta, E.E., Cancelli, A., Cottone, C., Simonelli, I., Tecchio, F., Bikson, M., Marangolo, P., 2015. Use of computational modeling to inform tDCS electrode montages for the promotion of language recovery in post-stroke aphasia. Brain Stimul. 8, 1108–1115.

Gomm, R., 2009. "Subject reactivity". Key Concepts in Social Research Methods. Palgrave Macmillan, London.

Gonzalez-Castillo, J., Chen, G., Nichols, T.E., Bandettini, P.A., 2016. Variance decomposition for single-subject task-based fMRI activity estimates across many sessions. Neuroimage.

Greicius, M.D., Krasnow, B., Reiss, A.L., Menon, V., 2003. Functional connectivity in the resting brain: a network analysis of the default mode hypothesis. Proc. Natl. Acad. Sci. USA 100, 253–258.

Hauser, T.U., Rutsche, B., Wurmitzer, K., Brem, S., Ruff, C.C., Grabner, R.H., 2016. Neurocognitive effects of transcranial direct current stimulation in arithmetic learning and performance: a simultaneous tDCS-fMRI study. Brain Stimul. 9, 850–858.

van den Heuvel, M.P., Hulshoff Pol, H.E., 2010. Exploring the brain network: a review on resting-state fMRI functional connectivity. Eur. Neuropsychopharmacol. 20, 519–534.

Holland, R., Leff, A.P., Josephs, O., Galea, J.M., Desikan, M., Price, C.J., Rothwell, J.C., Crinion, J., 2011. Speech facilitation by left inferior frontal cortex stimulation. Curr. Biol. 21, 1403–1407.

Horovitz, S.G., Braun, A.R., Carr, W.S., Picchioni, D., Balkin, T.J., Fukunaga, M., Duyn, J.H., 2009. Decoupling of the brain's default mode network during deep sleep. Proc. Natl. Acad. Sci. USA 106, 11376–11381.

Horvath, J.C., Vogrin, S.J., Carter, O., Cook, M.J., Forte, J.D., 2016. Effects of a common transcranial direct current stimulation (tDCS) protocol on motor evoked potentials found to be highly variable within individuals over 9 testing sessions. Exp. Brain Res 234, 2629–2642.

Insel, T.R., 2010. Faulty circuits. Sci. Am. 302, 44–51.
Jackson, M.P., Rahman, A., Lafon, B., Kronberg, G., Ling, D., Parra, L.C., Bikson, M., 2016. Animal models of transcranial direct current stimulation: methods and mechanisms. Clin. Neurophysiol. 127, 3425–3454.
Jamil, A., Batsikadze, G., Kuo, H.I., Labruna, L., Hasan, A., Paulus, W., Nitsche, M.A., 2016. Systematic evaluation of the impact of stimulation intensity on neuroplastic after-effects induced by transcranial direct current stimulation. J Physiol..
Jenkinson, M., Bannister, P., Brady, M., Smith, S., 2002. Improved optimization for the robust and accurate linear registration and motion correction of brain images. Neuroimage 17, 825–841.
Jung, Y.-J., Kim, J.-H., Im, C.-H., 2013. COMETS: a MATLAB toolbox for simulating local electric fields generated by transcranial direct current stimulation (tDCS). Biomed. Eng. Lett. 3, 39–46.
Kamen, G., 2004. Reliability of motor-evoked potentials during resting and active contraction conditions. Med Sci. Sport. Exerc 36, 1574–1579.
Keeser, D., Meindl, T., Bor, J., Palm, U., Pogarell, O., Mulert, C., Brunelin, J., Moller, H.J., Reiser, M., Padberg, F., 2011. Prefrontal transcranial direct current stimulation changes connectivity of resting-state networks during fMRI. J Neurosci. 31, 15284–15293.
Kekic, M., Boysen, E., Campbell, I.C., Schmidt, U., 2016. A systematic review of the clinical efficacy of transcranial direct current stimulation (tDCS) in psychiatric disorders. J Psychiatr. Res 74, 70–86.
Krishnamurthy, V., Gopinath, K., Brown, G.S., Hampstead, B.M., 2015. Resting-state fMRI reveals enhanced functional connectivity in spatial navigation networks after transcranial direct current stimulation. Neurosci. Lett. 604, 80–85.
Krohne, H.W., Egloff, B., Kohlmann, C.-W., Tausch, A., 1996. Untersuchungen mit einer deutschen Version der" Positive and Negative Affect Schedule"(PANAS). Diagnostica..
Kuo, M.F., Paulus, W., Nitsche, M.A., 2014. Therapeutic effects of non-invasive brain stimulation with direct currents (tDCS) in neuropsychiatric diseases. Neuroimage 85 (Pt 3), 948–960.
Lahey, M.A., Downey, R.G., Saal, F.E., 1983. Intraclass correlations: there's more there than meets the eye. Psychol. Bull. 93, 586–595.
Laird, A.R., Fox, P.M., Eickhoff, S.B., Turner, J.A., Ray, K.L., McKay, D.R., Glahn, D.C., Beckmann, C.F., Smith, S.M., Fox, P.T., 2011. Behavioral interpretations of intrinsic connectivity networks. J. Cogn. Neurosci. 23, 4022–4037.
Laumann, T.O., Gordon, E.M., Adeyemo, B., Snyder, A.Z., Joo, S.J., Chen, M.Y., Gilmore, A.W., McDermott, K.B., Nelson, S.M., Dosenbach, N.U., Schlaggar, B.L., Mumford, J.A., Poldrack, R.A., Petersen, S.E., 2015. Functional system and areal organization of a highly sampled individual human brain. Neuron 87, 657–670.
Laux, L., 1981. Das State-Trait-Angstinventar (STAI): theoretische Grundlagen und HandanweisungBeltz Test..
Laux, L., Spielberger, C.D., 1981. Das State-Trait-Angstinventar: stai.. Beltz, Weinheim.
Lefaucheur, J.P., Antal, A., Ayache, S.S., Benninger, D.H., Brunelin, J., Cogiamanian, F., Cotelli, M., De Ridder, D., Ferrucci, R., Langguth, B., Marangolo, P., Mylius, V., Nitsche, M.A., Padberg, F., Palm, U., Poulet, E., Priori, A., Rossi, S., Schecklmann, M., Vanneste, S., Ziemann, U., Garcia-Larrea, L., Paulus, W., 2016. Evidence-based guidelines on the therapeutic use of transcranial direct current stimulation (tDCS). Clin. Neurophysiol. 128, 56–92.
Liebetanz, D., Nitsche, M.A., Tergau, F., Paulus, W., 2002. Pharmacological approach to the mechanisms of transcranial DC-stimulation-induced after-effects of human motor cortex excitability. Brain 125, 2238–2247.
Livingston, S.C., Ingersoll, C.D., 2008. Intra-rater reliability of a transcranial magnetic stimulation technique to obtain motor evoked potentials. Int. J Neurosci. 118, 239–256.
Lopez-Alonso, V., Fernandez-Del-Olmo, M., Costantini, A., Gonzalez-Henriquez, J.J., Cheeran, B., 2015. Intra-individual variability in the response to anodal transcranial direct current stimulation. Clin. Neurophysiol. 126, 2342–2347.
Malcolm, M.P., Triggs, W.J., Light, K.E., Shechtman, O., Khandekar, G., Gonzalez Rothi, L.J., 2006. Reliability of motor cortex transcranial magnetic stimulation in four muscle representations. Clin. Neurophysiol. 117, 1037–1046.
McGonigle, D.J., 2012. Test-retest reliability in fMRI: or how I learned to stop worrying and love the variability. Neuroimage 62, 1116–1120.
Mega, M.S., Cummings, J.L., 1994. Frontal-subcortical circuits and neuropsychiatric disorders. J Neuropsychiatry Clin. Neurosci. 6, 358–370.
Meinzer, M., Antonenko, D., Lindenberg, R., Hetzer, S., Ulm, L., Avirame, K., Flaisch, T., Floel, A., 2012. Electrical brain stimulation improves cognitive performance by modulating functional connectivity and task-specific activation. J Neurosci. 32, 1859–1866.
Meinzer, M., Lindenberg, R., Antonenko, D., Flaisch, T., Floel, A., 2013. Anodal transcranial direct current stimulation temporarily reverses age-associated cognitive decline and functional brain activity changes. J Neurosci. 33, 12470–12478.
Meinzer, M., Lindenberg, R., Phan, M.T., Ulm, L., Volk, C., Floel, A., 2014. Transcranial direct current stimulation in mild cognitive impairment: behavioral effects and neural mechanisms. Alzheimers Dement 11, 1032–1040.
Mendonca, M.E., Santana, M.B., Baptista, A.F., Datta, A., Bikson, M., Fregni, F., Araujo, C.P., 2011. Transcranial DC stimulation in fibromyalgia: optimized cortical target supported by high-resolution computational models. J Pain 12, 610–617.
Menon, V., 2011. Large-scale brain networks and psychopathology: a unifying triple network model. Trends Cogn. Sci. 15, 483–506.
Miller, K.J., Weaver, K.E., Ojemann, J.G., 2009. Direct electrophysiological measurement of human default network areas. Proc. Natl. Acad. Sci. USA 106, 12174–12177.
Miranda, P.C., Lomarev, M., Hallett, M., 2006. Modeling the current distribution during transcranial direct current stimulation. Clin. Neurophysiol. 117, 1623–1629.
Monte-Silva, K., Kuo, M.F., Hessenthaler, S., Fresnoza, S., Liebetanz, D., Paulus, W., Nitsche, M.A., 2013. Induction of late LTP-like plasticity in the human motor cortex by repeated non-invasive brain stimulation. Brain Stimul. 6, 424–432.
Mueller, S., Wang, D., Fox, M.D., Yeo, B.T., Sepulcre, J., Sabuncu, M.R., Shafee, R., Lu, J., Liu, H., 2013. Individual variability in functional connectivity architecture of the human brain. Neuron 77, 586–595.
Nasseri, P., Nitsche, M.A., Ekhtiari, H., 2015. A framework for categorizing electrode montages in transcranial direct current stimulation. Front. Hum. Neurosci. 9, 54.
Nelson, J.T., McKinley, R.A., Golob, E.J., Warm, J.S., Parasuraman, R., 2014. Enhancing vigilance in operators with prefrontal cortex transcranial direct current stimulation (tDCS). Neuroimage 85 (Pt 3), 909–917.
Neuling, T., Wagner, S., Wolters, C.H., Zaehle, T., Herrmann, C.S., 2012. Finite-Element Model Predicts Current Density Distribution for Clinical Applications of tDCS and tACS. Front Psychiatry 3, 83.
Nichols, T.E., Das, S., Eickhoff, S.B., Evans, A.C., Glatard, T., Hanke, M., Kriegeskorte, N., Milham, M.P., Poldrack, R.A., Poline, J.-B., 2016. Best Practices in Data Analysis and Sharing in Neuroimaging using MRI. bioRxiv, 054262.
Nitsche, M.A., Paulus, W., 2000. Excitability changes induced in the human motor cortex by weak transcranial direct current stimulation. J Physiol. 527 (Pt 3), 633–639.
Nitsche, M.A., Paulus, W., 2001. Sustained excitability elevations induced by transcranial DC motor cortex stimulation in humans. Neurology 57, 1899–1901.
Nitsche, M.A., Liebetanz, D., Antal, A., Lang, N., Tergau, F., Paulus, W., 2003. Modulation of cortical excitability by weak direct current stimulation–technical, safety and functional aspects. Suppl. Clin. Neurophysiol. 56, 255–276.
Oldfield, R.C., 1971. The Assessment and Analysis of Handedness: the Edinburgh Inventory. Neuropsychologia 9, 97–113.
Palm, U., Keeser, D., Blautzik, J., Pogarell, O., Ertl-Wagner, B., Kupka, M.J., Reiser, M., Padberg, F., 2013a. Prefrontal transcranial direct current stimulation (tDCS) changes negative symptoms and functional connectivity MRI (fcMRI) in a single case of treatment-resistant schizophrenia. Schizophr. Res 150, 583–585.
Palm, U., Reisinger, E., Keeser, D., Kuo, M.-F., Pogarell, O., Leicht, G., Mulert, C., Nitsche, M.A., Padberg, F., 2013b. Evaluation of sham transcranial direct current stimulation for randomized, placebo-controlled clinical trials. Brain Stimul. 6, 690–695.
Palm, U., Feichtner, K.B., Hasan, A., Gauglitz, G., Langguth, B., Nitsche, M.A., Keeser, D., Padberg, F., 2014. The role of contact media at the skin-electrode interface during transcranial direct current stimulation (tDCS). Brain Stimul. 7, 762–764.
Palm, U., Keeser, D., Hasan, A., Kupka, M.J., Blautzik, J., Sarubin, N., Kaymakanova, F., Unger, I., Falkai, P., Meindl, T., Ertl-Wagner, B., Padberg, F., 2016. Prefrontal transcranial direct current stimulation for treatment of schizophrenia with predominant negative symptoms: a double-blind, sham-controlled proof-of-concept study. Schizophr. Bull. 42, 1253–1261.
Park, C.H., Chang, W.H., Park, J.Y., Shin, Y.I., Kim, S.T., Kim, Y.H., 2013. Transcranial direct current stimulation increases resting state interhemispheric connectivity. Neurosci. Lett. 539, 7–10.
Park, H.J., Friston, K., 2013. Structural and functional brain networks: from connections to cognition. Science 342, 579–587.
Parkin, B.L., Ekhtiari, H., Walsh, V.F., 2015. Non-invasive human brain stimulation in cognitive neuroscience: a primer. Neuron 87, 932–945.
Pena-Gomez, C., Sala-Lonch, R., Junque, C., Clemente, I.C., Vidal, D., Bargallo, N., Falcon, C., Valls-Sole, J., Pascual-Leone, A., Bartres-Faz, D., 2012. Modulation of large-scale brain networks by transcranial direct current stimulation evidenced by resting-state functional MRI. Brain Stimul. 5, 252–263.
Pereira, J.B., Junque, C., Bartres-Faz, D., Marti, M.J., Sala-Llonch, R., Compta, Y., Falcon, C., Vendrell, P., Pascual-Leone, A., Valls-Sole, J., Tolosa, E., 2013. Modulation of verbal fluency networks by transcranial direct current stimulation (tDCS) in Parkinson's disease. Brain Stimul. 6, 16–24.
Plichta, M.M., Schwarz, A.J., Grimm, O., Morgen, K., Mier, D., Haddad, L., Gerdes, A.B., Sauer, C., Tost, H., Esslinger, C., Colman, P., Wilson, F., Kirsch, P., Meyer-Lindenberg, A., 2012. Test-retest reliability of evoked BOLD signals from a cognitive-emotive fMRI test battery. Neuroimage 60, 1746–1758.
Polania, R., Paulus, W., Nitsche, M.A., 2012. Modulating cortico-striatal and thalamo-cortical functional connectivity with transcranial direct current stimulation. Hum. Brain Mapp. 33, 2499–2508.
Raemaekers, M., du Plessis, S., Ramsey, N.F., Weusten, J.M.H., Vink, M., 2012. Test–retest variability underlying fMRI measurements. Neuroimage 60, 717–727.
Ridding, M.C., Ziemann, U., 2010. Determinants of the induction of cortical plasticity by non-invasive brain stimulation in healthy subjects. J Physiol. 588, 2291–2304.
Sacco, K., Galetto, V., Dimitri, D., Geda, E., Perotti, F., Zettin, M., Geminiani, G.C., 2016. Concomitant use of transcranial direct current stimulation and computer-assisted training for the rehabilitation of attention in traumatic brain injured patients: behavioral and neuroimaging results. Front Behav. Neurosci. 10, 57.
Sallet, J., Mars, R.B., Noonan, M.P., Neubert, F.X., Jbabdi, S., O'Reilly, J.X., Filippini, N., Thomas, A.G., Rushworth, M.F., 2013. The organization of dorsal frontal cortex in humans and macaques. J Neurosci. 33, 12255–12274.
Schulz, R., Gerloff, C., Hummel, F.C., 2013. Non-invasive brain stimulation in neurological diseases. Neuropharmacology 64, 579–587.
Seibt, O., Brunoni, A.R., Huang, Y., Bikson, M., 2015. The pursuit of DLPFC: non-neuronavigated methods to target the left dorsolateral pre-frontal cortex with symmetric bicephalic Transcranial Direct Current Stimulation (tDCS). Brain Stimul. 8, 590–602.
Shine, J.M., Koyejo, O., Poldrack, R.A., 2016. Temporal metastates are associated with differential patterns of time-resolved connectivity, network topology, and attention. Proc. Natl. Acad. Sci. USA 113, 9888–9891.
Smith, S.M., 2002. Fast robust automated brain extraction. Hum. Brain Mapp. 17, 143–155.
Smith, S.M., Fox, P.T., Miller, K.L., Glahn, D.C., Fox, P.M., Mackay, C.E., Filippini, N., Watkins, K.E., Toro, R., Laird, A.R., Beckmann, C.F., 2009. Correspondence of the

brain's functional architecture during activation and rest. Proc. Natl. Acad. Sci. U S A 106, 13040–13045.
Spielberger, C.D., Gorsuch, R.L., Lushene, R.E., 1970. The State-Trait Anxiety Inventory (Test Manual). Consulting Psychologists, Palo Alto, CA.
Supino, P.G., 2012. Fundamental issues in evaluating the impact of interventions: sources and control of bias. In: Supino, P.G., Borer, J.S. (Eds.), Principles of Research Methodology: A Guide for Clinical Investigators.. Springer-Verlag, New York, 83.
Tandon, P., 2013. Not so "silent":the human prefrontal cortex. Neurol. India 61, 578–580.
Tavor, I., Parker Jones, O., Mars, R.B., Smith, S.M., Behrens, T.E., Jbabdi, S., 2016. Task-free MRI predicts individual differences in brain activity during task performance. Science 352, 216–220.
Tremblay, S., Lepage, J.-F., Latulipe-Loiselle, A., Fregni, F., Pascual-Leone, A., Théoret, H., 2014. The uncertain outcome of prefrontal tDCS. Brain Stimul. 7, 773–783.
van Minde, D., Klaming, L., Weda, H., 2014. Pinpointing moments of high anxiety during an MRI examination. Int. J. Behav. Med. 21, 487–495.
Vaz, S., Falkmer, T., Passmore, A.E., Parsons, R., Andreou, P., 2013. The case for using the repeatability coefficient when calculating test-retest reliability. PLoS One 8, e73990.
Vincent, J.L., Patel, G.H., Fox, M.D., Snyder, A.Z., Baker, J.T., Van Essen, D.C., Zempel, J.M., Snyder, L.H., Corbetta, M., Raichle, M.E., 2007. Intrinsic functional architecture in the anaesthetized monkey brain. Nature 447, 83–86.
Volpato, C., Piccione, F., Cavinato, M., Duzzi, D., Schiff, S., Foscolo, L., Venneri, A., 2013. Modulation of affective symptoms and resting state activity by brain stimulation in a treatment-resistant case of obsessive-compulsive disorder. Neurocase 19, 360–370.
Wassermann, E.M., Greenberg, B.D., Nguyen, M.B., Murphy, D.L., 2001. Motor cortex excitability correlates with an anxiety-related personality trait. Biol. Psychiatry 50, 377–382.
Watson, D., Clark, L.A., Tellegen, A., 1988. Development and validation of brief measures of positive and negative affect: the PANAS scales. J. Pers. Social. Psychol. 54, 1063.
Weber, M.J., Messing, S.B., Rao, H., Detre, J.A., Thompson-Schill, S.L., 2014. Prefrontal transcranial direct current stimulation alters activation and connectivity in cortical and subcortical reward systems: a tDCS-fMRI study. Hum. Brain Mapp. 35, 3673–3686.
Winkler, A.M., Ridgway, G.R., Webster, M.A., Smith, S.M., Nichols, T.E., 2014. Permutation inference for the general linear model. Neuroimage 92, 381–397.
Winkler, A.M., Webster, M.A., Vidaurre, D., Nichols, T.E., Smith, S.M., 2015. Multi-level block permutation. Neuroimage 123, 253–268.
Woods, A.J., Bryant, V., Sacchetti, D., Gervits, F., Hamilton, R., 2015. Effects of electrode drift in transcranial direct current stimulation. Brain Stimul. 8, 515–519.
Worsching, J., Padberg, F., Ertl-Wagner, B., Kumpf, U., Kirsch, B., Keeser, D., 2016. Imaging transcranial direct current stimulation (tDCS) of the prefrontal cortex-correlation or causality in stimulation-mediated effects? Neurosci. Biobehav Rev. 69, 333–356.
Zhou, J., Gennatas, E.D., Kramer, J.H., Miller, B.L., Seeley, W.W., 2012. Predicting regional neurodegeneration from the healthy brain functional connectome. Neuron 73, 1216–1227.
Ziemann, U., 2008. Pharmacology of TMS Measures. In: Wassermann, E.M., Epstein, C.M., Ziemann, U., Walsh, V., Paus, T., Lisanby, S.H. (Eds.), The Oxford Handbook of Transcranial Stimulation.. Oxford University Press, New York, 211–232.
Zuo, X.N., Kelly, C., Adelstein, J.S., Klein, D.F., Castellanos, F.X., Milham, M.P., 2010. Reliable intrinsic connectivity networks: test-retest evaluation using ICA and dual regression approach. Neuroimage 49, 2163–2177.

Supplementary Material

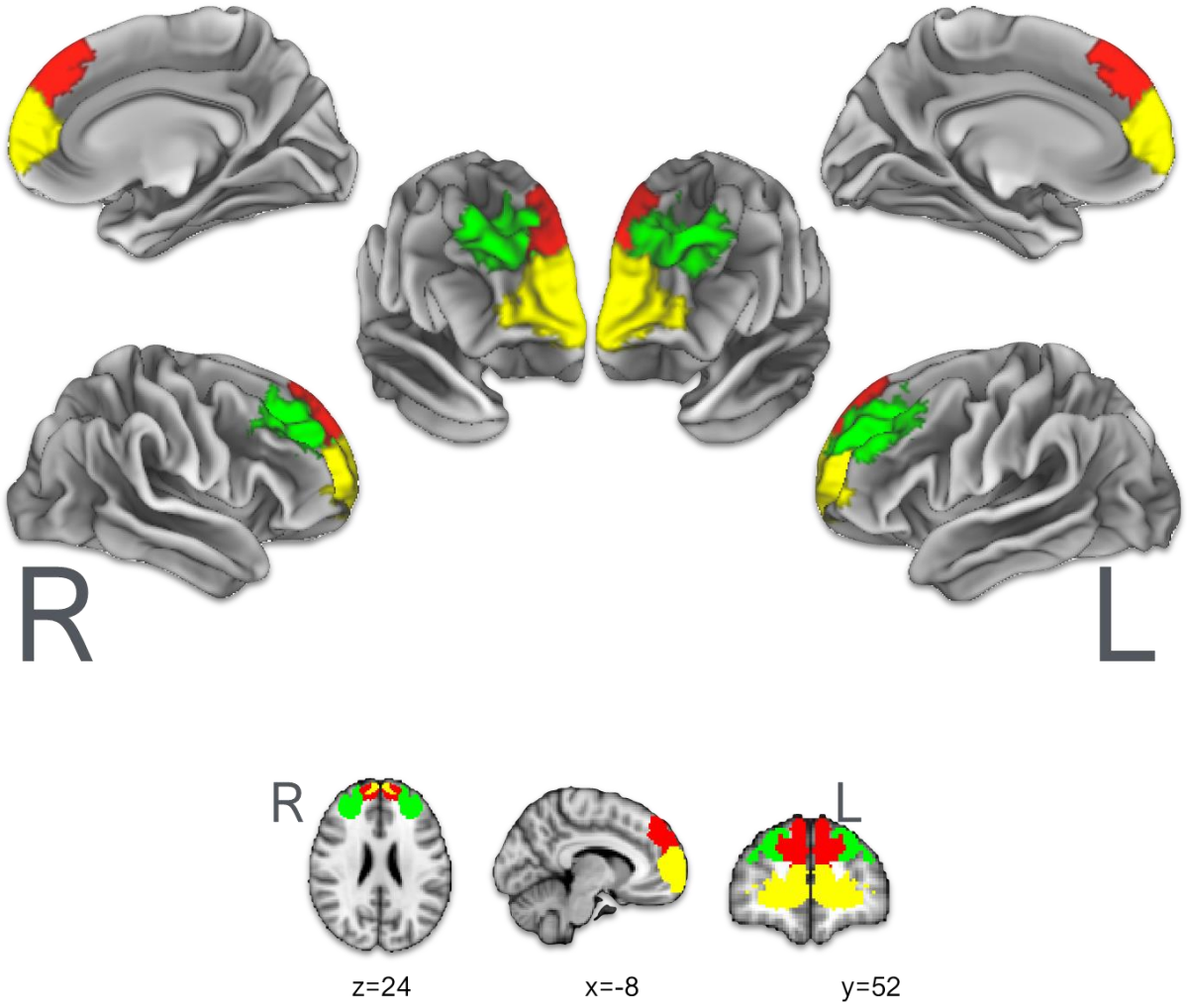

Supplementary Figure 1. Prefrontal regions of interest (ROI) selected for the ROI-based approach. Selection followed computational models. ROIs were extracted from the FSL atlas 'Sallet Dorsal Frontal connectivity-based parcellation' (Sallet et al., 2013) and drawn separately for the right and left hemisphere. yellow = area 10, green = area 46 dorsal part, red = area 9. Coordinates are given in MNI (x, y, z) space. L/R = left/right.

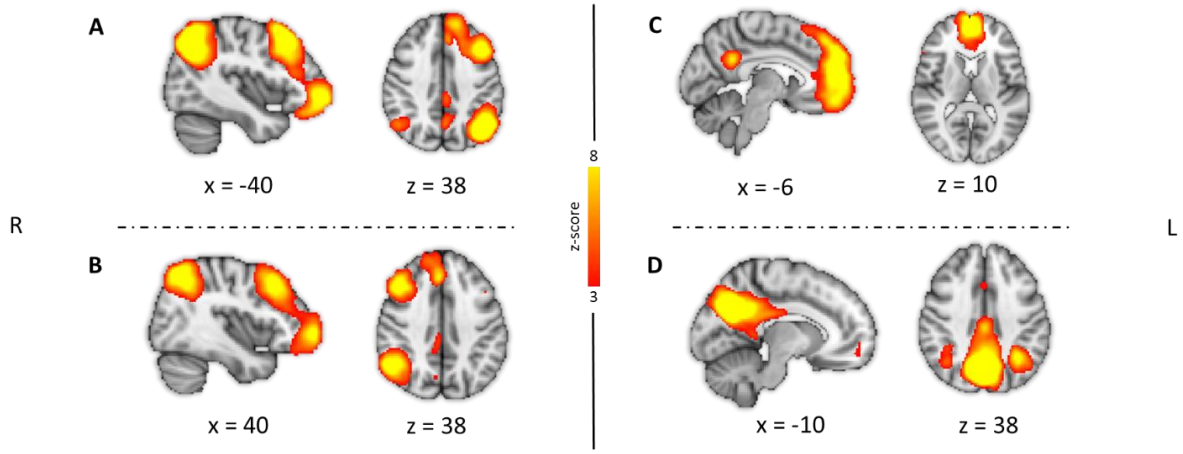

Supplementary Figure 2. Group analyses of resting-state network time series. Independent-component analyses (ICA) was run across all individuals and all conditions (baseline and post tDCS). Four networks were selected: a) left Frontal Parietal Network (FPN), b) right FPN, c) anterior Default Mode Network (DMN), d) posterior DMN. Coordinates (x, z) are given in MNI space. L/R = left/right.

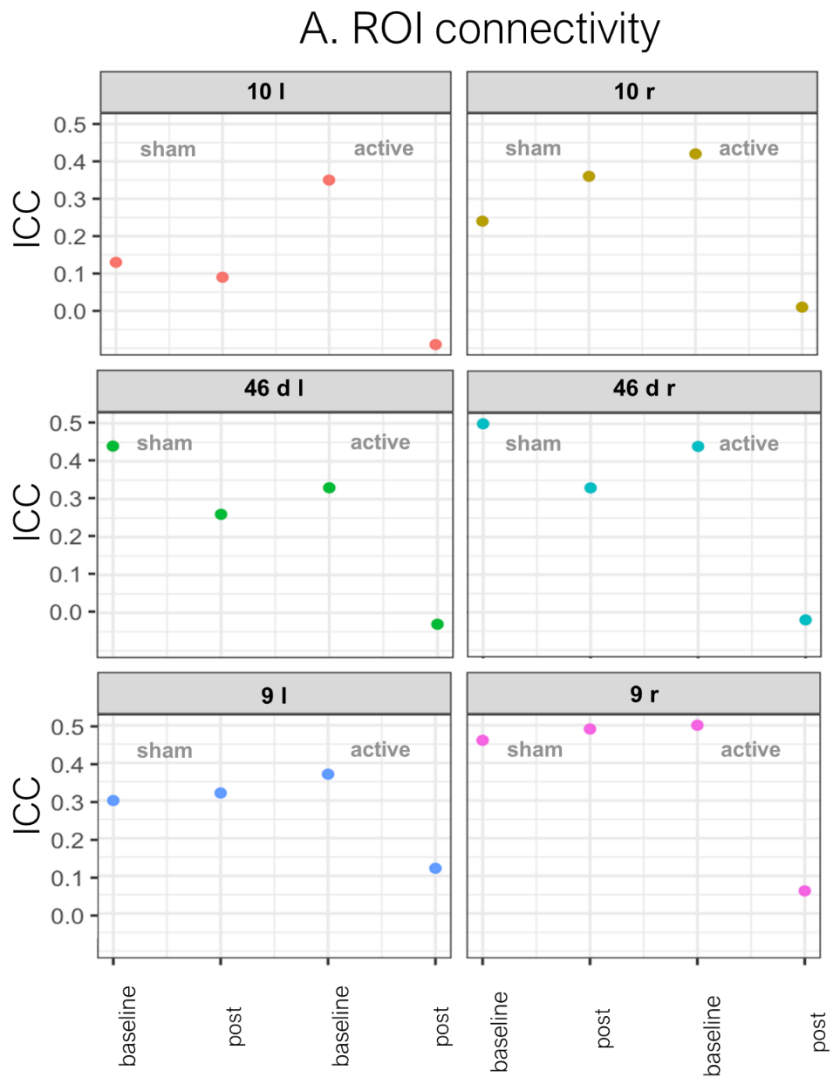

Supplementary Figure 3. Graphical illustration of median ICC-values resulting from voxel-wise ICC evaluations, separately for each measurement (baseline and post tDCS) and group (active and sham). a) Baseline and post-tDCS ICC-values of both groups (active and sham) resulting from the ROI-based approach. b) Baseline and post-tDCS ICC-values of both groups resulting from the ICA-based approach. DMN = Default Mode Network, FPN = Frontal Parietal Network, ICC = intra-class correlation coefficient, IC = independent component, l/r = left/right, ROI = region of interest, 10 = area 10 of the Sallet-atlas, 46d = area 46/9 dorsal of the Sallet-atlas, 9 = area 9 of the Sallet-atlas (Sallet et al., 2013).

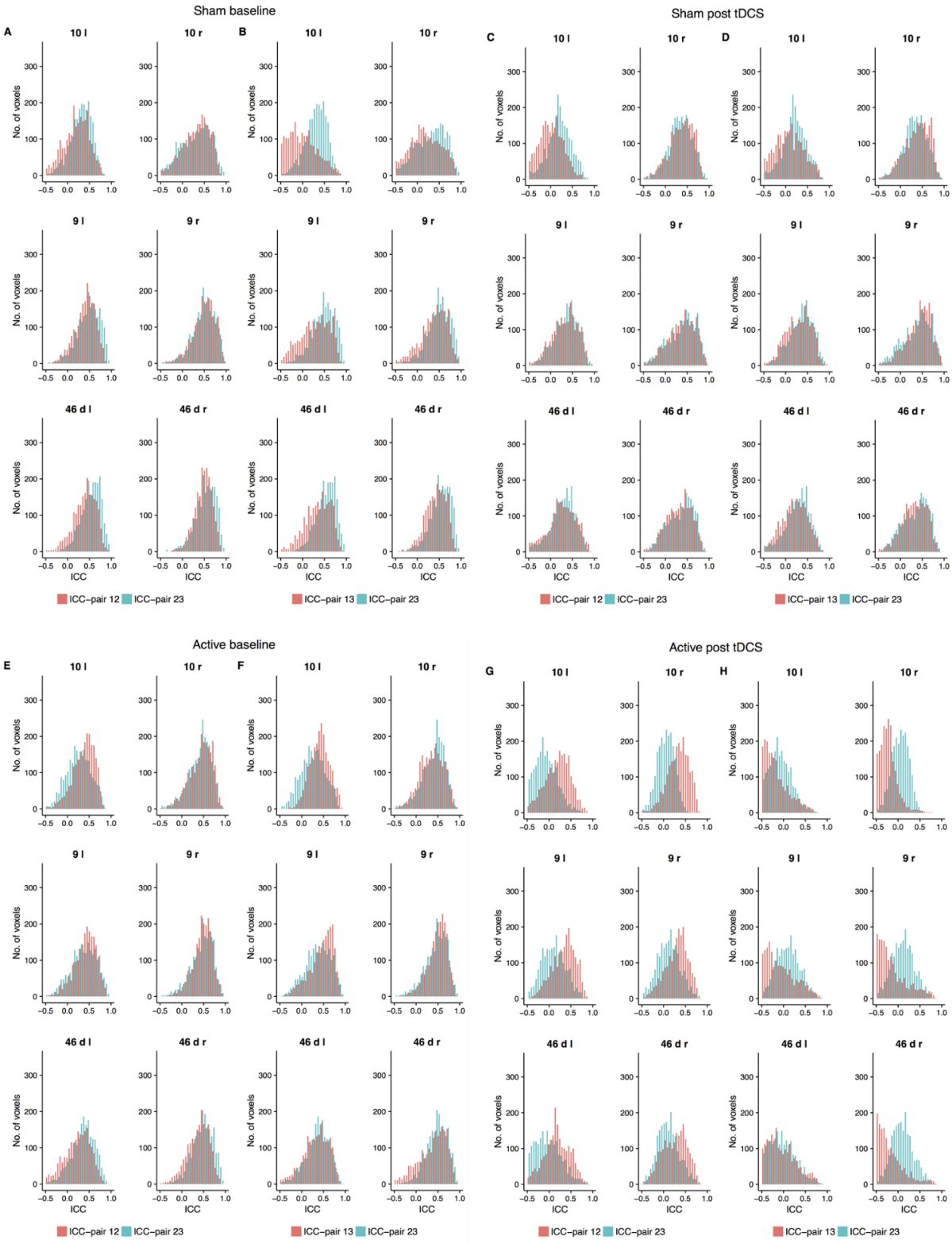

Supplementary Figure 4. Frequency distributions of voxel-wise ICC calculations within a region of interest (ROI). Colours represent frequency of ICC levels of ICC-pairs for the following conditions: a) + b) baseline sham, c) + d) post-tDCS sham, e) + f) baseline active, g) + h) post-tDCS active. ICC = intra-class correlation coefficient, l/r = left/right, 10 = area 10 of the Sallet-atlas, 46d = area 46/9 dorsal of the Sallet-atlas, 9 = area 9 of the Sallet-atlas (Sallet et al., 2013).

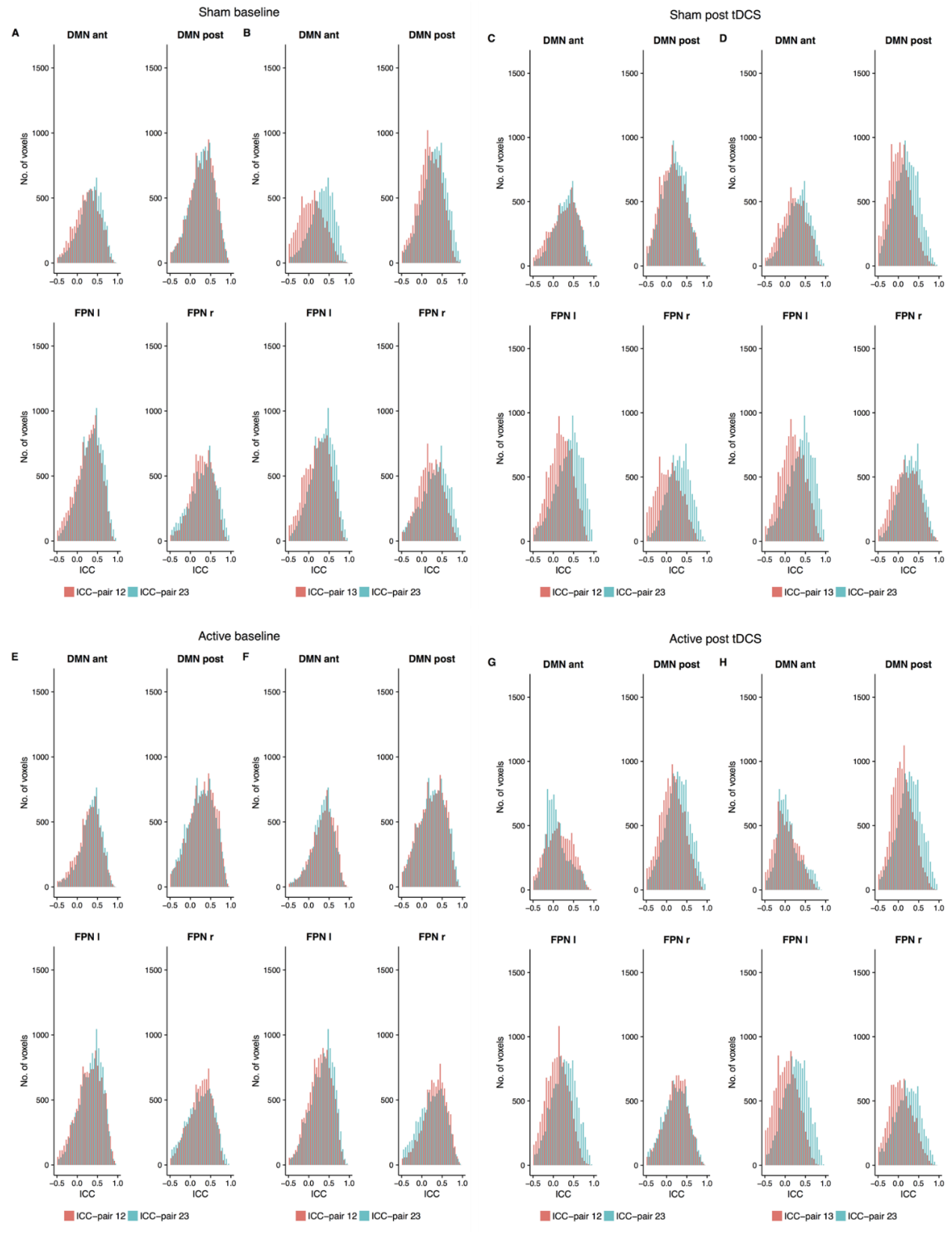

Supplementary Figure 5. Frequency distributions of voxel-wise ICC calculations within a resting-state network (RSN). Colours represent frequency of ICC levels of ICC-pairs for the following conditions: a) + b) baseline sham, c) + d) post-tDCS sham, e) + f) baseline active, g) + h) post-tDCS active. ant = anterior, DMN = Default Mode Network, FPN = Frontal Parietal Network, ICC = intra-class correlation coefficient, l/r = left/right, post = posterior.

RSN	Brain regions	Number of voxels	Brodman's area	Centre of gravity (MNI coordinates)		
				x	y	z
Post active tDCS > pre active tDCS						
t1						
RH						
	1) R Superior Frontal Gyrus	22	10	18.5	63.1	11.9
DMN anterior						
	1) Paracingulate Gyrus, BL Medial Frontal Gyrus	68	-, 10/9	-0.264	51.9	6.15
	2) R Superior Temporal Gyrus	37	22	43.2	-50.2	16.1
	3) R Causate, R Insula, R Claustrum	37	-, -, -	40.8	-21.5	-0.703
	4) R Paracentral Lobule	33	5/4	6.73	-36.6	62.2
	5) R Insula	32	13	47.4	-28.4	20.6
DMN posterior						
	1) R Middle Occipital Gyrus, R Middle Temporal Gyrus, R Superior Temporal Gyrus, R Superior Occipital Gyrus, R Sub-Gyral, R Angular Gyrus, R Precuneus	426	19, 39, 19, 19, 39, 39, 39	42.7	-68	28.7
	2) BL Medial Frontal Gyrus, BL Anterior Cingulate Gyrus	80	11/10, 32	-0.4	46.8	-14.5
	3) L Middle Occipital Gyrus, L Middle Temporal Gyrus	65	19, 39	-41.1	-74.4	16.9
	4) L Precuneus, L Sub-Gyral, L Paracentral Lobule	60	7, 40/7, 5/7	-20.7	-40	54.1
	5) R Superior Temporal Gyrus	44	22	40	-50.5	18.9

FPN l						
	1) R Postcentral Gyrus, R Precentral Gyrus, R Inferior Parietal Lobule	206	2/40/1/3, 4, 40	49	-20.4	48.3
	2) L Middle Frontal Gyrus, L Inferior Frontal Gyrus, L Sub-Gyral	61	10, 10, -	-37.4	44.2	-4.52
	3) L Middle Frontal Gyrus, L Inferior Frontal Gyrus, L Precentral Gyrus	50	8/9, 9, 6	-48.5	9.08	34.6
	4) R Precentral Gyrus, R Postcentral Gyrus	36	4, 3	33.8	-20.9	50.9
	5) R Parahippocampel Gyrus	36	27/30	25.6	-36.9	-1.06
	6) L Middle Occipital Gyrus, L Middle Temporal Gyrus	35	19,39	-40.6	-80.3	17.8
	7) L Middle Temporal Gyrus	21	21	-59.9	1.24	-19.7
FPN r						
	1) L Cuneus, L Posterior Cingulate, L Precuneus	31	18, 18, 31	-20	-67	24.3
	2) L Inferior Parietal Lobule	28	40	-56.4	-30.4	43.4
	3) R Precuneus, R Cuneus	24	19, 19	19.3	-82.1	44.8
	4) R Midbrain, R Thalamus	21	-, -	2.67	-17.7	-1.62
t2						
DMN anterior						
	1) R Transverse Temporal Gyrus, R Superior Temporal Gyrus, R Insula	28	41, 41, 13	42.5	-32	11.2
	2) L Thalamus	25	-	-20.1	-24.7	-0.8
	3) L Superior Temporal Gyrus, L Middle Temporal Gyrus	23	22	-52.3	-29.6	4

DMN posterior						
	1) R Medial Frontal Gyrus	54	9	8.7	51.5	14.3
	2) R Claustrum	41	-	32.7	-15.4	16.2
FPN l						
	1) R Middle Frontal Gyrus	167	6/8	32.2	14.7	38.8
	2) R Postcentral Gyrus, R Inferior Parietal Lobule, R Postcentral Gyrus	103	40, 40, 2/3	38.9	-33.2	50.9
	3) R Medial Frontal Gyrus, R Superior Frontal Gyrus	50	32, 6	17.3	19.9	46.5
	4) L Precentral Gyrus	36	9	-32.7	13.9	34.9
	5) R Precentral Gyrus	22	4	33.3	-21.6	55.3
FPN r						
	1) L Postcentral Gyrus, L Inferior Parietal Lobule	48	40/2, 40	-47.9	-27.6	53.2
	2) R Cuneus, R Precuneus	28	18/31, 31	18.7	-74.2	29.5
	3) L Superior Temporal Gyrus	26	13/22	-56.3	-39.8	21.7
t3						
DMN anterior						
	1) L Thalamus, L Caudate	52	-, -	-14.5	-12.8	17.8
DMN posterior						
	1) L Middle Frontal Gyrus, L Superior Frontal Gyrus	32	10, 9/10	-21.7	55.5	17.8
	2) L Medial Frontal Gyrus, L Superior Frontal Gyrus	25	8, 8	-5.36	39.8	43.3
FPN l						
	1) L Middle Frontal Gyrus, L Superior Frontal Gyrus, L Inferior Frontal Gyrus	83	10, 10, 10	-32.7	54.7	2.6
	2) BL Medial Frontal Gyrus, BL Anterior Cingulate	75	10, 10	3.92	55.4	-14.4

	3) L Middle Temporal Gyrus, L Inferior Temporal Gyrus	28	21, 21	-55.4	-13.4	-20.6
	4) R Cuneus, R Posterior Cingulate	26	30, 30	30.7	-71.7	15.5
FPN r						
	1) R Sub-Gyral, R Caudate, R Thalamus	175	-, -, -	27	-40.5	10.5
	2) R Parahippocampal Gyrus	51	36/35	22.5	-33.7	-14
	3) R Lentiform Nucleus, R Claustrum, R Caudate	38	-, -, -	20.9	19.1	-10.5
Post active tDCS < pre active tDCS						
t1						
DMN anterior						
	1) L Middle Frontal Gyrus, L Precentral Gyrus	226	8/9, 9	-38.2	28.8	30.6
	2) L Precentral Gyrus, L Postcentral Gyrus, L Sub-Gyral, L Middle Frontal	145	6/4, 3, 6, 6	-32.7	-3.32	53.5
	3) R Precentral Gyrus, R Middle Frontal Gyrus	71	6, 6	29.4	-5.83	52.6
	4) L Precentral Gyrus, L Inferior Frontal Gyrus	21	6, 44/9	-48.7	2.48	20.5
DMN posterior						
	1) L Precentral Gyrus, L Middle Frontal Gyrus	149	4/6, 6	-34.5	-7.18	54.7
	2) L Middle Frontal Gyrus, L Precentral Gyrus	116	8/9, 9	-39.2	31.7	36.3
	3) R Middle Frontal Gyrus	115	8/9	32.7	29.3	33
	4) R Middle Frontal Gyrus, R Superior Frontal Gyrus	78	9/10, 9/10	29.3	51.7	23.9
	5) R Inferior Frontal Gyrus	55	45/47	43.2	29.6	-1.75
	6) L Precentral Gyrus	45	4/6	-48.6	-5.47	44.8
	7) R Cingulate Gyrus	30	24	11.7	-2.67	38.1

	8) L Inferior Parietal Lobule, L Supramarginal Gyrus	25	40, 40	-52.8	-51.2	44.7
	9) R Middle Frontal Gyrus, R Precentral Gyrus	24	6, 6	38.8	-1.08	47.5
FPN l						
	1) L Medial Frontal Gyrus, L Cingulate Gyrus	62	6, 24	-7.58	-5.94	55.6
	2) L Middle Frontal Gyrus, L Precentral Gyrus	58	8/9, 9	-37.3	32.2	36.9
	3) R Medial Frontal Gyrus, R Cingulate Gyrus	56	6/8, 32	7.21	25.6	43.7
	4) BL Precuneus, R Paracentral Lobule	54	7, 5	1.26	-51.1	53.4
	5) L Precentral Gyrus	49	4/6	-34	-9.92	52.9
	6) L Superior Frontal Gyrus	29	9/10	-26.5	53.2	23.7
	7) R Middle Frontal Gyrus	23	6	37.7	-1.91	45.8
FPN r						
	-	-	-	-	-	-
t2						
DMN anterior						
	1) R Superiorr Frontal Gyrus, R Middle Frontal Gyrus	187	9, 9	43.6	40	26.6
	2) R Precentral Gyrus	53	6	35.5	5.69	32.7
	3) R Parahippocampal Gyrus, R Subcallosal Gyrus	23	4, 34	29.7	3.04	-16.2
DMN posterior						
	1) L Midbrain	24	-	-4.17	-35.2	-17.3

FPN l						
	1) L Middle Temporal Gyrus, L Middle Occipital Gyrus	136	19/37/39, 19/37	-46.8	-69.4	12.4
	2) L Superior Temporal Gyrus, L Middle Temporal Gyrus	52	39, 39	-51	-59.8	30.1
	3) L Posterior Cingulate	33	29/30	-0.303	-42.7	19.5
	4) Inferior Frontal Gyrus, L Extra-Nuclear	21	13, 13	-33.6	7.81	-15.4
	5) L Inferior Parietal Lobule, L Supramarginal Gyrus	21	40, 40	-54.3	-43.7	30.2
	6) R Precentral Gyrus, R Insula	21	44, 13	46	8.86	2
FPN r						
	1) R Middle Frontal Gyrus, R Superior Frontal Gyrus	133	9/10, 9/10	32.6	45.7	24.2
	2) L Anterior Cingulate, L Medial Frontal Gyrus, L Cingulate Gyrus	42	32, 9, 32	-7.05	28.7	26.2
	3) Anterior Cingulate Gyrus, Cingulate Gyrus	29	24, 32	2	32.1	21.8
	4) R Cingulate Gyrus	27	31	10	-28.9	39.3
	5) R Precentral Gyrus, L Inferior Frontal Gyrus	21	6, 44	-48.5	-1.62	18.3
t3						
DMN anterior						
	1) L Precuneus	31	7	-12.5	-65	49.2
DMN posterior						
	1) R Inferior Frontal Gyrus	67	45	53.2	33.1	-2.09
	2) L Superior Temporal Gyrus	51	22/42	-63.2	-31.7	15.8
	3) R Cingulate Gyrus	45	24/31	9.78	-2.53	44.7
	4) R Posterior Cingulate, R Precuneus	21	31, 31	13.8	-58.7	26.9

FPN l						
	1) R Precentral Gyrus, R Middle Frontal Gyrus	35	6, 6	36.9	-6.74	45.3
	2) L Claustrum, L Thalamus	25	-	-25.8	-19.3	17.1
FPN r						
	1) R Superior Frontal Gyrus, R Middle Frontal Gyrus	87	9, 8/9	31.3	47.2	30.3
	2) L Inferior Parietal Lobule, L Supramarginal Gyrus	81	40, 40	-63.4	-37.8	31.8
	3) L Cingulate Gyrus	78	24/32	-7.26	14.6	35.2
	4) R Anterior Cingulate, R Medial Frontal Gyrus, R Cingulate	75	32, 9, 32	14.1	37.7	23.5
	5) R Inferior Parietal Lobule, R Superior Parietal Lobule	53	7/39/40, 7	40.5	-56.9	46.8
	6) L Inferior Parietal Lobule, L Superior Parietal Lobule	46	40, 7	-37.7	-52.3	50.4
	7) R Middle Frontal Gyrus	37	10	41	45.9	15.6
	8) R Inferior Parietal Lobule, Supramarginal Gyrus	36	40, 40	48.1	-39.2	44.9
	9) R Precuneus	36	7	12	-51.6	66.3

Supplementary Table 1. Network-specific tDCS effects in the active group at each testing session.
Note. Clusters resulting from second-level random-effects analysis. Regions showing significantly increased and decreased functional connectivity with regions of interest (ROI) and RSNs after active stimulation as compared to baseline are listed. Sorting is after number of voxels. Brain regions are identified for clusters > 20 voxels; collection threshold $p_{unc.} < .01$. Coordinates (x, y, z) are given in MNI space. Brain regions were assigned after the Talairach atlas and, if for a certain region no label was available, after the Havard-Oxford (Sub-)Cortical Structural Atlas.
DMN = Default Mode Network, FPN = Frontal Parietal Network, L/R = left/right hemisphere, RH = right-hemispheric prefrontal ROI, RSN = resting-state network.

RSN	Brain regions	Number of voxels	Brodman's area	Centre of gravity (MNI coordinates)		
				x	y	z
	Post sham tDCS > pre sham tDCS					
t1						
DMN anterior						
	1) L Anterior Cingulate	92	24	-3.63	38.6	1.67
	2) R Inferior Frontal Gyrus, R Extra-Nuclear, R Insula	26	47, 13, -	40.7	16.5	-14.1
	3) L Cingulate Gyrus	26	24	-18.3	-14.9	36.8
	4) L Precentral Gyrus, L Postcentral Gyrus	24	5, 3	-34.8	-16.6	51.5
	5) L Precentral Gyrus	22	6	-35.1	-6.18	54.1
	6) L Postcentral Gyrus	21	1/3	-51	-12.3	54.2
DMN posterior						
	1) R Middle Occipital Gyrus, R Cuneus, R Inferior Temporal Gyrus	161	18/19/37, 18, -	36.6	-80.6	11.7
	2) R Postcentral Gyrus	130	2	55.4	-18.2	27.9
	3) L Insula	67	13	-39.9	-24.5	25
	4) L Postcentral Gyrus, L Inferior Parietal Lobule	56	1/2, 40	-54.6	-22.5	39.4
	5) R Cingulate Gyrus	39	31/24	12.2	-0.154	43.9
	6) L Inferior Temporal Gyrus, L Middle Temporal Gyrus	34	19/37, 37	-49.8	-60	3.53
	7) L Cuneus	25	18/29	-13.9	-91.2	28.2
	8) R Posterior Cingulate	25	30/29/23	4.88	-60.5	12
	9) R Medial Frontal Gyrus	24	6	8.33	-2.83	55.5
	10) L Superior Temporal Gyrus, L Postcentral Gyrus, L Inferior Parietal Lobule	22	42, 40, 40	-63.8	-29.4	20.9

	11) L Cuneus, L Posterior Cingulate, L Precuneus	21	18/23, 30/31, 31	-4	-70.9	18.5
FPN l						
	1) R Posterior Cingulate	32	30/23	3.81	-64.3	15
	2) L Precuneus	25	7	-15.6	-56.3	56.2
	3) R Superior Parietal Lobule, L Precuneus	24	7, 7	23.7	-53.5	66.3
FPN r						
	1) R Inferior Parietal Lobule, R Postcentral Gyrus	264	40, 2	56.7	-23.5	31.6
	2) L Insula	197	13	-36.5	29.5	7.41
	3) R Middle Occipital Gyrus, R Middle Temporal Gyrus	187	19, 19/39	46.6	-75.6	18.9
	4) R Medial Frontal Gyrus, R Cingulate Gyrus, R Superior Frontal Gyrus	140	32/6, 24, 6	8.37	6.34	50.6
	5) L Superior Temporal Gyrus, L Postcentral Gyrus, L Inferior Parietal Lobule	121	42/22, 40, 40	-62.6	-30.9	23.2
	6) L Precentral Gyrus, L Postcentral Gyrus	68	4, 3	-25.6	-23.4	50.9
	7) L Cingulate Gyrus	50	31	-8.72	-27.9	48.3
	8) L Inferior Frontal Gyrus, L Precentral Gyrus	50	44/45/9, 44	-59.9	11.7	14.1
	9) L Middle Temporal Gyrus	48	37	-50.1	-60.3	4.46
	10) L Superior Temporal Gyrus, L Transverse Temporal Gyrus, L Postcentral Gyrus	44	41/42, 41, 40	-54.1	-27.8	13.7
	11) R Superior Temporal Gyrus, R Insula	43	41, 13	45	-33.1	16.6
	12) L Precentral Gyrus	38	6	-41.6	-4.53	32.5
	13) R Insula	36	13	45.2	9.22	10.6
	14) L Precentral Gyrus, L Transverse Temporal Gyrus, L Postcentral Gyrus	34	6/4, -, -	-64.8	-1.76	11.4

	15) L Transverse Temporal Gyrus, L Postcentral Gyrus	33	41, 43	-55.8	-15.8	14.6
	16) R Cingulate Gyrus	32	32	13.3	24.7	26.4
	17) L Inferior Parietal Lobule	30	40	-63.8	-33.7	35.1
	18) L Middle Frontal Gyrus, L Inferior Frontal Gyrus	29	10/46, 46	-44.8	50.1	2.48
	19) R Precentral Gyrus, R Inferior Frontal Gyrus	27	6, 6/9	52.2	4.28	2
	20) R Cuneus, R Precuneus	23	19/18/7, 31	17.4	-77.7	36.1
t2						
DMN anterior						
	1) L Anterior Cingulate	118	24	1.37	10.7	14.7
	2) R Precentral Gyrus, R Middle Frontal Gyrus	102	9, 8/9	42.2	29.8	36.5
	3) R Middle Frontal Gyrus	51	6	37.6	8.59	43.9
	4) R Inferior Parietal Lobule	34	40	-17.6	-38.8	33.6
	5) R Inferior Parietal Lobule	32	40	44.8	-46.9	49.5
	6) L Cuneus, L Precuneus	27	7, 7	-9.63	-64.8	38.7
DMN posterior						
	1) L Precuneus, L Superior Parietal Lobule	117	7, 7	-12.9	-49.1	57.8
	2) L Middle Frontal Gyrus	95	6/8	-24.6	22.9	34.1
	3) L Preceneus, R Sub-Gyral, R Paracentral, R Superior Parietal Lobule	77	7, 40/7, 5, 7	27.3	-41.5	57.7
	4) L Sublobar Thalamus	76	-	-6.76	-4.82	16.7
	5) R Cingulate Gyrus, R Paracentral Lobule	71	31/24, 31	9.21	-17.3	42.7
	6) R Inferior Frontal Gyrus	63	47	34.5	24.6	-14.4
	7) L Postcentral Gyrus, L Inferior Parietal Lobule	53	40, 40	-35.5	-37.9	57.1

	8) R Precuneus, R Cingulate Gyrus, R Paracentral Lobule	33	7, 31, 5	5.94	-34.2	48.7
	9) R Precuneues, R Praracentral Lobule	26	7, 5	10.6	-40.9	60.1
	10) R Superior Temporal Gyrus, R Inferior Frontal Gyrus	26	-, 13	39	6.62	-15.7
FPN l						
	1) R Precuneus, R Sub-Gral, R Paracentral	82	7, 40/7, 7	25	-43.3	57.4
	2) R Cuneus, R Precuneus	71	7, 7	22.8	-70.2	40.7
FPN r						
	1) L Superior Temporal Gyrus, L Middle Temporal Gyrus	68	38/22, 21	-57.7	5.76	-8.41
t3						
DMN anterior						
	1) R Thalamus, R Caudate	53	-, -	13.8	-17.1	21
	2) L Superior Frontal Gyrus, R Middle Frontal Gyrus	45	9/8, 9	-25	49.8	32.4
DMN posterior						
	1) R Cingulate Gyrus	67	24	8.18	7.85	30.8
	2) Cingulate Gyrus	50	23/24	0.76	-13.2	35.6
	3) L Thalamus	38	-	-27.5	-30.9	2.42
FPN l						
	1) L Precuneus	29	31	-22.7	-73.9	31.2
FPN r						
	1) R Precuneus, R Cingulate Gyrus	71	31, 31	22.4	-41.2	32.3
	2) R Precentral Gyrus, R Inferior Parietal Lobule, R Postcentral Gyrus	41	4, 40, 2/1/3	59.6	-16.3	39.8

	3) L Caudate	35	-	-22.9	-18.5	24.7
	4) L Precentral Gyrus, L Postcentral Gyrus	31	4, 3	40.4	-6.77	35.6
	5) L Precentral Gyrus, L Postcentral Gyrus	28	4	-42.4	-14.9	42
	6) R Thalamus	21	-	2.38	-15.9	-1.9
Post sham tDCS < pre sham tDCS						
t1						
DMN anterior						
	1) R Midbrain, L Sub-lobar	99	-, -	2.1	-10.1	-13.2
	2) L Sublobar Caudate, L Sub-lobar Lentiform	56	-, -	-15.6	16.1	-2.68
	3) R Middle Frontal Gyrus	36	9/6/8	53.6	12.6	39.1
	4) L Midbrain, L Parahippocampal Gyrus	33	-, 28	-17	-13.2	-13.8
	5) L Insula	23	13	-40	-42.2	18.9
DMN posterior						
	1) L Middle Frontal Gyrus	58	8	-49.9	17.3	39.4
	2) R Midbrain, BL Sub-lobar	43	-	0.419	-6.74	-11.3
	3) L Parahippocampal Gyrus, L Superior Temporal Gyrus	33	34, 38	-27.4	-0.364	-21.3
	4) L Midbrain	30	-	29.2	-41.9	-16.1
	5) R Parahippocampal Gyrus	23	36/35	29.2	-23.2	-20.3
FPN l						
	1) R Medial Frontal Gyrus, BL Anterior Cingulate	190	11/10, 32/10	6.46	42	-11.5
	2) R Inferior Frontal Gyrus, R Middle Frontal Gyrus	138	45/46, 46	51.4	36.7	2.55
	3) L Inferior Frontal Gyrus, L Middle Frontal Gyrus	109	45/46, 46	-44.5	41.2	0.275

	4) L Anterior Cingulate, L Medial Frontal Gyrus, L Cingulate Gyrus	69	32, 9, 32	-8.41	37.4	23
	5) L Superior Temporal Gyrus, L Insula	63	22, 22	-42.9	-25.5	635
	6) R Inferior Frontal Gyrus, Middle Frontal Gyrus	21	47, 11	26.2	24.5	-20.6
FPN r						
	1) R Parahippocampal Gyrus	223	30/27	17.9	-41.7	7.17
	2) L Sublobar, L Parahippocampal Gyrus, L Midbrain, L Anterior Cingulate	115	-, 28, -, 25	-3.18	-3.44	-12.3
	3) R Precuneus	92	31/7	17.5	-49.2	38
	3) BL Sublobar	59	-	2.51	-3.93	5.56
	4) L Sublobar Caudate	51	-	-15	25.1	4.98
	5) R Midbrain	30	-	15.2	-9.07	-12.3
	6) R Parahippocampal	27	-	31.3	-21	-19.9
	7) R Medial Frontal Gyrus	24	8	0.833	49.7	39.5
t2						
DMN anterior						
	1) RLingual Gyrus, R Cuneus	84	18, 17/18/23	13.1	-77.6	10.2
	2) R Parahippocampal Gyrus	30	-	38.7	-15.9	-21.3
	3) R Sublobar Lentiform Nucleus	30	-	14.3	2.33	1.53
	4) R Midbrain, R Thalamus	28	-	12	-12.4	-7.14
	5) R Parahippocampal Gyrus	22	36	23.2	-44.4	-10.7

DMN posterior						
	1) L Inferior Parietal Lobule, L Angular Gyrus, L Precuneus, L Superior Parietal Lobule	340	40/39, 39, 19/39, 7	-43	-59.2	44.6
	2) R Cuneus	67	18	6.27	-78.9	24.3
	3) L Precentral Gyrus, L Middle Frontal Gyrus	57	9, 8	-45.5	28.8	33.6
	4) R Inferior Parietal Lobule	45	40	50.8	-53.7	49
	5) L Lentiform Nucleus, L Thalamus	37	-, -	-23.9	-15	6.49
	6) R Thalamus	31	-	29.5	-28.7	5.48
	7) L Middle Frontal Gyrus	28	46	-46.2	42.8	14.4
	8) L Cuneus	22	17	-14	-81.4	12.5
	9) L Parahippocampal	21	19	-24.7	-52.5	-2.95
FPN I						
	1) L Posterior Cingulate	166	29/30/31/23	-10.5	-55.5	14.4
	2) L Midbrain, L Parahippocampal Gyrus, L Thalamus	107	-, 27, -	-4.58	-30.3	-2.49
	3) R Anterior Cingulate, R Medial Frontal Gyrus, R Superior Frontal Gyrus	77	10, 10/6, 10	7.27	55.2	-8.75
	4) R Parahippocampal Gyrus	32	30	9.81	-44.4	187
	6) RThalamus	32	-	9.81	-44.4	0.187
	7) R Thalamus, R Lentiform Nucleus	27	-	18.5	-3.93	8.96
	8) R Midbrain	26	-	5.92	-17.4	-12.3
	9) R Insula, R Superior Temporal Gyrus	23	22, 22/41	44.8	-27.8	3.91

	10) Posterior Cingulate Gyrus	22	31/23	0.455	-29.5	32.5
	11) L Middle Temporal Gyrus, L Superior Temporal Gyrus	21	21, 21	-52.1	-8.19	-11.6
FPN r						
	1) R Midbrain	37	-	12.5	-37.9	-15.9
	2) L Precuneus, L Cuneus	33	7, 19	-9.94	-73.4	40.8
	3) R Inferior Parietal Lobule	31	40	52.8	-50.8	49.7
t3						
DMN anterior						
	1) Frontal Medial Cortex, Anterior Cingulate	45	10, 32	0.311	38.3	-14.6
	2) L Superior Temporal Gyrus	42	41/42	-61.7	-24.8	10.4
	3) L Postcentral Gyrus, L Inferior Parietal Lobule	38	40, 40	-39.2	-29.3	50.9
	4) R Parahippocampal Gyrus	33	35/28	21.9	-20.4	-11.4
	5) L Transverse Temporal Gyrus	26	42	-63.8	-13.5	9.08
	6) R Postcentral Gyrus, R Precentral Gyrus, R Inferior Parietal Lobule	24	40/3/4, 4, 40	36.5	-30.2	59.7
	6) R Inferior Frontal Gyrus	23	9/44	57.7	7.3	20.1
DMN posterior						
	1) L Insula, L Claustrum, L Superior Temporal Gyrus, L Transverse Temporal Gyrus	130	13, -, 41, 41	-38	-29.3	9.14
	2) L Lingual Gyrus, L Parahippocampal	63	19, 19	-24.4	-58.7	-2.48
	3) L Cuneus	54	17/18	-9.89	-85.5	17.1

	4) L Superior Temporal Gyrus	37	41/42	-56.9	-30.4	10.5
	5) R Lingual Gyrus, R Cuneus, R Posterior Cingulate	33	18, 30, 30	13.4	-64.8	9.94
	6) L Inferior Frontal Gyrus	21	46	-51	36.8	6
FPN l						
	1) L Middle Temporal Gyrus, L Superior Temporal Gyrus	53	21/22, 22	-51.7	-40.9	6.23
	2) L Middle Temporal Gyrus	51	21	-64.2	-42.2	-7.41
FPN r						
	1) L Precuneus, L Cingulate Gyrus	45	31, 31	-10.1	-47.1	32.5
	2) L Middle Frontal Gyrus	39	11/47	-25.6	38.7	-18.8
	3) L Sublobar Lentiform Nucleus, L Caudate	31	-, -	-19.1	18.6	-4.71
	4) L Superior Frontal Gyrus	22	10	-31	57	8.45

Supplementary Table 2. Network-specific tDCS effects in the sham group at each testing session.
Note. Clusters resulting from second-level random-effects analysis. Regions showing significantly increased and decreased functional connectivity with the FPN and DMN after sham stimulation as compared to baseline are listed. Sorting is after number of voxels. Brain regions are identified for clusters > 20 voxels; collection threshold $p_{unc.} < .01$. Coordinates (x, y, z) are given in MNI space. Brain regions were assigned after the Talairach atlas and, if for a certain region no label was available, after the Havard-Oxford Cortical Structural Atlas.
DMN = Default Mode Network, FPN = Frontal Parietal Network, L/R = left/right hemisphere, RSN = resting-state network.

ROI and hemisphere	sham		active	
	baseline	post	baseline	post
ICC 12				
46 d l	0.43	0.28	0.27	0.19
46 d r	0.50	0.35	0.41	0.30
9 l	0.39	0.35	0.42	0.42
9 r	0.64	0.44	0.54	0.34
10 l	0.24	0.01	0.42	0.24
10 r	0.36	0.40	0.49	0.37
ICC 13				
46 d l	0.39	0.23	0.37	-0.12
46 d r	0.46	0.34	0.45	-0.34
9 l	0.09	0.26	0.47	-0.02
9 r	0.33	0.56	0.52	-0.24
10 l	-0.07	0.07	0.43	-0.27
10 r	0.17	0.43	0.38	-0.25
ICC 23				
46 d l	0.55	0.29	0.37	-0.06
46 d r	0.54	0.37	0.49	0.08
9 l	0.44	0.38	0.26	0.05
9 r	0.48	0.49	0.48	0.09
10 l	0.32	0.19	0.24	-0.11
10 r	0.33	0.33	0.44	0.04

Supplementary Table 3. Inter-session test-retest reliability of ROIs between two testing sessions.
Note. Test-retest reliability of connectivity within ROIs, separately for both groups (active vs. sham) and both conditions (baselines and post tDCS). Test-retest reliability is expressed as median of voxel-wise intra-class correlation coefficients (ICC) for the following ICC pairs: t1 and t2 (first block), t1 and t3 (second block) and t2 and t3 (third block). d = dorsal, l/r = left/right, ROI = region of interest, 12/13/23 = pairs of ICC evaluation, 10 = area 10 of the Sallet-atlas, 46d = area 46/9 dorsal of the Sallet-atlas, 9 = area 9 of the Sallet-atlas (Sallet et al., 2013).

RSN	sham		active	
	baseline	post	baseline	post
ICC 12				
DMN anterior	0.27	0.30	0.33	0.15
DMN posterior	0.32	0.15	0.32	0.15
FPN l	0.32	0.20	0.33	0.12
FPN r	0.31	0.05	0.29	0.26
ICC 13				
DMN anterior	0.07	0.22	0.40	0.01
DMN posterior	0.21	0.03	0.27	0.11
FPN l	0.25	0.20	0.31	0.04
FPN r	0.22	0.20	0.35	0.06
ICC 23				
DMN anterior	0.33	0.33	0.35	0.02
DMN posterior	0.30	0.19	0.26	0.26
FPN l	0.35	0.40	0.35	0.26
FPN r	0.33	0.29	0.25	0.23

Supplementary Table 4. Inter-session test-retest reliability of RSNs between two testing sessions.
Note. Test-retest reliability of ICA-based RSNs, separately for both groups (active vs. sham) and both conditions (baselines and post tDCS). Test-retest reliability is expressed as median of voxel-wise intra-class correlation coefficients (ICC) for the following ICC pairs: t1 and t2 (first block), t1 and t3 (second block) and t2 and t3 (third block). DMN = Default Mode Network, FPN = Frontal Parietal Network, ICA = independent component analysis, l/r = left/right, RSN = resting-state network, 12/13/23 = pairs of ICC evaluation.

Approach	ROI or RSN	sham	active
		r	r
ROI			
	46 d l	0.05	-0.15
	46 d r	-0.01	-0.10
	9 l	0.08	0.04
	9 r	0.02	-0.08
	10 l	0.01	-0.05
	10 r	-0.05	-0.04
ICA			
	DMN anterior	-0.07	0.12
	DMN posterior	0.02	0.06
	FPN l	-0.01	0.07
	FPN r	-0.08	0.09

Supplementary table 5. Inter-session test-retest reliability of contrasts (post-pre maps).
Note. Test-retest reliability of connectivity within ROIs as well as of ICA-analyses-based RSN connectivity, separately for both groups (active vs. sham). Only contrasts (post tDCS – baseline) are shown. Test-retest reliability is expressed as median of voxel-wise intra-class correlations (ICC) between all testing sessions (t1, t2, t3). Confidence intervals are indicated by bracketed values. d = dorsal, DMN = Default Mode Network, FPN = Frontal Parietal Network, ICA = independent component analysis, l/r = left/right, LB = lower bound, r = correlation coefficient, ROI = region of interest, RSN = resting-state network, UB = upper bound, 10 = area 10 of the Sallet-atlas, 46d = area 46/9 dorsal of the Sallet-atlas, 9 = area 9 of the Sallet-atlas (Sallet et al., 2013).

Testing assumptions on prefrontal transcranial direct current stimulation: Comparison of electrode montages using multimodal fMRI

Brain Stimulation 11 (2018) 998–1007

Contents lists available at ScienceDirect

Brain Stimulation

journal homepage: http://www.journals.elsevier.com/brain-stimulation

Testing assumptions on prefrontal transcranial direct current stimulation: Comparison of electrode montages using multimodal fMRI

Jana Wörsching [a, *, 1], Frank Padberg [a, 1], Stephan Goerigk [a, b, c], Irmgard Heinz [a], Christine Bauer [a], Christian Plewnia [d], Alkomiet Hasan [a], Birgit Ertl-Wagner [e], Daniel Keeser [a, e]

[a] Department of Psychiatry and Psychotherapy, University Hospital, LMU, Nussbaumstrasse 7, 80336 Munich, Germany
[b] Department of Psychological Methodology and Assessment, LMU, Leopoldstrasse 13, 80802 Munich, Germany
[c] Hochschule Fresenius, University of Applied Sciences, Infanteriestrasse 11a, 80797 Munich, Germany
[d] Department of Psychiatry and Psychotherapy, Neurophysiology & Interventional, Neuropsychiatry and Werner Reichardt Center for Integrative Neuroscience (CIN), University of Tübingen, Calwerstrasse 14, 72076 Tübingen, Germany
[e] Department of Radiology, LMU, Marchioninistrasse 15, 81377 Munich, Germany

ARTICLE INFO

Article history:
Received 12 December 2017
Received in revised form
25 March 2018
Accepted 1 May 2018
Available online 4 May 2018

Keywords:
Cognitive control
Dorsolateral prefrontal cortex
Electrode montage
Resting state
fMRI
tDCS

ABSTRACT

Background: Transcranial direct current stimulation (tDCS) of the prefrontal cortex (PFC) has been widely applied in cognitive neurosciences and advocated as a therapeutic intervention, e.g. in major depressive disorder. Although several targets and protocols have been suggested, comparative studies of tDCS parameters, particularly electrode montages and their cortical targets, are still lacking.
Objective: This study investigated a priori hypotheses on specific effects of prefrontal-tDCS montages by using multimodal functional magnetic resonance imaging (fMRI) in healthy participants.
Methods: 28 healthy male participants underwent three common active-tDCS montages and sham tDCS in a pseudo-randomized order, comprising a total of 112 tDCS-fMRI sessions. Active tDCS was applied at 2 mA for 20 min. Before and after tDCS, a resting-state fMRI (RS fMRI) was recorded, followed by a task fMRI with a delayed-response working-memory (DWM) task for assessing cognitive control over emotionally negative or neutral distractors.
Results: After tDCS with a cathode-F3/anode-F4 montage, RS-fMRI connectivity decreased in a medial part of the left PFC. Also, after the same stimulation condition, regional brain activity during DWM retrieval decreased more in this area after negative than after neutral distraction, and responses to the DWM task were faster, independent of distractor type.
Conclusion: The current study does not confirm our a priori hypotheses on direction and localization of polarity-dependent tDCS effects using common bipolar electrode montages over PFC regions, but it provides evidence for montage-specific effects on multimodal neurophysiological and behavioral outcome measures. Systematic research on the actual targets and the respective dose-response relationships of prefrontal tDCS is warranted.

Introduction

Transcranial direct current stimulation (tDCS) is a non-invasive brain-stimulation (NIBS) technique that exerts non-focal effects on cellular, microcircuit, and network levels. Bidirectional effects of tDCS have been suggested depending on polarity, i.e. facilitatory or inhibitory effects are associated with the anode or cathode, respectively [1–3]. TDCS of the prefrontal cortex (PFC) may improve higher-order cognitive processes (for review see [4,5]), such as cognitive control (CC) [6], which is a crucial faculty for maintaining performance during distractive stimuli and which is impaired in major depressive disorder (MDD) [7–9]. In a recent study, deficits in an

* Corresponding author.
E-mail address: Jana.Woersching@med.uni-muenchen.de (J. Wörsching).
[1] both authors contributed equally to this work.

https://doi.org/10.1016/j.brs.2018.05.001
1935-861X/

emotionally loaded working-memory (WM) task in MDD were normalized after anodal tDCS over the left dorsolateral PFC (DLPFC) [10], pointing towards a potential clinical use.

For therapeutic applications in psychiatry, several tDCS protocols have been developed that are now widely used in preclinical and clinical research (for reviews see [11,12]). In MDD, repeated bifrontal tDCS has been shown to exert antidepressant effects superior to those of placebo [13,14]. Although these findings are promising, fundamental questions regarding dosage for devices and spatial distribution of stimulation effects remain unanswered [15]. Because tDCS can be more readily combined with functional magnetic resonance imaging (fMRI) than other NIBS methods, e.g. repetitive transcranial magnetic stimulation, imaging tDCS with multimodal approaches represents an ideal tool to reveal specific stimulation-brain interactions [16–18]. Only a few combined fMRI-tDCS studies are available for PFC targets, however, and previous studies have not made full use of multimodal neuroimaging and designs to compare stimulation parameters, e.g. electrode montages, and investigate the specificity of action (for review see [19]).

Therefore, this study used multimodal fMRI (resting state [RS] and task: CC in a WM paradigm) to investigate the specificity of target sites for effects mediated by prefrontal tDCS. For two of the active conditions, we used montages for anodal left DLPFC stimulation that are commonly used in MDD [13,14,20,21]. As the third active condition, we applied a cathodal left-DLPFC montage to further investigate polarity-dependent tDCS effects. By systematically varying tDCS electrode positions, we investigated two main hypotheses based on previous studies investigating effects of prefrontal tDCS on fMRI measures [22–24] and CC [10,25]: (1) Polarity-specific facilitatory and inhibitory effects of the anodal and cathodal condition, respectively, can be observed compared with sham tDCS in multimodal fMRI and on behavioral levels; (2) the two anodal conditions show similar effects but strongly differ from the cathodal condition (for review see [26]).

Material and methods

Description of the sample

The study was approved by the local ethics committee (Faculty of Medicine, Ludwig-Maximilians-University, Munich, Germany). All participants gave their written informed consent for participation in this study.

We studied 32 healthy male participants in a total of 128 tDCS-fMRI sessions (4 sessions per participant). All participants had to be right-handed according to the Edinburgh Handedness Questionnaire (EHQ; [27]); one participant had trained to use his right hand but was left-handed according to the EHQ and therefore excluded from analyses. The data of an additional three participants were excluded because of technical problems during recording, leaving 28 participants (i.e. 112 tDCS-fMRI sessions) in the final sample (age: $M = 26$ years, *range* = 21–32 years). A priori exclusion criteria were a history of neurological or psychiatric diseases, the intake of neuroactive medication, and smoking or drug consumption during the past 6 months.

Experimental procedure

This study was placebo-controlled and followed a single-blinded design with partially blinded operators (see Fig. 1A). Further details on blinding are provided in the supplementary information (see Sup. Info. A.1). All participants underwent four consecutive testing sessions in a pseudorandomized order, such that all 24 possible randomizations sequences were covered. Sessions differed only with respect to the stimulation condition and were separated by at least seven days to avoid carry-over effects. For each participant, measurements were performed at the same hour of the day across all testing sessions. Participants were asked to abstain from alcohol the day before and from caffeine the morning of the measurement.

At each testing session, participants received 20 min of one of three active-tDCS montages (anode F3, cathode F4; anode F3, cathode in proximity to the contralateral orbit; cathode F3, anode F4) or sham tDCS in the MRI scanner.

RS fMRI was recorded before tDCS (baseline measurement; 10 min recording time), during tDCS (20 min), and after tDCS (post-tDCS measurement; 10 min). Participants were asked to keep their eyes closed during RS fMRI and to not fall asleep, to think about nothing in particular and to avoid moving. After RS fMRI, participants performed a CC delayed-response WM (DWM) task in the scanner; instructions were given on the screen inside the scanner before the task-fMRI sequence started.

To control for confounding variables and safety, two questionnaires were collected at each testing session: The Positive And Negative Affect Schedule and the Comfort Rating Questionnaire. Detailed information on each questionnaire and its outcome are provided in Sup. Info. A.2, A.5 & B.1. Research questions on online RS measurements (i.e. RS fMRI during tDCS) are not presented here and will be addressed in a further publication.

Cognitive control — delayed working-memory task

After the three RS measurements (baseline and during and post-tDCS), fMRI was recorded while participants completed a DWM task with emotional distraction (CC-DWM task), adapted from Plewnia and colleagues [6]. Participants performed 60 trials of the CC-DWM task at each session. Each trial included an encoding phase in which a row of 6 letters was presented; a distraction phase, during which pictures were shown; and a recall phase comprising three successively presented letters. We used two types of trial, *negative* and *neutral*, in which a picture of negative or neutral valence was shown during the distraction phase. In the recall phase, participants had to indicate whether they detected a target (letter present in the row shown in the encoding phase) or a foil (letter absent in the encoding phase); participants indicated their response by pressing either a button below the index finger or one below the middle finger of their right hand. They were instructed to respond to each of the three target stimuli as quickly and accurately as possible. For each response, reaction time (RT) and response type (hit, miss, incorrect) were recorded. Trials were separated by a variable inter-trial interval. The task sequence is illustrated in Fig. 1B. For detailed information on stimulus presentation, see Sup. Info. A.3.

Transcranial direct current stimulation (tDCS)

TDCS was applied via two saline-soaked surface sponge-electrodes (area = 7×5 cm^2) that were connected to an Eldith stimulator MR (neuroCare Group GmbH, Munich, Germany). To target the DLPFC, we used three different bipolar montages (see Fig. 1A): atDCS-A (anode over F3, cathode over F4), atDCS-B (anode over F3, cathode over Fp2), and ctDCS (anode over F4, cathode over F3); for sham tDCS, we randomly selected one of the three active montages. Operators and participants were kept blind to treatment conditions.

Electrodes were positioned with a standardized system — as previously described by Padberg and colleagues [28] — that is based on the international 10–20 system. TDCS was delivered for 20 min at an intensity of 2 mA (15 s ramp in and 15 s ramp out), which is a protocol often used in experimental fMRI studies [22,24,29–33] as well as in pivotal clinical trials [20,21,34–36] of prefrontal tDCS; impedance was kept below 10 kΩ. For sham tDCS, the built-in study-mode was used that delivers a brief 2 mA DC

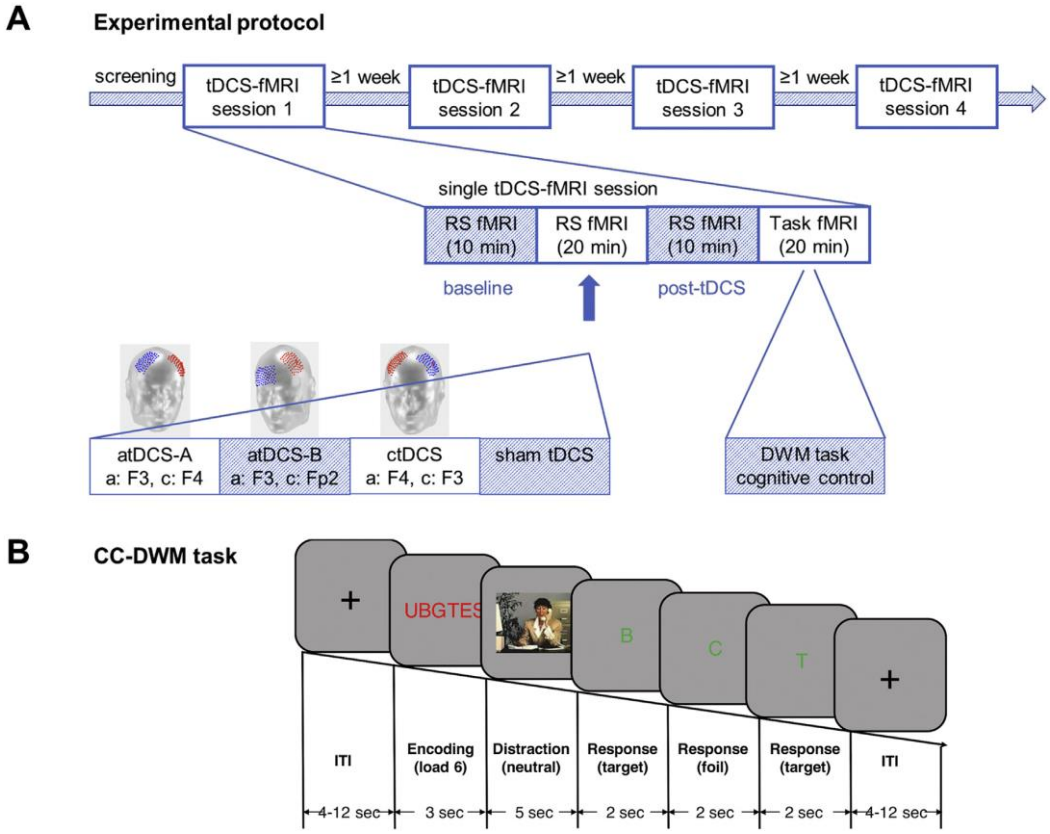

Fig. 1. Experimental procedure. A) The experimental protocol included four testing sessions. At each testing session, active or sham tDCS was preceded (baseline) and followed (post-tDCS) by a resting-state (RS) fMRI-scan. The post-tDCS RS-fMRI sequence was further followed by a delayed working-memory task requiring cognitive control (CC-DWM) with concomitant fMRI recordings (task fMRI). Between testing sessions, only stimulation differed, which was one out of four pseudorandomized tDCS conditions: 2x anodal tDCS (atDCS-A/B), cathodal (ctDCS), sham tDCS. The head models show the three different tDCS montages and were created with Matlab/Comets [91]. B) Sequence of the CC-DWM task. In each trial, six red letters or probe stimuli were presented for 3 s and had to be memorized. Next, either a neutral or a negative picture was shown for 5 s. Then, three times in succession a green letter was presented for 2 s on the screen. For each green letter, participants had to indicate via button press as fast and accurately as possible whether they saw a target (letter present in the row before) or a foil (letter absent in the row before). Trials were separated by a variable inter-trial interval (ITI), during which a fixation cross was shown.

plateau of 40 s (also 15 s ramp up and 15 s ramp down) at the beginning, followed by impedance measurements with impulses applied every 0.5 s of about 150 μA and 5 ms duration.

FMRI data processing

FMRI Data Pre-processing. For information on fMRI-data acquisition, see Sup. Info. A.4. The pre-processing steps for RS images have been described previously [30]. Task-fMRI images were pre-processed with the FEAT software tool implemented in FSL 5.0.9 (https://fsl.fmrib.ox.ac.uk/fsl/fslwiki). All raw functional time-series were slice-time corrected, reoriented, motion corrected, and linearly and nonlinearly spatially normalized to a standard EPI template in Montreal Neurological Institute (MNI) space and spatially smoothed with a 5 mm FWHM Gaussian kernel.

1st-level Analysis of Resting-State fMRI-Data. Single-subject RS-fMRI data were processed with two different approaches, i.e. functional connectivity was determined within specific regions-of-interest (ROI) and within resting-state networks (RSN). Three different ROIs (area 9/46 dorsal, area 9, and area 10; see Sup. Fig. 1) were positioned within the PFC by means of the Sallet Atlas [37] and drawn separately for each hemisphere. In addition to areas beyond the stimulation electrodes, the ROIs covered areas receiving the highest current density according to computation models of a bipolar-prefrontal tDCS montage [38–42]. In a next step, functional-connectivity values for the resulting hemisphere-specific ROIs were generated for each participant, stimulation condition, and RS measurement by cross-correlating RS time-series within each ROI (within-ROI functional-connectivity). RSNs were determined by the MELODIC (Multivariate Exploratory Linear Optimized Decomposition into Independent Components) routine, version 3.14, implemented in FSL [43], across all participants, stimulation conditions, and RS measurements. Four group-level independent-components (IC) were selected for further analyses: The Default Mode Network (DMN), the left Frontal Parietal Network (FPN), the right FPN, and the Executive Control Network (ECN) (see Sup. Fig. 2). All ICA-derived group-level ICs containing the four RSNs of interest were reconstructed into individual ICs by dual regression [44–46]. To only include activation within ICA-derived RSNs in the second-level analyses,

we masked individual ICs with an RSN template derived from binarization of group-level ICs.

1st-level Analysis of Task-fMRI Data. Subject-specific task-fMRI images were processed with FEAT (https://fsl.fmrib.ox.ac.uk/fsl/fslwiki/FEAT). Each recall phase was modelled as an event, separately for each trial type (neutral or negative), by convolving it with the FSL canonical hemodynamic response function. By means of a general-linear model, resulting parameter estimates were calculated for voxels within the same ROIs as used for RS analyses. For further analyses, standardized average z-scores were extracted within each ROI by using FEATQuery.

Statistical analyses

At the second level, individual RS functional-connectivity maps of both baseline and post-tDCS measurements were compared across stimulation conditions by means of a one-way repeated-measures ANOVA with 4 levels of the factor stimulation condition. Voxel-wise nonparametric statistical contrasts (with 10,000 permutations) between all stimulation conditions were determined with PALM alpha105 (Permutation Analysis of Linear Models; [47,48]; Linear Models, http://fsl.fmrib.ox.ac.uk/fsl/fslwiki/PALM/). Effects were considered significant at a false-discovery rate (FDR) corrected $p_{FDR} < .05$ (cluster size > 30 voxels). Because of the exploratory character of our study, trends towards significance at $p_{FDR} < .1$ were also reported.

We quantified the effects of the four stimulation conditions and the trial type (neutral or negative) on both ROI activation during retrieval and task-performance (RT for all responses, i.e. hits and incorrect responses, and accuracy) with linear-mixed-model analyses. This method of modelling was preferable because of its capacity to integrate missing-data cases (for further information see Sup. Info. A.6) and hence retain comparability between the behavioral and the RS-fMRI analyses. Task accuracy was not further analyzed because of ceiling effects (invariance) in participants' performance. Effects are reported as significant at $p < 0.05$. For detailed information on linear-mixed-model analyses, see Sup. Info A.6.

Results

Resting-state-fMRI connectivity

Testing session (i.e. stimulation condition) had no effect on baseline RS functional-connectivity for either the ROI- or the ICA-based approach. Post-tDCS RS-fMRI measurements showed several montage-specific effects on functional connectivity within ROIs (see Table 1 and Fig. 2). RS functional-connectivity decreased in the left area 10 after ctDCS as compared with atDCS-A ($p = 0.023$), atDCS-B ($p = 0.087$), and sham tDCS ($p = 0.053$). Also, after ctDCS, RS functional-connectivity decreased in the left area 9 as compared with atDCS-B ($p = 0.095$) and in the right area 9 as compared with both atDCS-A ($p = 0.053$) and atDCS-B ($p = 0.045$). Both the right ($p = 0.030$) and left area 9/46 dorsal ($p = 0.008$) showed an increase in RS functional-connectivity after ctDCS as compared with atDCS-B. The stimulation condition had no effect on post-tDCS RS-fMRI within ICA-derived RSNs.

Task-fMRI activity and task performance

Mixed-effect models of participants' brain activity in the retrieval phase showed a significant main effect for trial type in the left area 10 (see Fig. 3A) and the right area 9/46 dorsal (see Fig. 3B) and a significant disordinal interaction effect for stimulation condition and trial type in the left area 10 (see Fig. 3A). Although main effects should not be interpreted after significant disordinal interaction [49], stronger activation was generally observed after negative pictures ($t(112) = -2.79$, $p = 0.006$). Pairwise contrasts between factor levels revealed significantly different disordinal interaction between ctDCS and sham tDCS ($t(112) = -2.04$, $p = 0.043$).

In modelling participants' RTs, we found a significant interaction effect for stimulation condition and trial type (see Fig. 4). Pairwise contrasts revealed significantly different disordinal interactions, with crossover between atDCS-A and ctDCS ($t(107.01) = -2.31$, $p = 0.022$), and between atDCS-A and sham tDCS ($t(107.01) = -2.45$, $p = 0.015$).

For information on model comparisons, see Sup. Info. B.2.

Table 1
Location coordinates of fMRI clusters within regions-of-interest showing an effect of stimulation condition on post-tDCS resting-state connectivity-maps at different significance levels (cluster size > 30 voxels).

Regions (Talairach atlas)	Brodmann area	Center of mass (MNI space)			No. Voxels	Contrast
		x	y	z		
Left hemisphere						
Area 9/46 dorsal[c]						
Middle/Superior Frontal Gyrus[b]	8, 9	−30	34	26	193	ctDCS > atDCS-B
Area 9[c]						
Medial/Superior Frontal Gyrus[a]	9, 10	−14	60	12	224	atDCS-B > ctDCS
Area 10[c]						
Anterior Cingulate, Medial/Middle/Superior Frontal Gyrus[b]	9, 10, 32	−8	58	−16	1230	atDCS-A > ctDCS
Medial/Superior Frontal Gyrus[a]	9, 10	−8	58	−16	364	atDCS-B > ctDCS
Anterior Cingulate, Medial/Superior Frontal Gyrus[a]	9,10, 32	−10	60	−16	966	sham > ctDCS
Right hemisphere						
Area 9/46 dorsal[c]						
Middle/Superior Frontal Gyrus, Sub-Gyral[b]	8, 9	34	40	26	158	ctDCS > atDCS-B
Area 9[c]						
Medial/Superior Frontal Gyrus[a]	6, 8, 9	10	58	30	147	atDCS-A > ctDCS
Medial/Superior Frontal Gyrus[b]	6, 8, 9	8	62	26	137	atDCS-B > ctDCS

[a] $p_{FDR} < .1$.
[b] $p_{FDR} < .05$.
[c] Regions-of-interest selected from the FSL atlas 'Sallet Dorsal Frontal connectivity-based parcellation' [37].

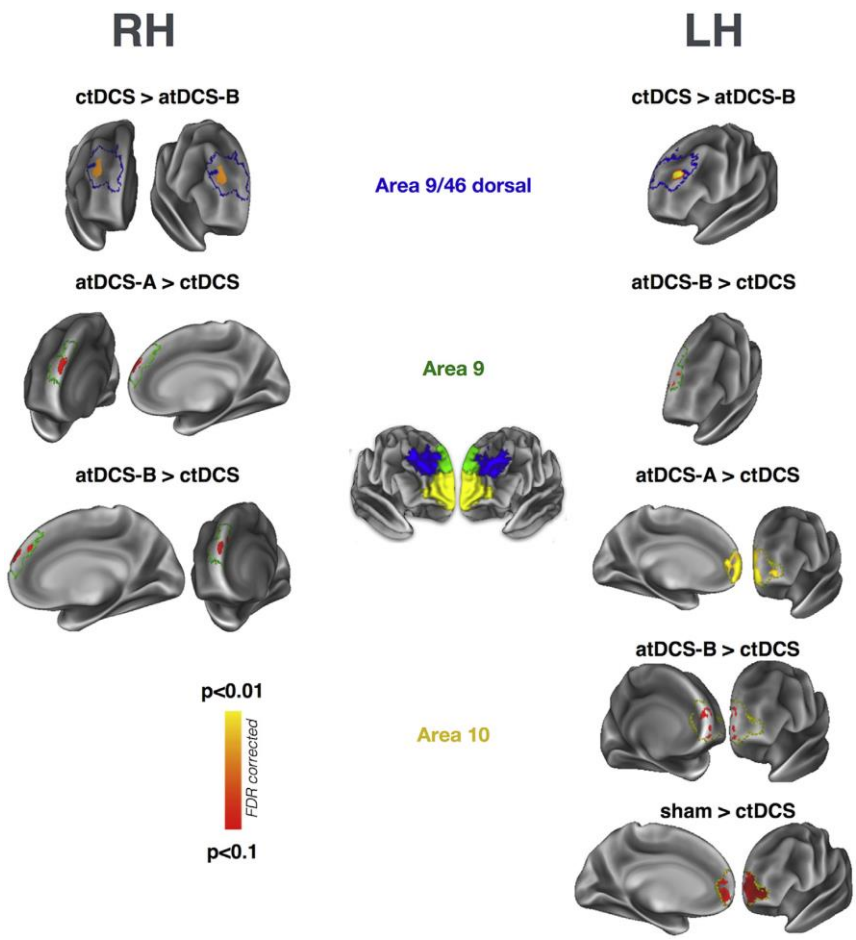

Fig. 2. Spatial distribution of fMRI clusters within regions-of-interest showing significant changes in post-tDCS resting-state connectivity for comparisons between stimulation conditions. Location of effects are given in Table 1. LH = left hemisphere, RH = right hemisphere.

Discussion

In this study, we investigated the effects on RS-fMRI functional-connectivity and DWM-task fMRI of a standard tDCS protocol with common electrode montages that were recently used in healthy volunteers and MDD patients. Our hypotheses were based on general assumptions in the field and on previous studies investigating effects of prefrontal tDCS on fMRI measures (for review see 19) and CC (for review see 6). Whereas our a priori hypotheses on the direction and localization of polarity-specific tDCS effects were not confirmed, we observed montage-specific effects of prefrontal tDCS across monitoring levels.

tDCS effects on RS fMRI

RS fMRI showed several changes in functional connectivity after tDCS but not between any of the baseline measurements, indicating that baseline functional-connectivity was stable across sessions and did not affect our results. Because post-tDCS changes were always associated with ctDCS, it is plausible that this electrode montage mediated the effects. In particular, RS functional-connectivity decreased (statistical trend) after ctDCS in an anterior-medial part of the left PFC (area 10) compared with sham tDCS. Assuming that sham tDCS had no effects [50–54], the finding that RS functional-connectivity within the same left-PFC area was significantly higher after atDCS-A and higher (statistical trend) after atDCS-B than after ctDCS was likely driven by a reduction after ctDCS. In addition, RS functional-connectivity significantly declined after ctDCS as compared with both atDCS-B in a left (statistical trend) and right (significant) dorso-medial part of the PFC (area 9) and atDCS-A in the right area 9 (statistical trend). Taken together, most ctDCS-related reductions of RS functional-connectivity were observed within the left medial PFC.

A reduction in left-hemispheric RS functional-connectivity by a montage with the cathode placed over the left hemisphere is consistent with the assumption of cathodal-tDCS-induced neural inhibition as shown in motor-cortex studies [1,3,55]. However, for prefrontal tDCS in combination with RS fMRI, potential tDCS effects may substantially differ from tDCS effects observed at motor regions. Pilot studies combining fMRI and tDCS showed an increase in RS functional-connectivity after anodal stimulation of the left DLPFC and concomitant cathodal stimulation above the right orbit as compared with a sham condition [22–24,50]. In the present

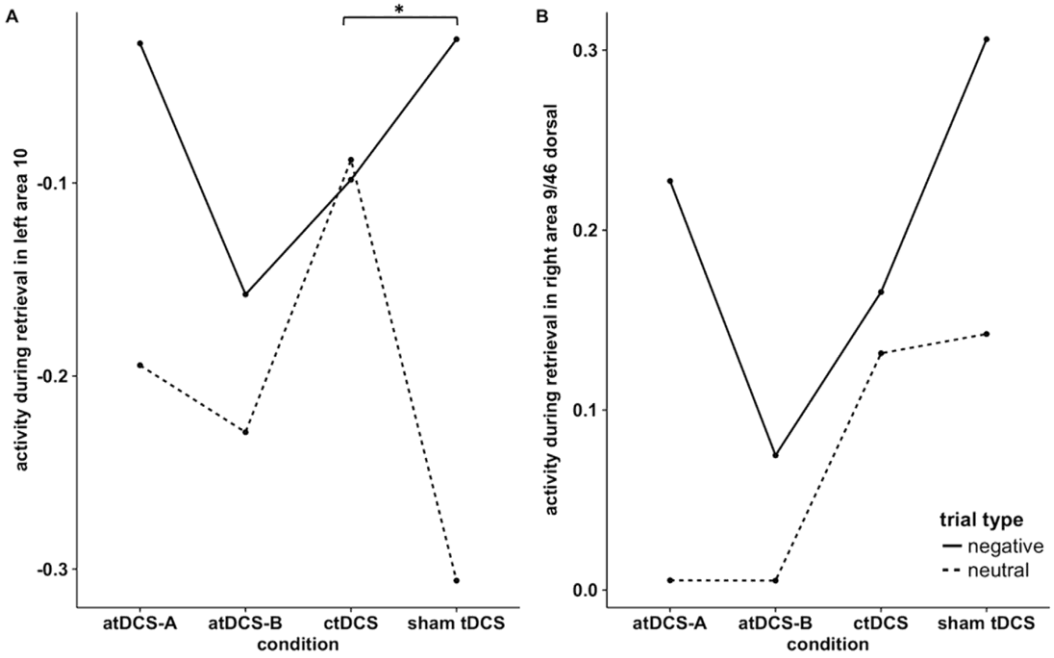

Fig. 3. Two-way interaction plot of brain activity in the retrieval phase for each stimulation condition and trial type. A) Activity in the left area 10. B) Activity in the right area 9/46 dorsal. Asterisk (*) indicates significant differences in contrasts between interaction effects of each factor level. Effects were considered significant at $\alpha = 0.05$.

study, we were not able to replicate such an anodal-tDCS-related increase in RS functional-connectivity, potentially as a result of diverse analyses methods. For example, in a previous study from our group [22], ROIs were determined based on electrode positions and not on computational models and the Sallet atlas, both of which were not available that time. However, also ICA-based

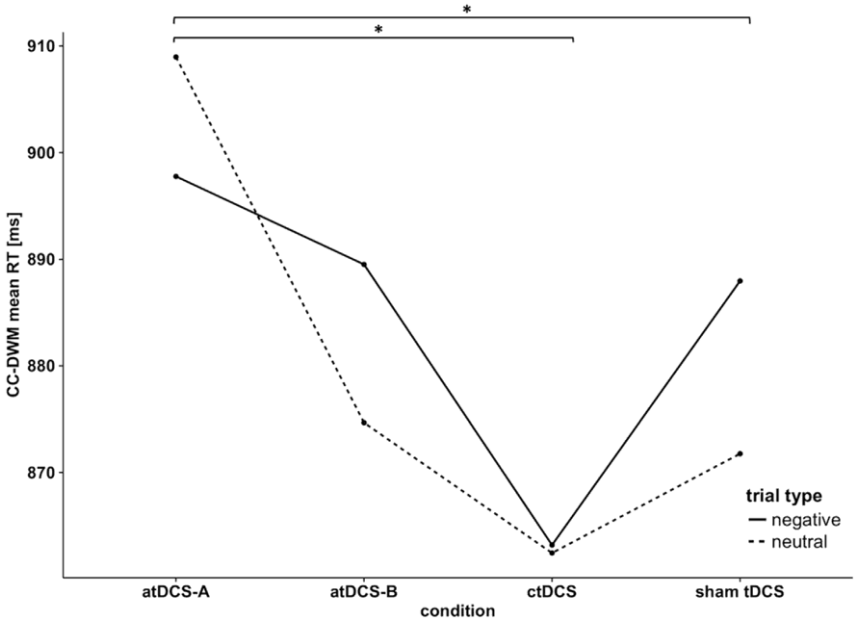

Fig. 4. Two-way interaction plot of mean reaction time (RT) in the behavioral task for each stimulation condition and trial type. Asterisk (*) indicates significant differences in contrasts between interaction effects of each factor level. Effects were considered significant at $\alpha = 0.05$.

analyses comparable to the analysis in our previous study [22], did not show such effects of tDCS on RSNs. In this context, the test-retest reliability of tDCS effects is currently a matter of debate in the NIBS field and tDCS appears to induce additional variability compared to sham stimulation [30,56–60]. Interestingly and also contrary to expectations, RS functional-connectivity significantly increased bilaterally after ctDCS as compared with atDCS-B in the DLPFC (area 9/46 dorsal).

tDCS effects on task fMRI

In task fMRI, both stimulation condition and trial type affected brain activity during retrieval and again effects were found in the anterior-medial part of the left PFC (area 10) and the right DLPFC (area 9/46 dorsal). In both areas, activity was overall higher after the presentation of emotionally negative pictures than after emotionally neutral pictures. Differential patterns of activity between negative and neutral distractors within medial and dorsolateral parts of the PFC is consistent with the model of affective-cognitive interaction [61], suggesting two brain systems representing CC [62]: one dorsal brain system, including the DLPFC, that is responsible for executive processing, such as maintaining goal-directed information in WM [63–68]; and one ventral system, comprising the medial PFC, which is involved in emotional processing [69–72]. Thus, activity patterns overserved within the left medial PFC and the right DLPFC may reflect both an enduring affective response to negative pictures and a greater need for maintenance of performance after negative than after neutral distractors. Strikingly, the affective response within the left medial PFC was diminished and even slightly reversed after ctDCS as compared with sham tDCS. Given that the medial PFC is part of a brain system subserving emotional processing, an alignment in activity during retrieval between negative and neutral trials after ctDCS may be consistent with the concept of neural facilitation [31]: A ctDCS-induced downregulation of the affective response may result in reduced distractibility [61]. Moreover, reduced activity in the ventral emotional system has been proposed to be accompanied by enhanced activity in the dorsal executive system [61,73–75]. In line with this assumption, the difference in activity in the right DLPFC between negative and neutral trials did not change after ctDCS.

tDCS effects on behavioral performance

In the CC-DWM task, we again found an effect of trial type, such that RTs were overall slower after negative trials than after neutral trials. This effect, referred to as negativity bias (NB), has been previously reported in MDD [9,76], and in one study was neutralized after anodal tDCS over the left DLPFC [10]. In our study, a NB was no longer present after ctDCS as compared with atDCS-A and reversed after atDCS-A as compared with sham tDCS (i.e. RTs were faster after neutral than after negative pictures). Improved RTs among healthy volunteers was previously reported for neutral pictures after anodal tDCS over the left DLPFC [10], possibly indicating an effective modulation of NB by atDCS-A. In addition, Plewnia and colleagues found an induction of a NB in healthy volunteers after cathodal tDCS over the left DLPFC [25], which is contrary to our finding that the fastest RTs were observed after ctDCS independently of the trial type. However, the montages and parameters used in both studies were fundamentally different: Plewnia and colleagues used extracephalic targets (i.e. deltoid muscle) for the second electrode and applied tDCS at 1 mA for 20 min [10,25], whereas we used bipolar-cephalic targets for both electrodes and applied tDCS at 2 mA for 20 min. Current intensity may indeed be critical as motor-cortex studies suggest that the effects of cathodal tDCS on amplitudes of motor-evoked potentials may be abolished or even inverted from inhibition to facilitation as intensity in increases from 1 to 2 mA [77,78].

Role of electrode montages

Contrary to classical assumptions derived from motor-cortex studies [1,3,79] and to findings of previous fMRI-tDCS studies [22–24,50], the most commonly applied active prefrontal-tDCS montages [28,34] did not differ from sham tDCS in the present study. Only the ctDCS montage seems to have been effective in that it showed a marginal difference from sham in addition to deviations from other tDCS conditions. Moreover, ctDCS-associated downregulations on a neurophysiological level were associated with excitatory effects on a behavioral level. At the same time, the direction of ctDCS effects changed across anatomical subdivision of the PFC (medial vs. dorsolateral parts), though F3-F4 electrode-positions have originally been chosen to stimulate DLPFC regions. A recent simulation study indicates that bipolar-frontal tDCS montages may lead to stimulation of the medial surface of the PFC at a similar magnitude as over the DLPFC [80]. Other computational models have shown that, for such montages, the electric field varies from medial to lateral parts of the PFC [38–42].

In sum, our findings argue against one-to-one translational assumptions, i.e. it seems to be difficult to transfer basic assumptions derived from motor-cortex studies to PFC stimulation conditions – just as it may be incorrect to transfer effects observed in healthy subject to psychiatric patients. So far, effects of prefrontal tDCS have been reported based on comparisons of one active-tDCS condition with sham tDCS or with an inversed electrode montage (often specified as atDCS vs. ctDCS) and not based on a range of comparator montages (for review see 19). There is a clear need to systematically test assumptions on electrode positions, also requiring modelling studies. Vice versa, multi-dimensional fMRI measurements (for review see 19) and other neurophysiological measures [81] will allow to experimentally validate computational models.

Limitations

The rigorous design in terms of control and comparator conditions for tDCS is a strength of this study. Nevertheless, it has some limitations that need to be considered when interpreting the data. Thirty-two participants underwent a total of 128 fMRI-tDCS sessions, which constitutes the largest number of fMRI scans in a single study in the tDCS-fMRI field to date. Still, higher sample sizes may be necessary for robust and reproducible results [82]. This is why we consider our study as exploratory and also reported findings that just reached a statistical trend. Consequently, our conclusions have to be regarded as preliminary and replications are warranted. At the same time, the striking difference between stable baseline versus changing post-tDCS RS-measurements points to the informative value of our findings. Moreover, several marginally significant results were close to a p-value smaller than 0.05 and therefore are likely to reach significance at a higher sample size. Beyond, the recently detected high inter- and intra-individual variability of tDCS responses [30,56,57,60,83–85] warrants the use of novel approaches based on analyses of individual data [84–86]. In this context, individual modelling of the electrical field may be of interest and is lacking in both this and previous studies.

A further shortcoming of our study concerns the selection of electrode montages. While we chose two montages for atDCS over the left DLPFC, both of which are commonly used for MDD, we included only one, exploratory montage for ctDCS over F3. In addition, we used only bipolar-cephalic montages and not an extracephalic montage, as used by Plewnia and colleagues [6]. The two

types of montage may differ significantly in terms of current distribution induced by prefrontal tDCS [87]. Noteworthy in this context is that the electrode montages used in randomized-controlled trials in MDD have also varied [13,14,20,21,35,88,89]. To date, it remains unclear whether differences in outcomes across studies may be related to differences in electrode montages. Future studies need to define dosages at stimulation sites and systematically establish optimal electrode positions for different cortical targets.

Finally, RS- and task-fMRI measures were acquired sequentially, i.e. they do not represent neurophysiological changes parallel in time. Although sustained effects of tDCS have previously been shown [2], tDCS mechanisms of action may change over time [77,90].

Conclusions

In this study, we were not able to prove our priori hypotheses on the localization and polarity-specificity of anodal versus cathodal tDCS on RS and DWM-task fMRI in healthy volunteers. We provide evidence, however, that prefrontal-tDCS effects depend on electrode montages. Thus, the effects of tDCS in experimental paradigms and clinical applications may be difficult to predict. The further development of prefrontal tDCS towards an effective therapeutic intervention requires systematic research on the actual targets (medial and dorsolateral PFC regions) and the respective dose-response relationships (e.g. based on electric field models) of prefrontal tDCS.

Funding sources

This work was supported by the German Center for Brain Stimulation (GCBS) research consortium (Work Package 5) [grant number 01EE1403E], funded by the Federal Ministry of Education and Research (BMBF).

Declarations of interest

F.P. has received speaker's honoraria from Mag&More GmbH and the neuroCare Group and support with equipment from neuroConn GmbH, Ilmenau, Germany, and Mag&More GmbH and Brainsway Inc., Jerusalem, Israel. A.H. has been invited to scientific meetings by Lundbeck, Janssen-Cilag, and Pfizer, and he has received paid speakerships from Desitin, Janssen-Colag, Otsuka and Lundbeck. He was member of Roche and Janssen-Cilag advisory boards. J.W., S.G., I.H., C.B., C.P., B.E.-W., and D.K. report no conflicts of interest.

Prior presentations

Wörsching, J.*, Padberg, F.*, Heinz, I., Bauer, C., Ertl-Wagner, B., & Keeser, D. (2017). Effects of different prefrontal-tDCS electrode montages on resting-state connectivity and cognitive control. *2nd European Conference on Brain Stimulation in Psychiatry, Munich, Germany.*

Acknowledgements

This work is part of the cumulative PhD thesis of J.W. (resting-state data) as well as of the M.D. projects of C.B. and I.H. (behavioral and task-fMRI data). The authors thank Jacquie Klesing, Board-certified Editor in the Life Sciences (ELS), for editing assistance with the manuscript.

Appendix A. Supplementary data

Supplementary data related to this article can be found at https://doi.org/10.1016/j.brs.2018.05.001.

References

[1] Nitsche MA, Nitsche MS, Klein CC, Tergau F, Rothwell JC, Paulus W. Level of action of cathodal DC polarisation induced inhibition of the human motor cortex. Clin Neurophysiol 2003;114(4):600–4.
[2] Nitsche MA, Paulus W. Sustained excitability elevations induced by transcranial DC motor cortex stimulation in humans. Neurology 2001;57(10):1899–901.
[3] Nitsche MA, Paulus W. Excitability changes induced in the human motor cortex by weak transcranial direct current stimulation. J Physiol 2000;527(3):633–9.
[4] Tremblay S, Lepage J-F, Latulipe-Loiselle A, Fregni F, Pascual-Leone A, Théoret H. The uncertain outcome of prefrontal tDCS. Brain Stimul 2014;7(6):773–83.
[5] Ironside M, O'Shea J, Cowen PJ, Harmer CJ. Frontal cortex stimulation reduces vigilance to threat: implications for the treatment of depression and anxiety. Biol Psychiatr 2016;79(10):823–30.
[6] Plewnia C, Schroeder PA, Wolkenstein L. Targeting the biased brain: non-invasive brain stimulation to ameliorate cognitive control. Lancet Psychiatr 2015;2(4):351–6.
[7] Baert S, De Raedt R, Schacht R, Koster EH. Attentional bias training in depression: therapeutic effects depend on depression severity. J Behav Ther Exp Psychiatr 2010;41(3):265–74.
[8] Beck AT. The evolution of the cognitive model of depression and its neurobiological correlates. Am J Psychiatr 2008;165(8):969–77.
[9] Ochsner KN, Gross JJ. The cognitive control of emotion. Trends Cognit Sci 2005;9(5):242–9.
[10] Wolkenstein L, Plewnia C. Amelioration of cognitive control in depression by transcranial direct current stimulation. Biol Psychiatr 2013;73(7):646–51.
[11] Lefaucheur JP, Antal A, Ayache SS, Benninger DH, Brunelin J, Cogiamanian F, et al. Evidence-based guidelines on the therapeutic use of transcranial direct current stimulation (tDCS). Clin neurophysiol: Off J Int Fed Clin Neurophysiol 2017;128(1):56–92.
[12] Kuo MF, Chen PS, Nitsche MA. The application of tDCS for the treatment of psychiatric diseases. Int Rev Psychiatr 2017;29(2):146–67.
[13] Brunoni AR, Ferrucci R, Bortolomasi M, Scelzo E, Boggio PS, Fregni F, et al. Interactions between transcranial direct current stimulation (tDCS) and pharmacological interventions in the Major Depressive Episode: findings from a naturalistic study. Europ psych : J Assoc Eur Psychiat 2013;28(6):356–61.
[14] Brunoni AR, Moffa AH, Sampaio-Junior B, Borrione L, Moreno ML, Fernandes RA, et al. Trial of electrical direct-current therapy versus escitalopram for depression. N Engl J Med 2017;376(26):2523–33.
[15] Lisanby SH. Noninvasive brain stimulation for depression - the devil is in the dosing. N Engl J Med 2017;376(26):2593–4.
[16] Antonenko D, Schubert F, Bohm F, Ittermann B, Aydin S, Hayek D, et al. Tdcs-induced modulation of GABA levels and resting-state functional connectivity in older adults. J Neurosci : Off J Soc Neurosci 2017;37(15):4065–73.
[17] Fischer DB, Fried PJ, Ruffini G, Ripolles O, Salvador R, Banus J, et al. Multifocal tDCS targeting the resting state motor network increases cortical excitability beyond traditional tDCS targeting unilateral motor cortex. Neuroimage 2017;157:34–44.
[18] Hone-Blanchet A, Edden RA, Fecteau S. Online effects of transcranial direct current stimulation in real time on human prefrontal and striatal metabolites. Biol Psychiatr 2016;80(6):432–8.
[19] Worsching J, Padberg F, Ertl-Wagner B, Kumpf U, Kirsch B, Keeser D. Imaging transcranial direct current stimulation (tDCS) of the prefrontal cortex-correlation or causality in stimulation-mediated effects? Neurosci Biobehav Rev 2016;69:333–56.
[20] Loo CK, Alonzo A, Martin D, Mitchell PB, Galvez V, Sachdev P. Transcranial direct current stimulation for depression: 3-week, randomised, sham-controlled trial. Brit J psych : J Ment Sci 2012;200(1):52–9.
[21] Boggio PS, Rigonatti SP, Ribeiro RB, Myczkowski ML, Nitsche MA, Pascual-Leone A, et al. A randomized, double-blind clinical trial on the efficacy of cortical direct current stimulation for the treatment of major depression. Int J neuropsychopharmacol/Off Sci J Coll Int Internationale Neuropsychopharmacologicum 2008;11(2):249–54.
[22] Keeser D, Meindl T, Bor J, Palm U, Pogarell O, Mulert C, et al. Prefrontal transcranial direct current stimulation changes connectivity of resting-state networks during fMRI. The Journal of neuroscience : Off J Soc Neurosci 2011;31(43):15284–93.
[23] Park CH, Chang WH, Park JY, Shin YI, Kim ST, Kim YH. Transcranial direct current stimulation increases resting state interhemispheric connectivity. Neurosci Lett 2013;539:7–10.
[24] Pena-Gomez C, Sala-Lonch R, Junque C, Clemente IC, Vidal D, Bargallo N, et al. Modulation of large-scale brain networks by transcranial direct current stimulation evidenced by resting-state functional MRI. Brain Stimul 2012;5(3):252–63.

[25] Wolkenstein L, Zeiller M, Kanske P, Plewnia C. Induction of a depression-like negativity bias by cathodal transcranial direct current stimulation. Cortex 2014;59:103–12.
[26] Simonsmeier BA, Grabner RH, Hein J, Krenz U, Schneider M. Electrical brain stimulation (tES) improves learning more than performance: a meta-analysis. Neurosci Biobehav Rev 2018;84:171–81.
[27] Oldfield RC. The assessment and analysis of handedness: the Edinburgh inventory. Neuropsychologia 1971;9:97–113.
[28] Padberg F, Kumpf U, Mansmann U, Palm U, Plewnia C, Langguth B, et al. Prefrontal transcranial direct current stimulation (tDCS) as treatment for major depression: study design and methodology of a multicenter triple blind randomized placebo controlled trial (DepressionDC). Eur Arch Psychiatr Clin Neurosci 2017;267(8):751–66.
[29] Cavaliere C, Aiello M, Di Perri C, Amico E, Martial C, Thibaut A, et al. Functional connectivity substrates for tDCS response in minimally conscious state patients. Front Cell Neurosci 2016;10:257.
[30] Worsching J, Padberg F, Helbich K, Hasan A, Koch L, Goerigk S, et al. Test-retest reliability of prefrontal transcranial Direct Current Stimulation (tDCS) effects on functional MRI connectivity in healthy subjects. Neuroimage 2017;155:187–201.
[31] Holland R, Leff AP, Josephs O, Galea JM, Desikan M, Price CJ, et al. Speech facilitation by left inferior frontal cortex stimulation. Curr Biol : CB 2011;21(16):1403–7.
[32] Holland R, Leff AP, Penny WD, Rothwell JC, Crinion J. Modulation of frontal effective connectivity during speech. Neuroimage 2016;140:126–33.
[33] Pereira JB, Junque C, Bartres-Faz D, Marti MJ, Sala-Llonch R, Compta Y, et al. Modulation of verbal fluency networks by transcranial direct current stimulation (tDCS) in Parkinson's disease. Brain Stimul 2013;6(1):16–24.
[34] Brunoni AR, Valiengo L, Baccaro A, Zanao TA, de Oliveira JF, Goulart A, et al. The sertraline vs. electrical current therapy for treating depression clinical study: results from a factorial, randomized, controlled trial. JAMA Psychiatr 2013;70(4):383–91.
[35] Palm U, Schiller C, Fintescu Z, Obermeier M, Keeser D, Reisinger E, et al. Transcranial direct current stimulation in treatment resistant depression: a randomized double-blind, placebo-controlled study. Brain Stimul 2012;5(3):242–51.
[36] Palm U, Keeser D, Hasan A, Kupka MJ, Blautzik J, Sarubin N, et al. Prefrontal transcranial direct current stimulation for treatment of schizophrenia with predominant negative symptoms: a double-blind, sham-controlled proof-of-concept study. Schizophr Bull 2016;42(5):1253–61.
[37] Sallet J, Mars RB, Noonan MP, Neubert FX, Jbabdi S, O'Reilly JX, et al. The organization of dorsal frontal cortex in humans and macaques. The Journal of neuroscience : Off J Soc Neurosci 2013;33(30):12255–74.
[38] Bai S, Dokos S, Ho KA, Loo C. A computational modelling study of transcranial direct current stimulation montages used in depression. Neuroimage 2014;87:332–44.
[39] DaSilva AF, Truong DQ, DosSantos MF, Toback RL, Datta A, Bikson M. State-of-art neuroanatomical target analysis of high-definition and conventional tDCS montages used for migraine and pain control. Front Neuroanat 2015;9:89.
[40] Nelson JT, McKinley RA, Golob EJ, Warm JS, Parasuraman R. Enhancing vigilance in operators with prefrontal cortex transcranial direct current stimulation (tDCS). Neuroimage 2014;85(3):909–17.
[41] Seibt O, Brunoni AR, Huang Y, Bikson M. The pursuit of DLPFC: non-neuronavigated methods to target the left dorsolateral pre-frontal cortex with symmetric bicephalic transcranial direct current stimulation (tDCS). Brain Stimul 2015;8(3):590–602.
[42] Woods AJ, Bryant V, Sacchetti D, Gervits F, Hamilton R. Effects of electrode drift in transcranial direct current stimulation. Brain Stimul 2015;8(3):515–9.
[43] Beckmann CF, Smith SM. Probabilistic independent component analysis for functional magnetic resonance imaging. IEEE Trans Med Imag 2004;23(2):137–52.
[44] Biswal BB, Mennes M, Zuo XN, Gohel S, Kelly C, Smith SM, et al. Toward discovery science of human brain function. Proc. Natl. Acad. Sci. U.S.A. 2010;107(10):4734–9.
[45] Filippini N, MacIntosh BJ, Hough MG, Goodwin GM, Frisoni GB, Smith SM, et al. Distinct patterns of brain activity in young carriers of the APOE-epsilon4 allele. Proc. Natl. Acad. Sci. U.S.A. 2009;106(17):7209–14.
[46] Zuo XN, Kelly C, Adelstein JS, Klein DF, Castellanos FX, Milham MP. Reliable intrinsic connectivity networks: test-retest evaluation using ICA and dual regression approach. Neuroimage 2010;49(3):2163–77.
[47] Winkler AM, Ridgway GR, Webster MA, Smith SM, Nichols TE. Permutation inference for the general linear model. Neuroimage 2014;92:381–97.
[48] Winkler AM, Webster MA, Vidaurre D, Nichols TE, Smith SM. Multi-level block permutation. Neuroimage 2015;123:253–68.
[49] Aiken LS, West SG, Reno RR. Multiple regression: testing and interpreting interactions. Sage. 1991.
[50] Stagg CJ, Lin RL, Mezue M, Segerdahl A, Kong Y, Xie J, et al. Widespread modulation of cerebral perfusion induced during and after transcranial direct current stimulation applied to the left dorsolateral prefrontal cortex. J Neurosci : Off J Soc Neurosci 2013;33(28):11425–31.
[51] Vanneste S, De Ridder D. Bifrontal transcranial direct current stimulation modulates tinnitus intensity and tinnitus-distress-related brain activity. Eur J Neurosci 2011;34(4):605–14.
[52] Chib VS, Yun K, Takahashi H, Shimojo S. Noninvasive remote activation of the ventral midbrain by transcranial direct current stimulation of prefrontal cortex. Transl Psychiatry 2013;3. e268.
[53] Hoy KE, Bailey NW, Arnold SL, Fitzgerald PB. The effect of transcranial Direct Current Stimulation on gamma activity and working memory in schizophrenia. Psychiatr Res 2015;228(2):191–6.
[54] Volpato C, Piccione F, Cavinato M, Duzzi D, Schiff S, Foscolo L, et al. Modulation of affective symptoms and resting state activity by brain stimulation in a treatment-resistant case of obsessive-compulsive disorder. Neurocase 2013;19(4):360–70.
[55] Nitsche MA, Seeber A, Frommann K, Klein CC, Rochford C, Nitsche MS, et al. Modulating parameters of excitability during and after transcranial direct current stimulation of the human motor cortex. J Physiol 2005;568(Pt 1):291–303.
[56] Chew T, Ho KA, Loo CK. Inter- and intra-individual variability in response to transcranial direct current stimulation (tDCS) at varying current intensities. Brain Stimul 2015;8(6):1130–7.
[57] Dyke K, Kim S, Jackson GM, Jackson SR. Intra-subject consistency and reliability of response following 2 mA transcranial direct current stimulation. Brain Stimul 2016;9(6):819–25.
[58] Horvath JC, Vogrin SJ, Carter O, Cook MJ, Forte JD. Effects of a common transcranial direct current stimulation (tDCS) protocol on motor evoked potentials found to be highly variable within individuals over 9 testing sessions. Exp Brain Res 2016;234(9):2629–42.
[59] Jamil A, Batsikadze G, Kuo HI, Labruna L, Hasan A, Paulus W, et al. Systematic evaluation of the impact of stimulation intensity on neuroplastic after-effects induced by transcranial direct current stimulation. J Physiol 2017;595(4):1273–88.
[60] Lopez-Alonso V, Fernandez-Del-Olmo M, Costantini A, Gonzalez-Henriquez JJ, Cheeran B. Intra-individual variability in the response to anodal transcranial direct current stimulation. Clinical neurophysiology : Off J Int Fed Clin Neurophysiol 2015;126(12):2342–7.
[61] Dolcos F, McCarthy G. Brain systems mediating cognitive interference by emotional distraction. J neurosci : Off J Soc Neurosci 2006;26(7):2072–9.
[62] Miller EK, Cohen JD. An integrative theory of prefrontal cortex function. Annu Rev Neurosci 2001;24:167–202.
[63] Chafee MV, Goldman-Rakic PS. Inactivation of parietal and prefrontal cortex reveals interdependence of neural activity during memory-guided saccades. J Neurophysiol 2000;83(3):1550–66.
[64] Kragel PA, Kano M, Van Oudenhove L, Ly HG, Dupont P, Rubio A, et al. Generalizable representations of pain, cognitive control, and negative emotion in medial frontal cortex. Nat Neurosci 2018;21(2):283–9.
[65] Wallis CU, Cardinal RN, Alexander L, Roberts AC, Clarke HF. Opposing roles of primate areas 25 and 32 and their putative rodent homologs in the regulation of negative emotion. Proc. Natl. Acad. Sci. U.S.A. 2017;114(20):E4075–84.
[66] Courtney SM, Ungerleider LG, Keil K, Haxby JV. Transient and sustained activity in a distributed neural system for human working memory. Nature 1997;386(6625):608–11.
[67] Fuster JM. Network memory. Trends Neurosci 1997;20(10):451–9.
[68] Smith EE, Jonides J. Storage and executive processes in the frontal lobes. Science 1999;283(5408):1657–61.
[69] Davidson RJ, Irwin W. The functional neuroanatomy of emotion and affective style. Trends Cognit Sci 1999;3(1):11–21.
[70] Davis M, Whalen PJ. The amygdala: vigilance and emotion. Mol Psychiatr 2001;6(1):13–34.
[71] Phan KL, Wager T, Taylor SF, Liberzon I. Functional neuroanatomy of emotion: a meta-analysis of emotion activation studies in PET and fMRI. Neuroimage 2002;16(2):331–48.
[72] Zald DH. The human amygdala and the emotional evaluation of sensory stimuli. Brain Res Brain Res Rev. 2003;41(1):88–123.
[73] Dolan RJ, Bench CJ, Liddle PF, Friston KJ, Frith CD, Grasby PM, et al. Dorsolateral prefrontal cortex dysfunction in the major psychoses; symptom or disease specificity? J Neurol Neurosurg Psychiatr 1993;56(12):1290–4.
[74] Mayberg HS, Liotti M, Brannan SK, McGinnis S, Mahurin RK, Jerabek PA, et al. Reciprocal limbic-cortical function and negative mood: converging PET findings in depression and normal sadness. Am J Psychiatr 1999;156(5):675–82.
[75] Yamasaki H, LaBar KS, McCarthy G. Dissociable prefrontal brain systems for attention and emotion. Proc. Natl. Acad. Sci. U.S.A. 2002;99(17):11447–51.
[76] Disner SG, Beevers CG, Haigh EA, Beck AT. Neural mechanisms of the cognitive model of depression. Nat Rev Neurosci 2011;12(8):467–77.
[77] Batsikadze G, Moliadze V, Paulus W, Kuo MF, Nitsche MA. Partially non-linear stimulation intensity-dependent effects of direct current stimulation on motor cortex excitability in humans. J Physiol 2013;591(7):1987–2000.
[78] Jamil A, Batsikadze G, Kuo HI, Labruna L, Hasan A, Paulus W, et al. Systematic evaluation of the impact of stimulation intensity on neuroplastic after-effects induced by transcranial direct current stimulation. J Physiol 2017;595(4):1273–88.
[79] Nitsche MA, Liebetanz D, Antal A, Lang N, Tergau F, Paulus W. Modulation of cortical excitability by weak direct current stimulation–technical, safety and functional aspects. Suppl Clin neurophysiol 2003;56:255–76.
[80] Csifcsak G, Boayue NM, Puonti O, Thielscher A, Mittner M. Effects of transcranial direct current stimulation for treating depression: a modeling study. J Affect Disord 2018;234:164–73.

[81] Huang Y, Liu AA, Lafon B, Friedman D, Dayan M, Wang X, et al. Measurements and models of electric fields in the in vivo human brain during transcranial electric stimulation. Elife 2017:6.
[82] Minarik T, Berger B, Althaus L, Bader V, Biebl B, Brotzeller F, et al. The importance of sample size for reproducibility of tDCS effects. Front Hum Neurosci 2016;10(453).
[83] Wiethoff S, Hamada M, Rothwell JC. Variability in response to transcranial direct current stimulation of the motor cortex. Brain Stimul 2014;7(3):468–75.
[84] Strube W, Bunse T, Nitsche MA, Nikolaeva A, Palm U, Padberg F, et al. Bidirectional variability in motor cortex excitability modulation following 1 mA transcranial direct current stimulation in healthy participants. Phys Rep 2016;4(15).
[85] Lopez-Alonso V, Cheeran B, Rio-Rodriguez D, Fernandez-Del-Olmo M. Inter-individual variability in response to non-invasive brain stimulation paradigms. Brain Stimul 2014;7(3):372–80.
[86] Hsu TY, Juan CH, Tseng P. Individual differences and state-dependent responses in transcranial direct current stimulation. Front Hum Neurosci 2016;10:643.
[87] Martin DM, Alonzo A, Mitchell PB, Sachdev P, Galvez V, Loo CK. Fronto-extracephalic transcranial direct current stimulation as a treatment for major depression: an open-label pilot study. J Affect Disord 2011;134(1–3):459–63.
[88] Loo CK, Husain MM, McDonald WM, Aaronson S, O'Reardon JP, Alonzo A, et al. International randomized-controlled trial of transcranial Direct Current Stimulation in depression. Brain Stimul 2018;11(1):125–33.
[89] Loo CK, Sachdev P, Martin D, Pigot M, Alonzo A, Malhi GS, et al. A double-blind, sham-controlled trial of transcranial direct current stimulation for the treatment of depression. Int J neuropsychopharmacol/Off Sci J Coll Int Internationale Neuropsychopharmacologicum 2010;13(1):61–9.
[90] Ohn SH, Park CI, Yoo WK, Ko MH, Choi KP, Kim GM, et al. Time-dependent effect of transcranial direct current stimulation on the enhancement of working memory. Neuroreport 2008;19(1):43–7.
[91] Jung Y-J, Kim J-H, Im C-H. COMETS: a MATLAB toolbox for simulating local electric fields generated by transcranial direct current stimulation (tDCS). Biomed Eng Lett. 2013;3(1):39–46.

Supplementary Material

Supplementary Information

Methods and Materials

1. Experimental Procedure

Due to the difference in electrode positions across conditions, the design was not fully blinded to the experimenters. Operators were aware that only one sham condition was delivered, and therefore could realize that one of those two sessions, for which the electrodes have been placed in the same scalp locations, must be the sham condition, while the remaining two sessions must be active. By contrast, participants were not informed about the design and therefore were fully blinded.

2. Questionnaires

To measure the impact of tDCS on emotions, participants filled in the state scale of the Positive And Negative Affect Schedule (PANAS, missing the item “enthusiastic” on the positive affect scale) (Krohne et al. 1996; Watson et al. 1988) at the beginning and end of each testing session. After each tDCS-fMRI session, the Comfort Rating Questionnaire (CRQ; Palm et al. 2014) was completed to control for potential side effects that could result in unblinding of the participants. In addition, at the first testing session, the Edinburgh Handedness Questionnaire (EHQ; Oldfield 1971) and a questionnaire for sociodemographic data were administered**.** Questionnaire data were collected using an in-house programmed software on a digital 10-inch Android tablet system (Padberg et al. 2017).

3. Cognitive Control – Delayed Working Memory task

Stimuli were presented using Presentation version 18.0 (https://www.neurobs.com/) on a MRI compatible 40” NordicNeuroLab screen

(http://www.nordicneurolab.com/products/InroomViewingDevice.html). In total, the paradigm continued for approximately 20 min and consisted of 60 trials. Half of the trials contained a neutral picture (neutral trials) and the other half a negative picture (negative trials). Pictures were taken from the International Affective Picture System (IAPS; Lang et al. 2008); negative pictures with a high valence/arousal according to normative ratings were chosen. Participants were instructed to always look at the pictures even if they contained severely injured or dead bodies. Trial type was presented in a pseudorandomised order: maximal three equal trials were allowed to appear in succession. The experiment was triggered by the 6th volume of the fMRI sequence and began with an inter-trial interval (ITI). During the ITI, randomly lasting between 4 and 12 s plus a randomly added jitter between 0 and 0.99999 s, a white fixation cross on a black background was visible and participants were instructed to fixate this cross. The subsequently appearing probe stimuli, presented horizontally in the center of the screen, were randomly chosen from the alphabet with no letter being allowed to appear twice within one row. Regarding required responses, the mapping between buttons and target type was counterbalanced across participants; target type (targets and foils) was counterbalanced across trials. Responses were given via a Diamond 4 button response system (http://www.curdes.com/mainforp/responsedevices/hhsc-1x4-d.html). At the first testing session, before participants went into the MRI scanner, they completed a practice run outside the scanner, consisting of 10 trials and containing only neutral pictures, which did not appear again during the main experiment.

4. FMRI-Data Acquisition

Brain imaging was performed on a 3-Tesla MR-scanner (Magneton Skyra, Siemens Healthineers, Erlangen, Germany) with a 20-channel head-coil. To acquire functional whole-brain images, we employed a T2*-weighted echo-planar-image (EPI) sequence with the following parameters: repetition time (TR), 2000 ms; echo time (TE), 30 ms; flip angle (FA),

80° for RS- and 87° for task-fMRI sequences; spatial resolution, 3 x 3 x 3 mm^3. For anatomical reference, a high-resolution MPRAGE sequence was performed. Participants were lying in the scanner in a head-first supine position and their head was fixed using plastic foam.

5. Statistical Analyses of Questionnaires

Behavioral data derived from the surveys and the CC-DWM task were analyzed using R (R Development Core Team (2008). R: A language and environment for statistical computing. R Foundation for Statistical Computing, Vienna, Austria. ISBN 3-900051-07-0, URL http://www.R-project.org). Cumulative negative and positive values of the PANAS state were evaluated with a repeated-measures ANOVA with the within-subject factors stimulation condition (4 stages: atDCS-A, atDCS-B, ctDCS, sham tDCS) and RS measurement (2 stages: baseline and post-tDCS). For CRQ analyses, participant-specific sum scores were created and compared between stimulation conditions by means of a repeated-measures ANOVA. Because of missing values resulting from incomplete data entry, only five items related to sensations of side effects during stimulation (pain, tingling, burning, fatigue, headache) and four items related to sensations after stimulation (pain, tingling, burning, fatigue) could be included in the analyses. The item “discomfort” was separately analyzed. For comparisons of side effects during versus after tDCS, paired t-tests were conducted separately for each stimulation condition and only for the four items (pain, tingling, burning, fatigue) available for both observation periods (during and after stimulation).

6. Statistical Analyses of Task Data

The effects of the four types of stimulation condition and the trial type (neutral and negative) on the participant's task-performance measures (reaction time [RT]) were quantified using linear-mixed-model analyses, in order to efficiently handle inter-individual variability in the data. This method of modelling was also preferable due to its capability to integrate missing-data cases and hence retain comparability between the behavioral and fMRI analyses. Missing-data cases only emerged for behavioral readouts and originated from a communication problem between the response system and the recording device (computer). This problem was present in five participants (1, 15, 22, 23, 26) in one testing session / stimulation condition (t4: atDCS-B, t2: sham, t4: atDCS-A, t4: ctDCS, t1: sham). Because missing data were derived from technical difficulties in the measurement process and never appeared twice in one participant, missing cases were considered to be missing at random.

Subject-specific ROI-activity and RTs and interpersonal differences in the reaction to the different stimulation conditions were accounted for by treating both the model intercept and the stimulation-based change rate as random factors. Superior model-fit of the random-effects models was assessed by $\chi 2$-likelihood-ratio tests. Model parameters were calculated with maximum-likelihood (ML) estimations rather than restricted maximum-likelihood estimations because MLs produce more accurate estimates for fixed regression parameters (Twisk 2006) and allow for model comparisons. Models were fit by Satterthwaite approximations to degrees of freedom. All regression-based calculations were carried out with the R package lme4 (Bates et al. 2014).

Results

1. Questionnaires

Neither negative nor positive emotional affect as investigated with the PANAS state-scale changed significantly between testing sessions ($F(3,81) = .89$, $p = .448$) or between RS measurements ($F(1,27) = 3.01$, $p = .094$).

Sum score analyses of CRQ showed that tDCS-related side-effects and discomfort was low independent of the stimulation condition, indicating blinding integrity. During sham tDCS, mean sum score of side effects was 7.25 ± 4.51, after sham tDCS 1.57 ± 3.32. During atDCS-A, mean sum score of side effects was 8.21 ± 5.35, after atDCS-A .89 ± 1.37. During atDCS-B, mean sum score of side effects was 8.57 ± 5.80, after atDCS-B 1.61 ± 2.62. During ctDCS stimulation, mean sum score of side effects was 7.29 ± 5.16, after ctDCS stimulation 1.43 ± 2.67. Repeated measures ANOVA showed no significant difference between mean sum scores during any of the active stimulations and the sham stimulation ($F(3,81) = 1.84$, $p = .146$) and between mean sum scores after any of the active stimulations and the sham stimulation ($F(3,81) = 1.15$, $p = .336$). Phosphenes were not reported by any participant. Also, general discomfort showed no statistically significant difference between active (anodal: 1.5 ± 1.37; cathodal: 1.75 ± 1.65; supraorbital: 1.75 ± 1.80) and sham (1.25 ± 1.38) stimulation ($F(3,81) = 1.61$; $p = .195$). Side effects were significantly lower after stimulation compared to during stimulation in the atDCS-A ($t(27) = 6.97$; $p < 0.001$), atDCS-B ($t(27) = 8.24$; $p < 0.001$), ctDCS ($t(27) = 7.17$; $p < 0.001$), and in the sham condition ($t(27) = 10.24$; $p < 0.001$).

2. Task-fMRI activity and task performance

We used χ^2-likelihood-ratio tests to compare models that allowed the change rate to vary with models that assumed a fixed change rate for all participants. The results were significant for the left area 10 in the retrieval phase ($\Delta AIC = 20; \Delta df = 9; p < .001$) and for the RTs ($\Delta AIC = 50.3; \Delta df = 9; p < .001$), indicating that allowing for individual differences between the participants sufficiently improved model-fit to the data.

References

1. Krohne HW, Egloff B, Kohlmann C-W, Tausch A. Untersuchungen mit einer deutschen Version der" Positive and Negative Affect Schedule"(PANAS). Diagnostica. 1996.
2. Watson D, Clark LA, Tellegen A. Development and validation of brief measures of positive and negative affect: the PANAS scales. Journal of personality and social psychology. 1988;54(6):1063.
3. Palm U, Feichtner KB, Hasan A, Gauglitz G, Langguth B, Nitsche MA, et al. The role of contact media at the skin-electrode interface during transcranial direct current stimulation (tDCS). Brain stimulation. 2014;7(5):762-4.
4. Oldfield RC. The Assessment and Analysis of Handedness: The Edinburgh Inventory. Neuropsychologia. 1971;9:97-113.
5. Padberg F, Kumpf U, Mansmann U, Palm U, Plewnia C, Langguth B, et al. Prefrontal transcranial direct current stimulation (tDCS) as treatment for major depression: study design and methodology of a multicenter triple blind randomized placebo controlled trial (DepressionDC). European archives of psychiatry and clinical neuroscience. 2017.
6. Lang PJ, Bradley MM, Cuthbert BN. International affective picture system (IAPS): Affective ratings of pictures and instruction manual. Technical report A-8. 2008.
7. Twisk JW. Applied multilevel analysis: a practical guide for medical researchers. Cambridge (GB): Cambridge University Press; 2006.
8. Bates D, Maechler M, Bolker B, Walker S. lme4: Linear mixed-effects models using Eigen and S4. R package version. 2014;1(7).

Supplementary Figures

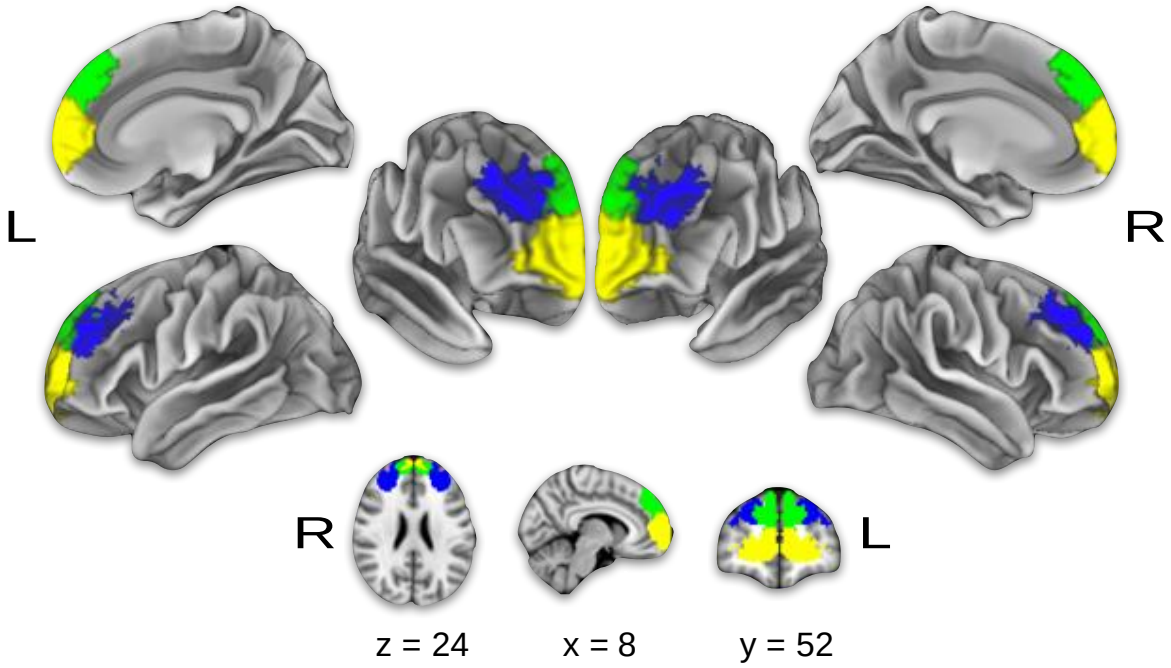

Supplementary Figure 1. Prefrontal regions-of-interest (ROI) within each hemisphere. ROIs were selected from the FSL atlas 'Sallet Dorsal Frontal connectivity-based parcellation' (33) such that parts of the prefrontal cortex were covered, which are most likely stimulated by a bilateral prefrontal-tDCS montage according to computational models: yellow = area 10, green = area 9, blue = area 9/46 dorsal. Coordinates are given in MNI (x, y, z) space.

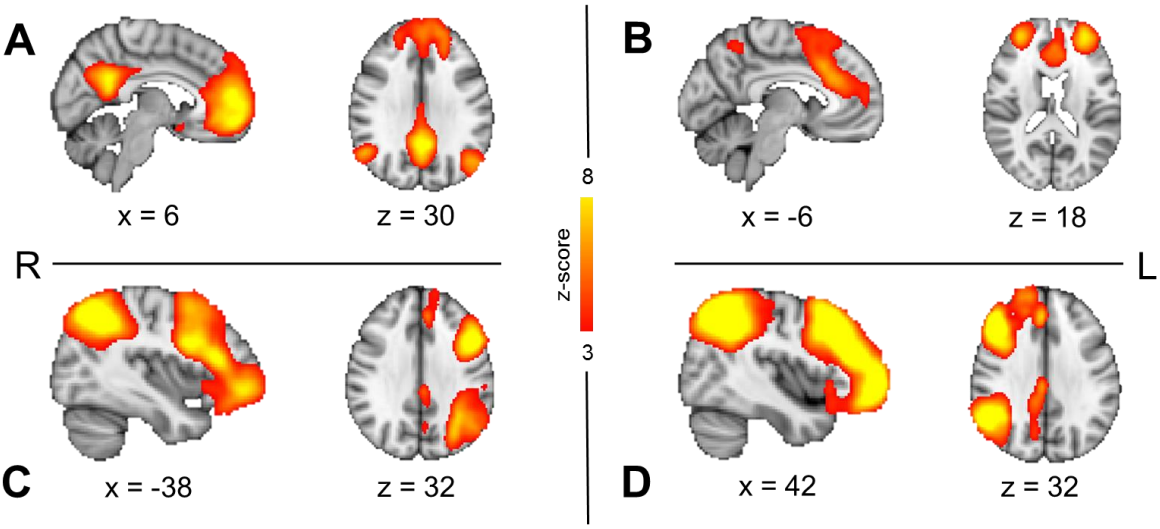

Supplementary Figure 2. Resting-state (RS) networks (RSN) resulting from group independent-component analysis (ICA). ICA was run across all individuals, all stimulation conditions and all RS measurements (baseline and post-tDCS). RSN selection was oriented towards previous findings and anatomical targets (regions within the DLPFC), resulting in four RSNs of interest: A) Default Mode Network (DMN), B) Executive Control Network (ECN), C) left Frontal Parietal Network (FPN), D) right FPN. Coordinates (x, z) are given in MNI space.

References

Antal A, Alekseichuk I, Bikson M, Brockmoller J, Brunoni AR, Chen R, Cohen LG, Dowthwaite G, Ellrich J, Floel A, et al. 2017. Low intensity transcranial electric stimulation: Safety, ethical, legal regulatory and application guidelines, Clin Neurophysiol, 128: 1774-1809.

Arul-Anandam AP, Loo C, Martin D, Mitchell PB. 2009. Chronic neuropathic pain alleviation after transcranial direct current stimulation to the dorsolateral prefrontal cortex, Brain Stimul, 2: 149-151.

Bai S, Dokos S, Ho KA, Loo C. 2014. A computational modelling study of transcranial direct current stimulation montages used in depression, Neuroimage, 87: 332-344.

Barr MS, Farzan F, Tran LC, Fitzgerald PB, Daskalakis ZJ. 2012. A randomized controlled trial of sequentially bilateral prefrontal cortex repetitive transcranial magnetic stimulation in the treatment of negative symptoms in schizophrenia, Brain Stimul, 5: 337-346.

Bates D, Maechler M, Bolker B, Walker S. 2014. lme4: Linear mixed-effects models using Eigen and S4, R package version, 1.

Batsikadze G, Moliadze V, Paulus W, Kuo MF, Nitsche MA. 2013. Partially non-linear stimulation intensity-dependent effects of direct current stimulation on motor cortex excitability in humans, J Physiol, 591: 1987-2000.

Been G, Ngo TT, Miller SM, Fitzgerald PB. 2007. The use of tDCS and CVS as methods of non-invasive brain stimulation, Brain Res Rev, 56: 346-361.

Benwell CS, Learmonth G, Miniussi C, Harvey M, Thut G. 2015. Non-linear effects of transcranial direct current stimulation as a function of individual baseline performance: Evidence from biparietal tDCS influence on lateralized attention bias, Cortex, 69: 152-165.

Bestmann S, de Berker AO, Bonaiuto J. 2015. Understanding the behavioural consequences of noninvasive brain stimulation, Trends Cogn Sci, 19: 13-20.

Bikson M, Grossman P, Thomas C, Zannou AL, Jiang J, Adnan T, Mourdoukoutas AP, Kronberg G, Truong D, Boggio P, et al. 2016. Safety of Transcranial Direct Current Stimulation: Evidence Based Update 2016, Brain Stimul, 9: 641-661.

Bikson M, Inoue M, Akiyama H, Deans JK, Fox JE, Miyakawa H, Jefferys JG. 2004. Effects of uniform extracellular DC electric fields on excitability in rat hippocampal slices in vitro, J Physiol, 557: 175-190.

Bindman LJ, Lippold OC, Redfearn JW. 1963. Comparison of the effects on electrocortical activity of general body cooling of the surface of the brain, Electroencephalogr Clin Neurophysiol, 15: 238-245.

Bindman LJ, Lippold OCJ, Redfearn JWT. 1962. Long-lasting Changes in the Level of the Electrical Activity of the Cerebral Cortex produced by Polarizing Currents, Nature, 196: 584-585.

Biswal BB, Mennes M, Zuo XN, Gohel S, Kelly C, Smith SM, Beckmann CF, Adelstein JS, Buckner RL, Colcombe S, et al. 2010. Toward discovery science of human brain function, Proc Natl Acad Sci U S A, 107: 4734-4739.

Boggio PS, Ferrucci R, Rigonatti SP, Covre P, Nitsche M, Pascual-Leone A, Fregni F. 2006. Effects of transcranial direct current stimulation on working memory in patients with Parkinson's disease, J Neurol Sci, 249: 31-38.

Boggio PS, Liguori P, Sultani N, Rezende L, Fecteau S, Fregni F. 2009. Cumulative priming effects of cortical stimulation on smoking cue-induced craving, Neurosci Lett, 463: 82-86.

Boggio PS, Rigonatti SP, Ribeiro RB, Myczkowski ML, Nitsche MA, Pascual-Leone A, Fregni F. 2008. A randomized, double-blind clinical trial on the efficacy of cortical direct current stimulation for the treatment of major depression, Int J Neuropsychopharmacol, 11: 249-254.

Brunelin J, Mondino M, Gassab L, Haesebaert F, Gaha L, Suaud-Chagny MF, Saoud M, Mechri A, Poulet E. 2012. Examining transcranial direct-current stimulation (tDCS) as a treatment for hallucinations in schizophrenia, Am J Psychiatry, 169: 719-724.

Brunoni AR, Ferrucci R, Bortolomasi M, Scelzo E, Boggio PS, Fregni F, Dell'Osso B, Giacopuzzi M, Altamura AC, Priori A. 2013. Interactions between transcranial direct current stimulation (tDCS) and pharmacological interventions in the Major Depressive Episode: findings from a naturalistic study, Eur Psychiatry, 28: 356-361.

Brunoni AR, Moffa AH, Sampaio-Junior B, Borrione L, Moreno ML, Fernandes RA, Veronezi BP, Nogueira BS, Aparicio LVM, Razza LB, et al. 2017. Trial of Electrical Direct-Current Therapy versus Escitalopram for Depression, N Engl J Med, 376: 2523-2533.

Brunoni AR, Nitsche MA, Bolognini N, Bikson M, Wagner T, Merabet L, Edwards DJ, Valero-Cabre A, Rotenberg A, Pascual-Leone A, et al. 2012. Clinical research with transcranial direct current stimulation (tDCS): challenges and future directions, Brain Stimul, 5: 175-195.

Brunoni AR, Valiengo L, Baccaro A, Zanao TA, de Oliveira JF, Goulart A, Boggio PS, Lotufo PA, Bensenor IM, Fregni F. 2013. The sertraline vs. electrical current therapy for treating depression clinical study: results from a factorial, randomized, controlled trial, JAMA Psychiatry, 70: 383-391.

Cavaliere C, Aiello M, Di Perri C, Amico E, Martial C, Thibaut A, Laureys S, Soddu A. 2016. Functional Connectivity Substrates for tDCS Response in Minimally Conscious State Patients, Front Cell Neurosci, 10: 257.

Chew T, Ho KA, Loo CK. 2015. Inter- and Intra-individual Variability in Response to Transcranial Direct Current Stimulation (tDCS) at Varying Current Intensities, Brain Stimul, 8: 1130-1137.

Conti CL, Nakamura-Palacios EM. 2014. Bilateral transcranial direct current stimulation over dorsolateral prefrontal cortex changes the drug-cued reactivity in the anterior cingulate cortex of crack-cocaine addicts, Brain Stimul, 7: 130-132.

Creutzfeldt OD, Fromm GH, Kapp H. 1962. Influence of transcortical d-c currents on cortical neuronal activity, Exp Neurol, 5: 436-452.

da Silva MC, Conti CL, Klauss J, Alves LG, do Nascimento Cavalcante HM, Fregni F, Nitsche MA, Nakamura-Palacios EM. 2013. Behavioral effects of transcranial direct current stimulation (tDCS) induced dorsolateral prefrontal cortex plasticity in alcohol dependence, J Physiol Paris, 107: 493-502.

DaSilva AF, Truong DQ, DosSantos MF, Toback RL, Datta A, Bikson M. 2015. State-of-art neuroanatomical target analysis of high-definition and conventional tDCS montages used for migraine and pain control, Front Neuroanat, 9: 89.

Datta A, Baker JM, Bikson M, Fridriksson J. 2011. Individualized model predicts brain current flow during transcranial direct-current stimulation treatment in responsive stroke patient, Brain Stimul, 4: 169-174.

Datta A, Bansal V, Diaz J, Patel J, Reato D, Bikson M. 2009. Gyri-precise head model of transcranial direct current stimulation: improved spatial focality using a ring electrode versus conventional rectangular pad, Brain Stimul, 2: 201-207, 207 e201.

Dedoncker J, Brunoni AR, Baeken C, Vanderhasselt MA. 2016. A Systematic Review and Meta-Analysis of the Effects of Transcranial Direct Current Stimulation (tDCS) Over the Dorsolateral Prefrontal Cortex in Healthy and Neuropsychiatric Samples: Influence of Stimulation Parameters, Brain Stimul, 9: 501-517.

Dmochowski JP, Datta A, Bikson M, Su Y, Parra LC. 2011. Optimized multi-electrode stimulation increases focality and intensity at target, J Neural Eng, 8: 046011.

Dmochowski JP, Datta A, Huang Y, Richardson JD, Bikson M, Fridriksson J, Parra LC. 2013. Targeted transcranial direct current stimulation for rehabilitation after stroke, Neuroimage, 75: 12-19.

Dubljevic V, Saigle V, Racine E. 2014. The rising tide of tDCS in the media and academic literature, Neuron, 82: 731-736.

Dyke K, Kim S, Jackson GM, Jackson SR. 2016. Intra-Subject Consistency and Reliability of Response Following 2 mA Transcranial Direct Current Stimulation, Brain Stimul, 9: 819-825.

Edwards AD, Richardson C, van der Zee P, Elwell C, Wyatt JS, Cope M, Delpy DT, Reynolds EO. 1993. Measurement of hemoglobin flow and blood flow by near-infrared spectroscopy, J Appl Physiol (1985), 75: 1884-1889.

Edwards D, Cortes M, Datta A, Minhas P, Wassermann EM, Bikson M. 2013. Physiological and modeling evidence for focal transcranial electrical brain stimulation in humans: a basis for high-definition tDCS, Neuroimage, 74: 266-275.

Filmer HL, Dux PE, Mattingley JB. 2014. Applications of transcranial direct current stimulation for understanding brain function, Trends Neurosci, 37: 742-753.

Finn ES, Shen X, Scheinost D, Rosenberg MD, Huang J, Chun MM, Papademetris X, Constable RT. 2015. Functional connectome fingerprinting: identifying individuals using patterns of brain connectivity, Nat Neurosci, 18: 1664-1671.

Fitzgerald PB, McQueen S, Daskalakis ZJ, Hoy KE. 2014. A negative pilot study of daily bimodal transcranial direct current stimulation in schizophrenia, Brain Stimul, 7: 813-816.

Flöel A. 2014. tDCS-enhanced motor and cognitive function in neurological diseases, Neuroimage, 85, Part 3: 934-947.

Fox MD, Buckner RL, Liu H, Chakravarty MM, Lozano AM, Pascual-Leone A. 2014. Resting-state networks link invasive and noninvasive brain stimulation across diverse psychiatric and neurological diseases, Proc Natl Acad Sci U S A, 111: E4367-4375.

Fox MD, Buckner RL, White MP, Greicius MD, Pascual-Leone A. 2012. Efficacy of transcranial magnetic stimulation targets for depression is related to intrinsic functional connectivity with the subgenual cingulate, Biol Psychiatry, 72: 595-603.

Frank E, Schecklmann M, Landgrebe M, Burger J, Kreuzer P, Poeppl TB, Kleinjung T, Hajak G, Langguth B. 2012. Treatment of chronic tinnitus with repeated sessions of prefrontal transcranial direct current stimulation: outcomes from an open-label pilot study, J Neurol, 259: 327-333.

Fregni F, Boggio PS, Santos MC, Lima M, Vieira AL, Rigonatti SP, Silva MT, Barbosa ER, Nitsche MA, Pascual-Leone A. 2006. Noninvasive cortical stimulation with transcranial direct current stimulation in Parkinson's disease, Mov Disord, 21: 1693-1702.

Galletta EE, Cancelli A, Cottone C, Simonelli I, Tecchio F, Bikson M, Marangolo P. 2015. Use of Computational Modeling to Inform tDCS Electrode Montages for the Promotion of Language Recovery in Post-stroke Aphasia, Brain Stimul, 8: 1108-1115.

Gozenman F, Berryhill ME. 2016. Working memory capacity differentially influences responses to tDCS and HD-tDCS in a retro-cue task, Neurosci Lett, 629: 105-109.

Heinen K, Sagliano L, Candini M, Husain M, Cappelletti M, Zokaei N. 2016. Cathodal transcranial direct current stimulation over posterior parietal cortex enhances distinct aspects of visual working memory, Neuropsychologia, 87: 35-42.

Horvath JC, Forte JD, Carter O. 2015. Evidence that transcranial direct current stimulation (tDCS) generates little-to-no reliable neurophysiologic effect beyond MEP amplitude modulation in healthy human subjects: A systematic review, Neuropsychologia, 66: 213-236.

Horvath JC, Vogrin SJ, Carter O, Cook MJ, Forte JD. 2016. Effects of a common transcranial direct current stimulation (tDCS) protocol on motor evoked potentials found to be highly variable within individuals over 9 testing sessions, Exp Brain Res, 234: 2629-2642.

Hoy KE, Emonson MR, Arnold SL, Thomson RH, Daskalakis ZJ, Fitzgerald PB. 2013. Testing the limits: Investigating the effect of tDCS dose on working memory enhancement in healthy controls, Neuropsychologia, 51: 1777-1784.

Hsu TY, Juan CH, Tseng P. 2016. Individual Differences and State-Dependent Responses in Transcranial Direct Current Stimulation, Front Hum Neurosci, 10: 643.

Ironside M, O'Shea J, Cowen PJ, Harmer CJ. 2016. Frontal Cortex Stimulation Reduces Vigilance to Threat: Implications for the Treatment of Depression and Anxiety, Biol Psychiatry, 79: 823-830.

Iwabuchi SJ, Krishnadas R, Li C, Auer DP, Radua J, Palaniyappan L. 2015. Localized connectivity in depression: a meta-analysis of resting state functional imaging studies, Neurosci Biobehav Rev, 51: 77-86.

Iyer MB, Mattu U, Grafman J, Lomarev M, Sato S, Wassermann EM. 2005. Safety and cognitive effect of frontal DC brain polarization in healthy individuals, Neurology, 64: 872-875.

Jacobson L, Koslowsky M, Lavidor M. 2012. tDCS polarity effects in motor and cognitive domains: a meta-analytical review, Exp Brain Res, 216: 1-10.

Kaiser RH, Andrews-Hanna JR, Wager TD, Pizzagalli DA. 2015. Large-Scale Network Dysfunction in Major Depressive Disorder: A Meta-analysis of Resting-State Functional Connectivity, JAMA Psychiatry, 72: 603-611.

Keeser D, Meindl T, Bor J, Palm U, Pogarell O, Mulert C, Brunelin J, Moller HJ, Reiser M, Padberg F. 2011. Prefrontal transcranial direct current stimulation changes connectivity of resting-state networks during fMRI, J Neurosci, 31: 15284-15293.

Kessler SK, Minhas P, Woods AJ, Rosen A, Gorman C, Bikson M. 2013. Dosage considerations for transcranial direct current stimulation in children: a computational modeling study, PLoS One, 8: e76112.

Krohne HW, Egloff B, Kohlmann C-W, Tausch A. 1996. Untersuchungen mit einer deutschen Version der" Positive and Negative Affect Schedule"(PANAS), Diagnostica.

Kuo MF, Paulus W, Nitsche MA. 2014. Therapeutic effects of non-invasive brain stimulation with direct currents (tDCS) in neuropsychiatric diseases, Neuroimage, 85 Pt 3: 948-960.

Laakso I, Tanaka S, Koyama S, De Santis V, Hirata A. 2015. Inter-subject Variability in Electric Fields of Motor Cortical tDCS, Brain Stimul, 8: 906-913.

Laird AR, Fox PM, Eickhoff SB, Turner JA, Ray KL, McKay DR, Glahn DC, Beckmann CF, Smith SM, Fox PT. 2011. Behavioral interpretations of intrinsic connectivity networks, Journal of Cognitive Neuroscience, 23: 4022-4037.

Lang PJ, Bradley MM, Cuthbert BN. 2008. International affective picture system (IAPS): Affective ratings of pictures and instruction manual, Technical report A-8.

Learmonth G, Thut G, Benwell CS, Harvey M. 2015. The implications of state-dependent tDCS effects in aging: Behavioural response is determined by baseline performance, Neuropsychologia, 74: 108-119.

Looi CY, Duta M, Brem AK, Huber S, Nuerk HC, Cohen Kadosh R. 2016. Combining brain stimulation and video game to promote long-term transfer of learning and cognitive enhancement, Sci Rep, 6: 22003.

Lopez-Alonso V, Cheeran B, Rio-Rodriguez D, Fernandez-Del-Olmo M. 2014. Inter-individual variability in response to non-invasive brain stimulation paradigms, Brain Stimul, 7: 372-380.

Lopez-Alonso V, Fernandez-Del-Olmo M, Costantini A, Gonzalez-Henriquez JJ, Cheeran B. 2015. Intra-individual variability in the response to anodal transcranial direct current stimulation, Clin Neurophysiol, 126: 2342-2347.

Meinzer M, Antonenko D, Lindenberg R, Hetzer S, Ulm L, Avirame K, Flaisch T, Floel A. 2012. Electrical brain stimulation improves cognitive performance by modulating functional connectivity and task-specific activation, J Neurosci, 32: 1859-1866.

Meinzer M, Lindenberg R, Antonenko D, Flaisch T, Floel A. 2013. Anodal transcranial direct current stimulation temporarily reverses age-associated cognitive decline and functional brain activity changes, J Neurosci, 33: 12470-12478.

Meinzer M, Lindenberg R, Phan MT, Ulm L, Volk C, Floel A. 2015. Transcranial direct current stimulation in mild cognitive impairment: Behavioral effects and neural mechanisms, Alzheimers Dement, 11: 1032-1040.

Miranda PC, Lomarev M, Hallett M. 2006. Modeling the current distribution during transcranial direct current stimulation, Clin Neurophysiol, 117: 1623-1629.

Monte-Silva K, Kuo MF, Hessenthaler S, Fresnoza S, Liebetanz D, Paulus W, Nitsche MA. 2013. Induction of late LTP-like plasticity in the human motor cortex by repeated non-invasive brain stimulation, Brain Stimul, 6: 424-432.

Monte-Silva K, Kuo MF, Liebetanz D, Paulus W, Nitsche MA. 2010. Shaping the optimal repetition interval for cathodal transcranial direct current stimulation (tDCS), J Neurophysiol, 103: 1735-1740.

Moreno-Duarte I, Gebodh N, Schestatsky P, Guleyupoglu B, Reato D, Bikson M, Fregni F. 2014. Transcranial electrical stimulation: transcranial direct current stimulation (tDCS), transcranial alternating current stimulation (tACS), transcranial pulsed current stimulation (tPCS), and transcranial random noise stimulation (tRNS)editor. The Stimulated Brain: Elsevier. 35-59.

Mueller S, Wang D, Fox MD, Yeo BT, Sepulcre J, Sabuncu MR, Shafee R, Lu J, Liu H. 2013. Individual variability in functional connectivity architecture of the human brain, Neuron, 77: 586-595.

Nakamura-Palacios EM, de Almeida Benevides MC, da Penha Zago-Gomes M, de Oliveira RW, de Vasconcellos VF, de Castro LN, da Silva MC, Ramos PA, Fregni F. 2012. Auditory event-related potentials (P3) and cognitive changes induced by frontal direct current stimulation in alcoholics according to Lesch alcoholism typology, Int J Neuropsychopharmacol, 15: 601-616.

Nasseri P, Nitsche MA, Ekhtiari H. 2015. A framework for categorizing electrode montages in transcranial direct current stimulation, Front Hum Neurosci, 9: 54.

Nawani H, Bose A, Agarwal SM, Shivakumar V, Chhabra H, Subramaniam A, Kalmady S, Narayanaswamy JC, Venkatasubramanian G. 2014. Modulation of corollary discharge dysfunction in schizophrenia by tDCS: preliminary evidence, Brain Stimul, 7: 486-488.

Nelson JT, McKinley RA, Golob EJ, Warm JS, Parasuraman R. 2014. Enhancing vigilance in operators with prefrontal cortex transcranial direct current stimulation (tDCS), Neuroimage, 85 Pt 3: 909-917.

Neuling T, Wagner S, Wolters CH, Zaehle T, Herrmann CS. 2012. Finite-Element Model Predicts Current Density Distribution for Clinical Applications of tDCS and tACS, Front Psychiatry, 3: 83.

Nitsche MA, Cohen LG, Wassermann EM, Priori A, Lang N, Antal A, Paulus W, Hummel F, Boggio PS, Fregni F, et al. 2008. Transcranial direct current stimulation: State of the art 2008, Brain Stimulation: Basic, Translational, and Clinical Research in Neuromodulation, 1: 206-223.

Nitsche MA, Fricke K, Henschke U, Schlitterlau A, Liebetanz D, Lang N, Henning S, Tergau F, Paulus W. 2003. Pharmacological modulation of cortical excitability shifts induced by transcranial direct current stimulation in humans, J Physiol, 553: 293-301.

Nitsche MA, Liebetanz D, Antal A, Lang N, Tergau F, Paulus W. 2003. Modulation of cortical excitability by weak direct current stimulation--technical, safety and functional aspects, Suppl Clin Neurophysiol, 56: 255-276.

Nitsche MA, Liebetanz D, Lang N, Antal A, Tergau F, Paulus W. 2003. Safety criteria for transcranial direct current stimulation (tDCS) in humans, Clinical Neurophysiology, 114: 2220-2222.

Nitsche MA, Nitsche MS, Klein CC, Tergau F, Rothwell JC, Paulus W. 2003. Level of action of cathodal DC polarisation induced inhibition of the human motor cortex, Clinical Neurophysiology, 114: 600-604.

Nitsche MA, Paulus W. 2000. Excitability changes induced in the human motor cortex by weak transcranial direct current stimulation, J Physiol, 527 Pt 3: 633-639.

Nitsche MA, Paulus W. 2001. Sustained excitability elevations induced by transcranial DC motor cortex stimulation in humans, Neurology, 57: 1899-1901.

Nitsche MA, Seeber A, Frommann K, Klein CC, Rochford C, Nitsche MS, Fricke K, Liebetanz D, Lang N, Antal A, et al. 2005. Modulating parameters of excitability during and after transcranial direct current stimulation of the human motor cortex, J Physiol, 568: 291-303.

Ohn SH, Park CI, Yoo WK, Ko MH, Choi KP, Kim GM, Lee YT, Kim YH. 2008. Time-dependent effect of transcranial direct current stimulation on the enhancement of working memory, Neuroreport, 19: 43-47.

Oldfield RC. 1971. The Assessment and Analysis of Handedness: The Edinburgh Inventory, Neuropsychologia, 9: 97-113.

Padberg F, Kumpf U, Mansmann U, Palm U, Plewnia C, Langguth B, Zwanzger P, Fallgatter A, Nolden J, Burger M, et al. 2017. Prefrontal transcranial direct current stimulation (tDCS) as treatment for major depression: study design and methodology of a multicenter triple blind randomized placebo controlled trial (DepressionDC), Eur Arch Psychiatry Clin Neurosci.

Palm U, Feichtner KB, Hasan A, Gauglitz G, Langguth B, Nitsche MA, Keeser D, Padberg F. 2014. The role of contact media at the skin-electrode interface during transcranial direct current stimulation (tDCS), Brain Stimul, 7: 762-764.

Palm U, Keeser D, Blautzik J, Pogarell O, Ertl-Wagner B, Kupka MJ, Reiser M, Padberg F. 2013. Prefrontal transcranial direct current stimulation (tDCS)

changes negative symptoms and functional connectivity MRI (fcMRI) in a single case of treatment-resistant schizophrenia, Schizophr Res, 150: 583-585.

Palm U, Keeser D, Hasan A, Kupka MJ, Blautzik J, Sarubin N, Kaymakanova F, Unger I, Falkai P, Meindl T, et al. 2016. Prefrontal Transcranial Direct Current Stimulation for Treatment of Schizophrenia With Predominant Negative Symptoms: A Double-Blind, Sham-Controlled Proof-of-Concept Study, Schizophr Bull, 42: 1253-1261.

Palm U, Kumpf U, Behler N, Wulf L, Kirsch B, Worsching J, Keeser D, Hasan A, Padberg F. 2017. Home Use, Remotely Supervised, and Remotely Controlled Transcranial Direct Current Stimulation: A Systematic Review of the Available Evidence, Neuromodulation.

Park CH, Chang WH, Park JY, Shin YI, Kim ST, Kim YH. 2013. Transcranial direct current stimulation increases resting state interhemispheric connectivity, Neurosci Lett, 539: 7-10.

Parkin BL, Ekhtiari H, Walsh VF. 2015. Non-invasive Human Brain Stimulation in Cognitive Neuroscience: A Primer, Neuron, 87: 932-945.

Paulus W. 2004. Outlasting excitability shifts induced by direct current stimulation of the human brain, Suppl Clin Neurophysiol, 57: 708-714.

Pena-Gomez C, Sala-Lonch R, Junque C, Clemente IC, Vidal D, Bargallo N, Falcon C, Valls-Sole J, Pascual-Leone A, Bartres-Faz D. 2012. Modulation of large-scale brain networks by transcranial direct current stimulation evidenced by resting-state functional MRI, Brain Stimul, 5: 252-263.

Plewnia C, Schroeder PA, Wolkenstein L. 2015. Targeting the biased brain: non-invasive brain stimulation to ameliorate cognitive control, Lancet Psychiatry, 2: 351-356.

Prehn-Kristensen A, Munz M, Goder R, Wilhelm I, Korr K, Vahl W, Wiesner CD, Baving L. 2014. Transcranial oscillatory direct current stimulation during sleep improves declarative memory consolidation in children with attention-deficit/hyperactivity disorder to a level comparable to healthy controls, Brain Stimul, 7: 793-799.

Priori A, Berardelli A, Rona S, Accornero N, Manfredi M. 1998. Polarization of the human motor cortex through the scalp, Neuroreport, 9: 2257-2260.

Purpura DP, McMurtry JG. 1965. INTRACELLULAR ACTIVITIES AND EVOKED POTENTIAL CHANGES DURING POLARIZATION OF MOTOR CORTEX, J Neurophysiol, 28: 166-185.

Radman T, Datta A, Ramos RL, Brumberg JC, Bikson M. 2009. One-dimensional representation of a neuron in a uniform electric field, Conf Proc IEEE Eng Med Biol Soc, 2009: 6481-6484.

Radman T, Ramos RL, Brumberg JC, Bikson M. 2009. Role of cortical cell type and morphology in subthreshold and suprathreshold uniform electric field stimulation in vitro, Brain Stimul, 2: 215-228, 228 e211-213.

Rahman A, Reato D, Arlotti M, Gasca F, Datta A, Parra LC, Bikson M. 2013. Cellular effects of acute direct current stimulation: somatic and synaptic terminal effects, J Physiol, 591: 2563-2578.

Rosso C, Valabregue R, Arbizu C, Ferrieux S, Vargas P, Humbert F, Attal Y, Messe A, Zavanone C, Meunier S, et al. 2014. Connectivity between right inferior frontal gyrus and supplementary motor area predicts after-effects of right frontal cathodal tDCS on picture naming speed, Brain Stimul, 7: 122-129.

Russell M, Goodman T, Wang Q, Groshong B, Lyeth BG. 2014. Gender Differences in Current Received during Transcranial Electrical Stimulation, Front Psychiatry, 5: 104.

Russell MJ, Goodman TA, Visse JM, Beckett L, Saito N, Lyeth BG, Recanzone GH. 2017. Sex and Electrode Configuration in Transcranial Electrical Stimulation, Front Psychiatry, 8: 147.

Seibt O, Brunoni AR, Huang Y, Bikson M. 2015. The Pursuit of DLPFC: Non-neuronavigated Methods to Target the Left Dorsolateral Pre-frontal Cortex With Symmetric Bicephalic Transcranial Direct Current Stimulation (tDCS), Brain Stimul, 8: 590-602.

Sotnikova A, Soff C, Tagliazucchi E, Becker K, Siniatchkin M. 2017. Transcranial Direct Current Stimulation Modulates Neuronal Networks in Attention Deficit Hyperactivity Disorder, Brain Topogr, 30: 656-672.

Stagg CJ, Lin RL, Mezue M, Segerdahl A, Kong Y, Xie J, Tracey I. 2013. Widespread modulation of cerebral perfusion induced during and after transcranial direct current stimulation applied to the left dorsolateral prefrontal cortex, J Neurosci, 33: 11425-11431.

Stagg CJ, Nitsche MA. 2011. Physiological basis of transcranial direct current stimulation, Neuroscientist, 17: 37-53.

Strube W, Bunse T, Nitsche MA, Nikolaeva A, Palm U, Padberg F, Falkai P, Hasan A. 2016. Bidirectional variability in motor cortex excitability modulation following 1 mA transcranial direct current stimulation in healthy participants, Physiol Rep, 4.

Teo F, Hoy KE, Daskalakis ZJ, Fitzgerald PB. 2011. Investigating the Role of Current Strength in tDCS Modulation of Working Memory Performance in Healthy Controls, Front Psychiatry, 2: 45.

Thibaut A, Bruno MA, Ledoux D, Demertzi A, Laureys S. 2014. tDCS in patients with disorders of consciousness: sham-controlled randomized double-blind study, Neurology, 82: 1112-1118.

Tremblay S, Lepage J-F, Latulipe-Loiselle A, Fregni F, Pascual-Leone A, Théoret H. 2014. The Uncertain Outcome of Prefrontal tDCS, Brain Stimul, 7: 773-783.

Truong DQ, Magerowski G, Blackburn GL, Bikson M, Alonso-Alonso M. 2013. Computational modeling of transcranial direct current stimulation (tDCS) in obesity: impact of head fat and dose guidelines, Neuroimage (Amst), 2: 759-766.

Tseng P, Chang YT, Chang CF, Liang WK, Juan CH. 2016. The critical role of phase difference in gamma oscillation within the temporoparietal network for binding visual working memory, Sci Rep, 6: 32138.

Tseng P, Hsu TY, Chang CF, Tzeng OJ, Hung DL, Muggleton NG, Walsh V, Liang WK, Cheng SK, Juan CH. 2012. Unleashing potential: transcranial direct current stimulation over the right posterior parietal cortex improves change detection in low-performing individuals, J Neurosci, 32: 10554-10561.

Twisk JW. 2006. Applied multilevel analysis: a practical guide for medical researchers. Cambridge (GB): Cambridge University Press.

Utz KS, Dimova V, Oppenlander K, Kerkhoff G. 2010. Electrified minds: transcranial direct current stimulation (tDCS) and galvanic vestibular stimulation (GVS) as methods of non-invasive brain stimulation in neuropsychology--a review of current data and future implications, Neuropsychologia, 48: 2789-2810.

Valle A, Roizenblatt S, Botte S, Zaghi S, Riberto M, Tufik M, Boggio PS, Fregni F. 2009. Efficacy of anodal transcranial direct current stimulation (tDCS) for the treatment of fibromyalgia: results of a randomized, shamcontrolled longitudinal clinical trial, J Pain Manag, 2: 353–361.

van den Heuvel MP, Hulshoff Pol HE. 2010. Exploring the brain network: a review on resting-state fMRI functional connectivity, Eur Neuropsychopharmacol, 20: 519-534.

van den Heuvel MP, Sporns O. 2013. An anatomical substrate for integration among functional networks in human cortex, J Neurosci, 33: 14489-14500.

Vanneste S, De Ridder D. 2011. Bifrontal transcranial direct current stimulation modulates tinnitus intensity and tinnitus-distress-related brain activity, Eur J Neurosci, 34: 605-614.

Vanneste S, Focquaert F, Van de Heyning P, De Ridder D. 2011. Different resting state brain activity and functional connectivity in patients who respond and not respond to bifrontal tDCS for tinnitus suppression, Exp Brain Res, 210: 217-227.

Vanneste S, Plazier M, Ost J, van der Loo E, Van de Heyning P, De Ridder D. 2010. Bilateral dorsolateral prefrontal cortex modulation for tinnitus by transcranial direct current stimulation: a preliminary clinical study, Exp Brain Res, 202: 779-785.

Vercammen A, Rushby JA, Loo C, Short B, Weickert CS, Weickert TW. 2011. Transcranial direct current stimulation influences probabilistic association learning in schizophrenia, Schizophr Res, 131: 198-205.

Volpato C, Piccione F, Cavinato M, Duzzi D, Schiff S, Foscolo L, Venneri A. 2013. Modulation of affective symptoms and resting state activity by brain stimulation in a treatment-resistant case of obsessive-compulsive disorder, Neurocase, 19: 360-370.

Wagner T, Valero-Cabre A, Pascual-Leone A. 2007. Noninvasive human brain stimulation, Annu Rev Biomed Eng, 9: 527-565.

Watson D, Clark LA, Tellegen A. 1988. Development and validation of brief measures of positive and negative affect: the PANAS scales, Journal of personality and social psychology, 54: 1063.

Weaver L, Williams R, Rush S. 1976. Current density in bilateral and unilateral ECT, Biol Psychiatry, 11: 303-312.

Weber MJ, Messing SB, Rao H, Detre JA, Thompson-Schill SL. 2014. Prefrontal transcranial direct current stimulation alters activation and connectivity in cortical and subcortical reward systems: a tDCS-fMRI study, Hum Brain Mapp, 35: 3673-3686.

Woods AJ, Bryant V, Sacchetti D, Gervits F, Hamilton R. 2015. Effects of Electrode Drift in Transcranial Direct Current Stimulation, Brain Stimul, 8: 515-519.

Worsching J, Padberg F, Ertl-Wagner B, Kumpf U, Kirsch B, Keeser D. 2016. Imaging transcranial direct current stimulation (tDCS) of the prefrontal cortex-correlation or causality in stimulation-mediated effects?, Neurosci Biobehav Rev, 69: 333-356.

Yang LZ, Shi B, Li H, Zhang W, Liu Y, Wang H, Zhou Y, Wang Y, Lv W, Ji X, et al. 2017. Electrical stimulation reduces smokers' craving by modulating the coupling between dorsal lateral prefrontal cortex and parahippocampal gyrus, Soc Cogn Affect Neurosci, 12: 1296-1302.

Zaghi S, Acar M, Hultgren B, Boggio PS, Fregni F. 2010. Noninvasive brain stimulation with low-intensity electrical currents: putative mechanisms of action for direct and alternating current stimulation, Neuroscientist, 16: 285-307.

Acknowledgements

Ich möchte mich zu gleichen Maßen bei Herrn Prof. Dr. Frank Padberg und Herrn Dr. Daniel Keeser ganz herzlich bedanken. Hierbei ist neben der fachlichen Unterstützung auch die emotionale herauszustellen. Danke für die kurzen Dienstwege, 24-h Verfügbarkeit, ausführlichen Diskussionen, aufbauenden Gespräche, zahlreichen Fortbildungsmöglichkeiten und Konferenz-Reisen sowie für euer Vertrauen und euren Glauben in meine Fähigkeiten!

Weiterhin möchte ich mich auch bei PD Dr. Alkomiet Hasen bedanken für die statistische Beratung, welche nach Anfrage mit einer maximalen Latenz von 5 min zur Verfügung stand. Und natürlich auch Danke für den herausforderndsten Lauf meines Lebens im Göttinger Forst!

Im Zuge der statistischen Mithilfe ist auch Stephan Goerigk zu nennen – danke für deine Geduld und die Bereitstellung deines Statistik-Wissens!

Als unendlich unterstützend habe ich in meinem Arbeitsumfeld auch meine lieben Kolleginnen erlebt – Linda Wulf, Nora Behler, Eva Metzger, Tabea Matt und Lucia Bulubas. Vielen Dank für euren Zuspruch, den bereichernden Austausch, die ausgedehnten Mittagspausen, den Tratsch etc. Kurzum: Es war wunderbar mit euch ein Büro teilen zu dürfen!

Danke an Irmgard Heinz, Christine Bauer und Konstantin Helbich für euren phänomenalen Rekrutierungs- und Datenerhebungs-Marathon! Danke an Julia Dillard für die unermüdliche Erstellung von Tabellen! Und für die IT-Hilfestellung ein großes Dankeschön an Temmuz Karali.

Last but not least, möchte ich mich bei meiner Familie, meinen Freunden und vor allem bei meinem Mann Lukas bedanken für die die vielen Ratschläge und den wertvollen Ausgleich zum Arbeitsalltag, ohne den ich den beschrittenen und hiermit beendeten Weg der Promotion nicht erreicht hätte.

Die im Rahmen der Doktorarbeit durchgeführten Projekte wurden gefördert von dem Bundesministerium für Bildung und Forschung (BMBF).